



**Figure S1. Lower Panel**

abs@504nm	normalized abs@504nm	#cycle	calculated abs.	R.I. assumed
2.69	1	0	1.000	0.90
2.42	0.900	1	0.900	
2.14	0.796	2	0.810	
2.08	0.773	3	0.729	
1.82	0.677	4	0.656	
1.54	0.572	5	0.590	
1.41	0.524	6	0.531	
1.26	0.468	7	0.478	
1.23	0.457	8	0.430	
1.05	0.390	9	0.387	

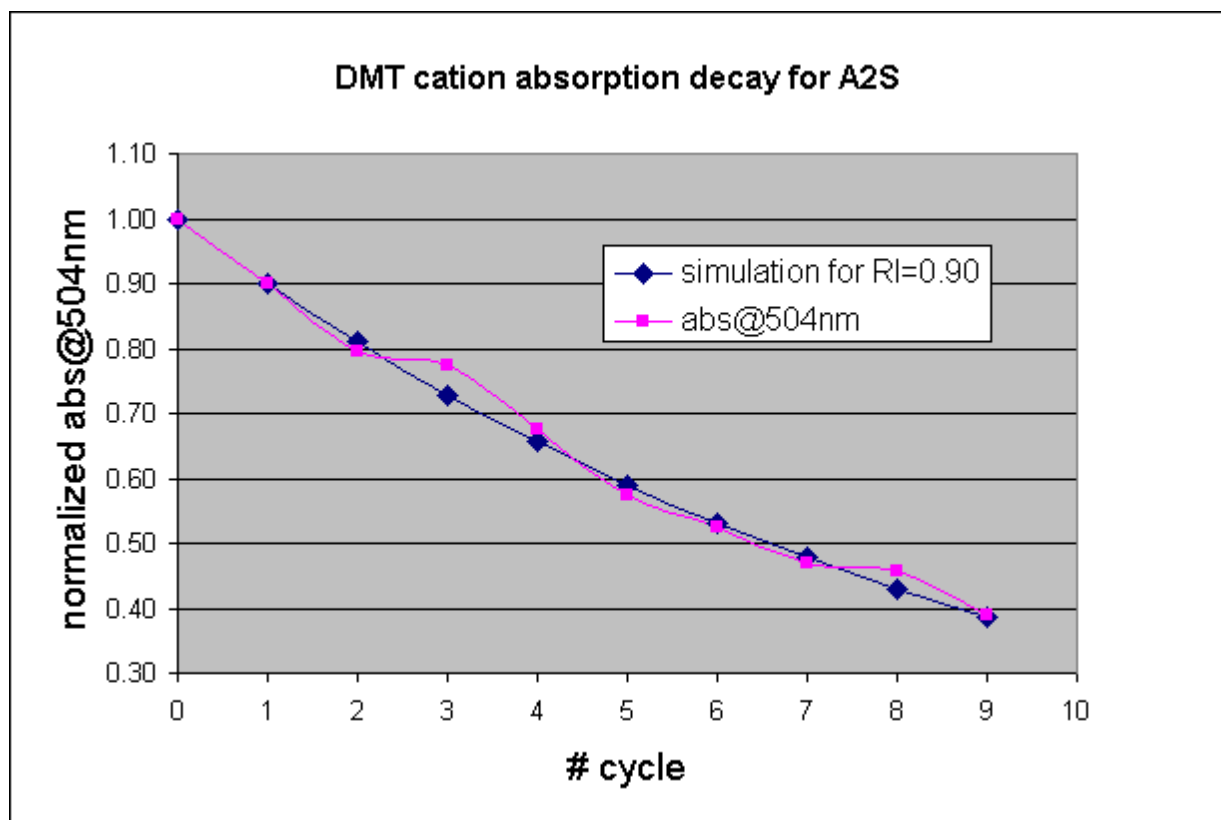


Figure S1. Upper Panel: Overlaid VIS spectra for measurement of the DMT<sup>+</sup> cation absorption ( $\lambda_{\max}$ =504 nm) after consecutive detritylation steps during the synthesis of the **A2S** oligomer (5'-[S<sub>p</sub>-PS]-d(GACA<sub>L</sub>TCA<sub>L</sub>CTAG)-3') at 1  $\mu$ mole scale. Lower Panel: Calculation of the Average Repetitive Yield (RI) and plot for the normalized absorption measured @ 504 nm (pink rectangles) and values calculated at RI=0.90 (blue diamonds). Cycle #0 – detritylation of the nucleoside attached to the support.

## II. Separation of OTP-LNA monomers into P-diastereomers.

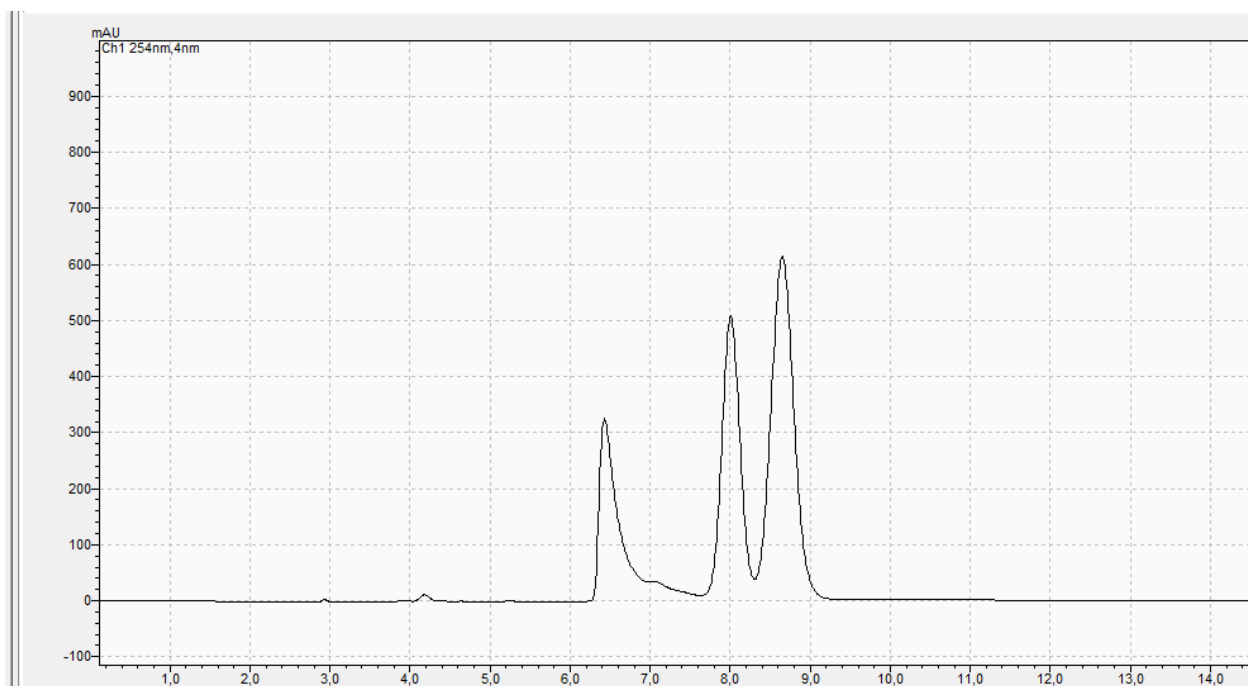


Figure S2. An HPLC profile from search for conditions for semi-preparative separation of P-diastereomers of **2d**. The conditions were identified using a Phenomenex Luna 5u Silica column (100Å; 250×10 mm; flow rate 5 mL/min)

### III. Melting experiment

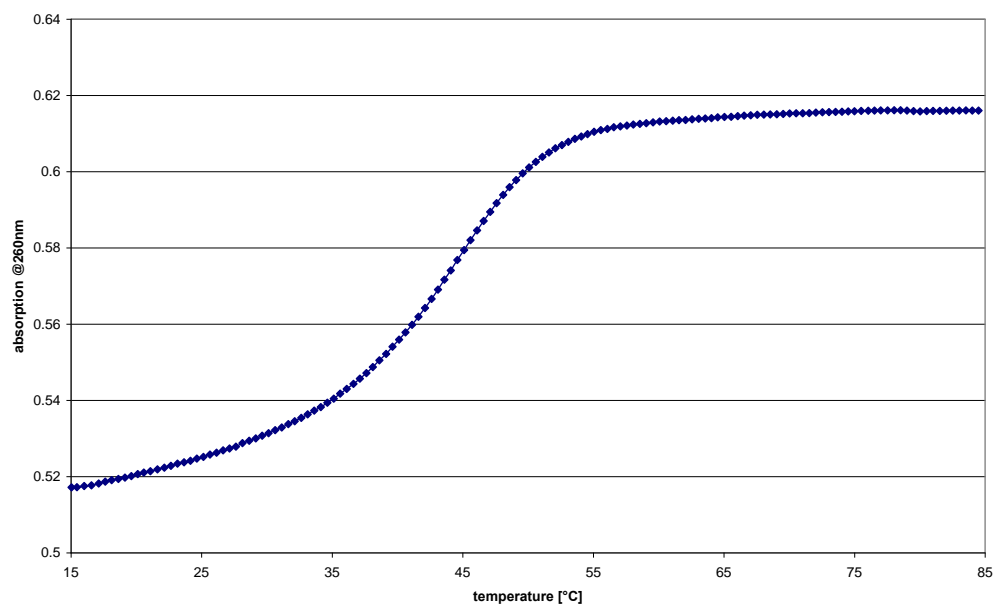


Figure S3. The melting profile for **C2R/M1<sub>D</sub>** in a pH 7.2 buffer containing 10 mM Tris-HCl, 100 mM NaCl, and 10 mM MgCl<sub>2</sub>. The oligonucleotides were mixed at 2.0  $\mu$ M concentration each. Temperature gradient 0.5°C/min.

## IV. CD measurements

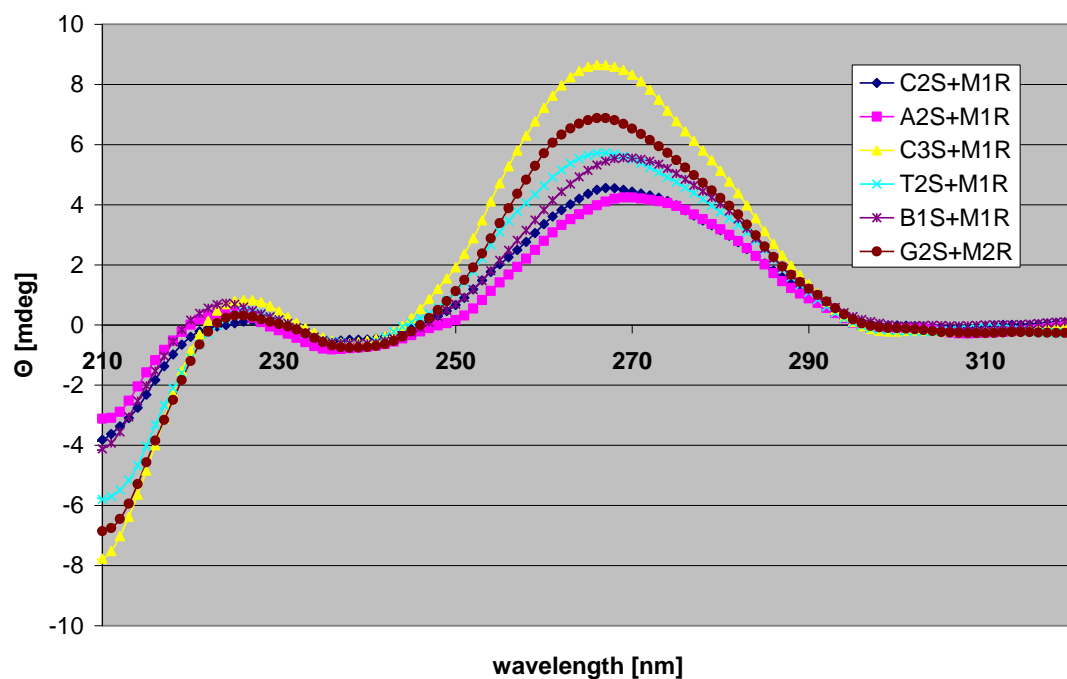


Figure S4. The CD spectra recorded for  $[S_p\text{-PS}]$ -(DNA/LNA)/RNA duplexes and the reference spectrum.

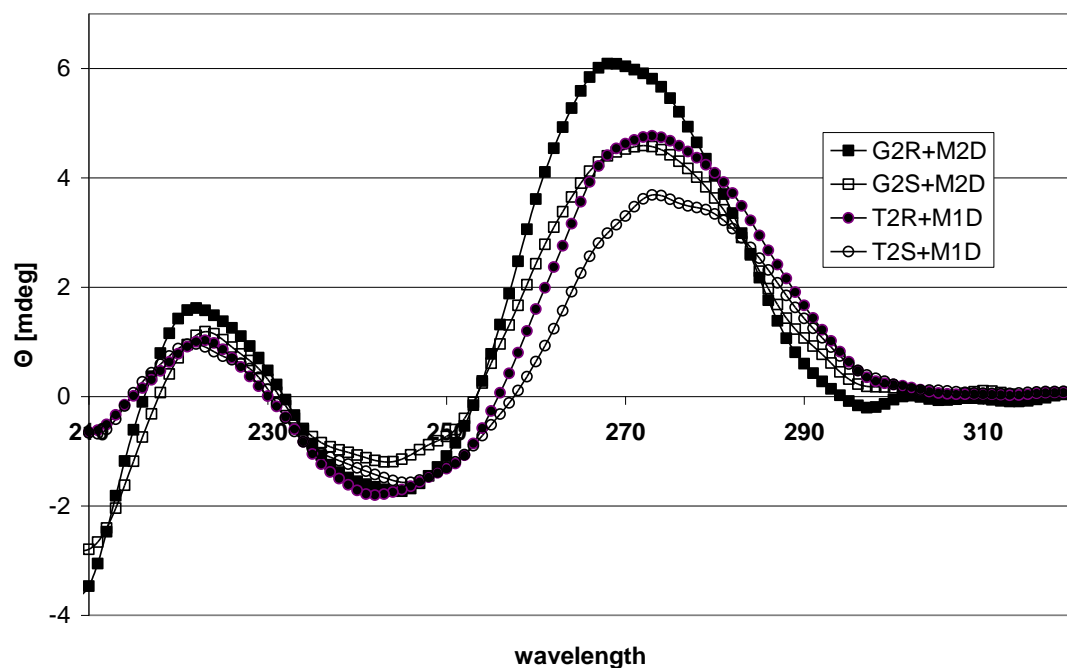


Figure S5. The CD spectra recorded for complexes of T2R and T2S with M1<sub>D</sub>, and G2R and G2S with M2<sub>D</sub>.

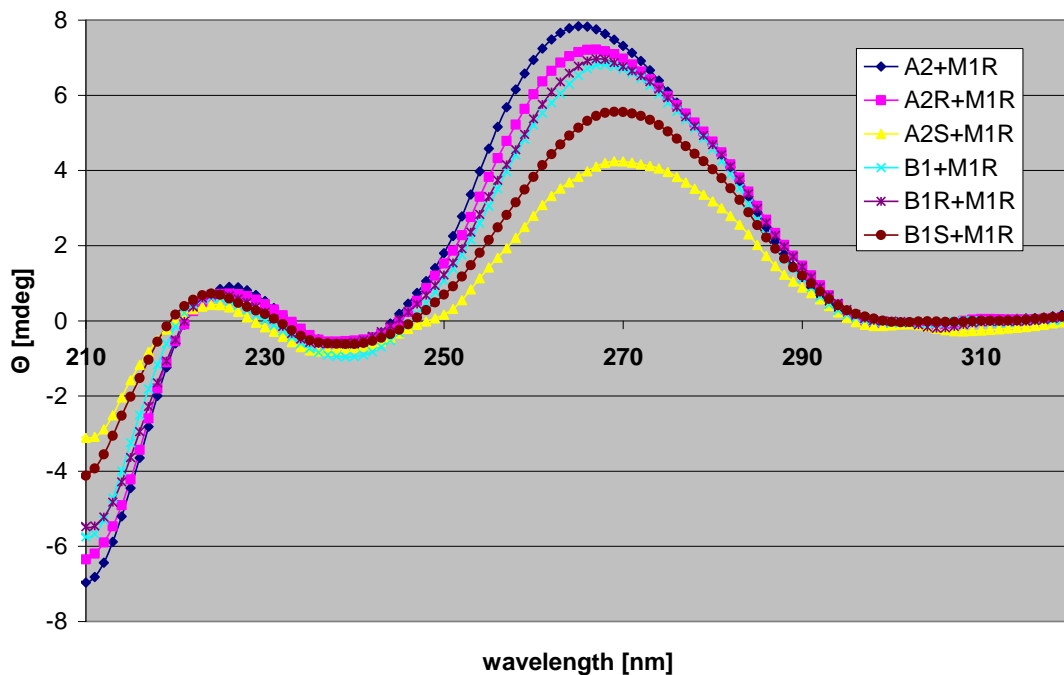


Figure S6. The CD spectra recorded for complexes of **A2**, **A2R** and **A2S** with **M1<sub>R</sub>** and for the reference duplexes.

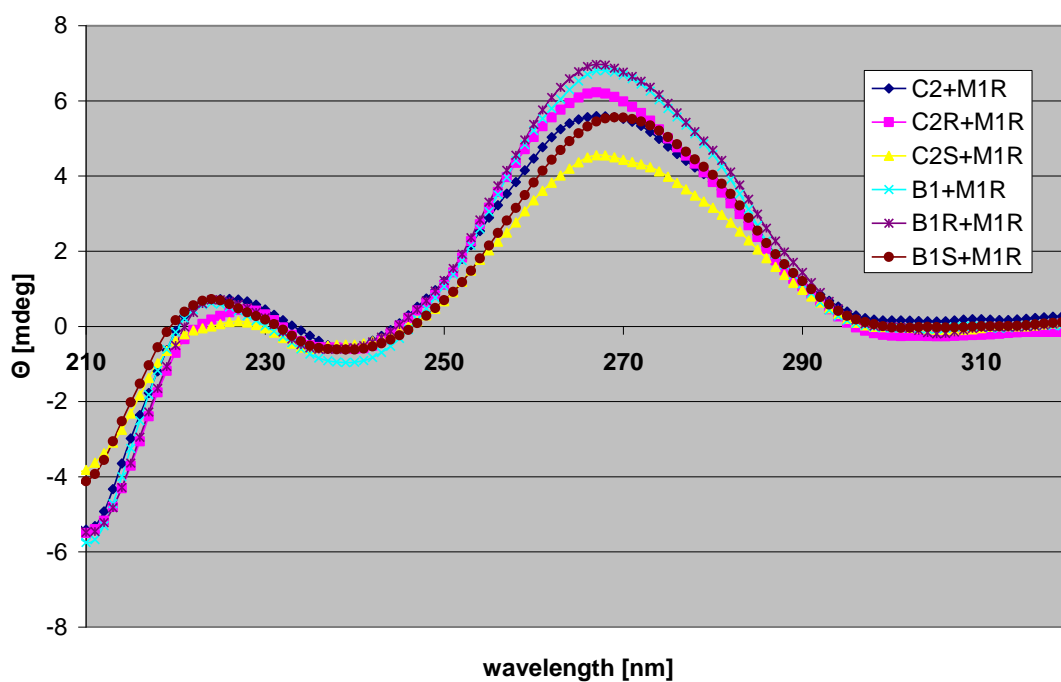


Figure S7. The CD spectra recorded for complexes of **C2**, **C2R** and **C2S** with **M1<sub>R</sub>** and for the reference duplexes.

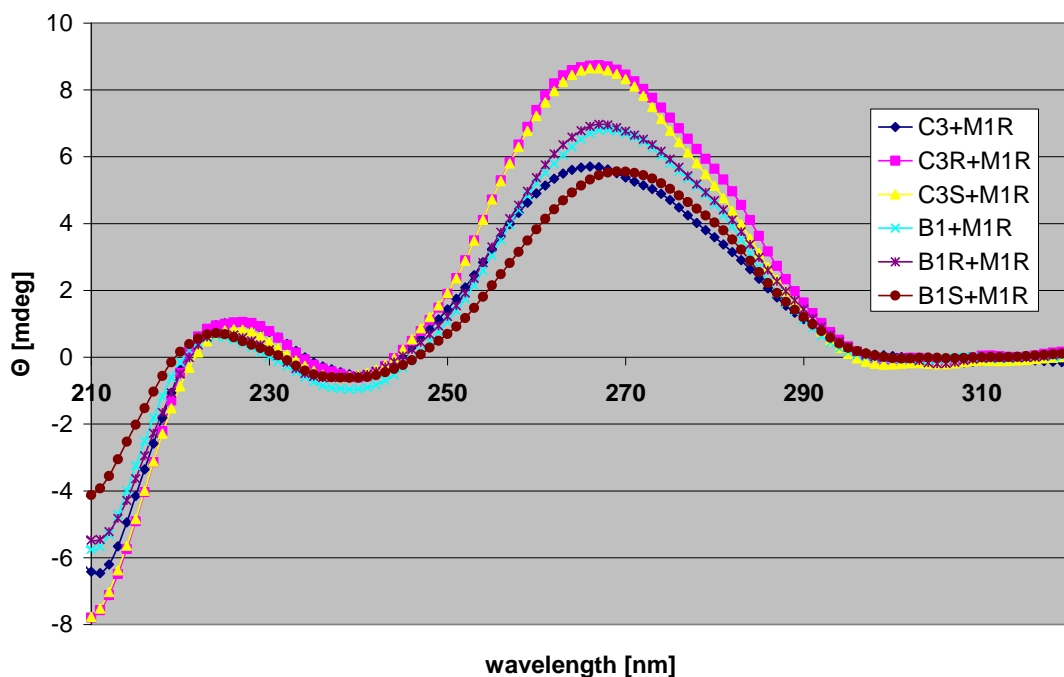


Figure S8. The CD spectra recorded for complexes of **C3**, **C3R** and **C3S** with **M1<sub>R</sub>** and for the reference duplexes.

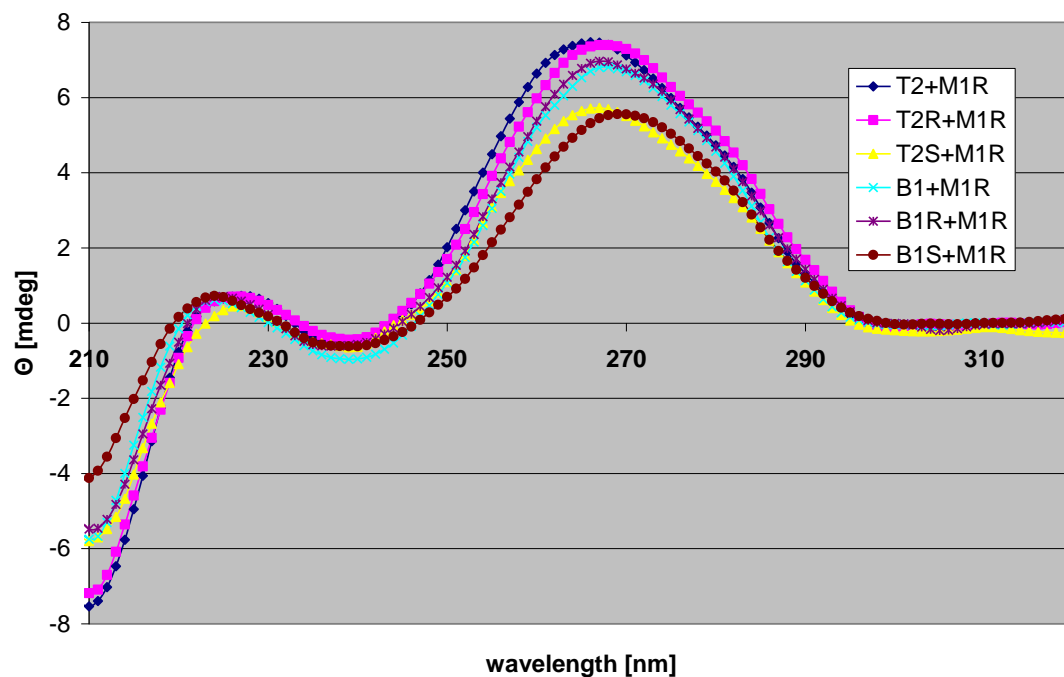


Figure S9. The CD spectra recorded for complexes of **T2**, **T2R** and **T2S** with **M1<sub>R</sub>** and for the reference duplexes.

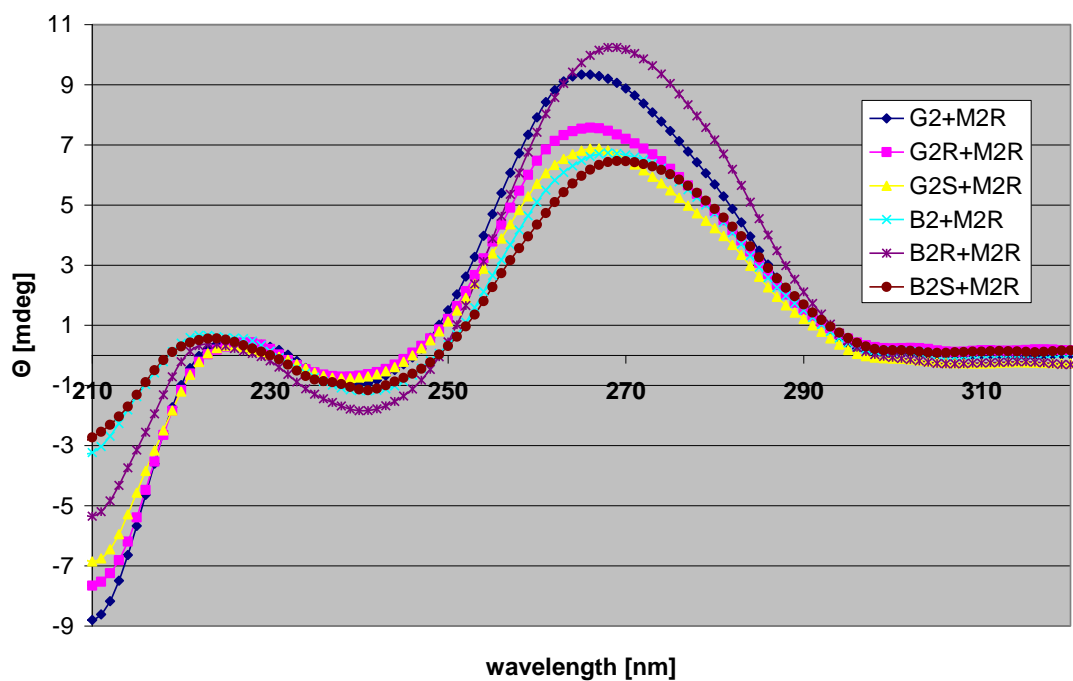


Figure S10. The CD spectra recorded for complexes of **G2**, **G2R** and **G2S** with **M2<sub>R</sub>** and for the reference duplexes.



## V. X-ray analysis of **3**.

Table S1. Crystal data for X-ray analysis of **3**.

Empirical formula	C <sub>18</sub> H <sub>25</sub> N <sub>2</sub> O <sub>7</sub> PS <sub>2</sub>
Formula weight	476.51
Temperature (K)	100
Wavelength (Å)	1.54184
Crystal system, space group	Orthorhombic, P2 <sub>1</sub> 2 <sub>1</sub> 2 <sub>1</sub>
Unit cell dimensions: a, b, c (Å)	6.3711 (1), 12.1422 (3), 27.2294 (7)
Volume (Å <sup>3</sup> )	2106.44 (8)
Z	4
Calculated density (Mg m <sup>-3</sup> )	1.502
Absorption coefficient (mm <sup>-1</sup> )	3.41
F(000)	1000
Crystal size (mm <sup>3</sup> )	0.10 × 0.05 × 0.02

Table S2. Parameters for data collection and refinement for X-ray analysis of **3**

Data collection	
Diffractometer	SuperNova single-crystal diffractometer (Agilent Technologies) with Cu K $\alpha$ radiation ( $\lambda = 1.5418 \text{ \AA}$ ).
No. of measured reflection	7619
No. of independent reflection	4177
No. of reflections with $I > 2\sigma(I)$	3851
R <sub>int</sub>	0.034
$(\sin \theta / \lambda)_{\max}$	0.626
Limiting indices	-7 $\leq h \leq$ 5, -14 $\leq k \leq$ 13, -34 $\leq l \leq$ 28
Theta range for data collection	4.0° $< \theta <$ 75.0°
Refinement	
Refinement method	Full-matrix least-squares on F <sup>2</sup>
Completeness to theta = 75.0°	0.979
Data / restraints / parameters	4177/0/273
Goodness-of-fit on F <sup>2</sup>	1.032
Final R indices [ $I > 2\sigma(I)$ ]	R1=0.031, wR2=0.073
R indices (all data)	R1=0.036, wR2=0.075
Absolute structure parameter	0.010 (15)
Largest diff. peak and hole (e Å <sup>-3</sup> )	0.268, -0.323

VI.  $^1\text{H}$  NMR spectra for separated OTP-LNA monomers, recorded with a Bruker AV-200 spectrometer (200 MHz)

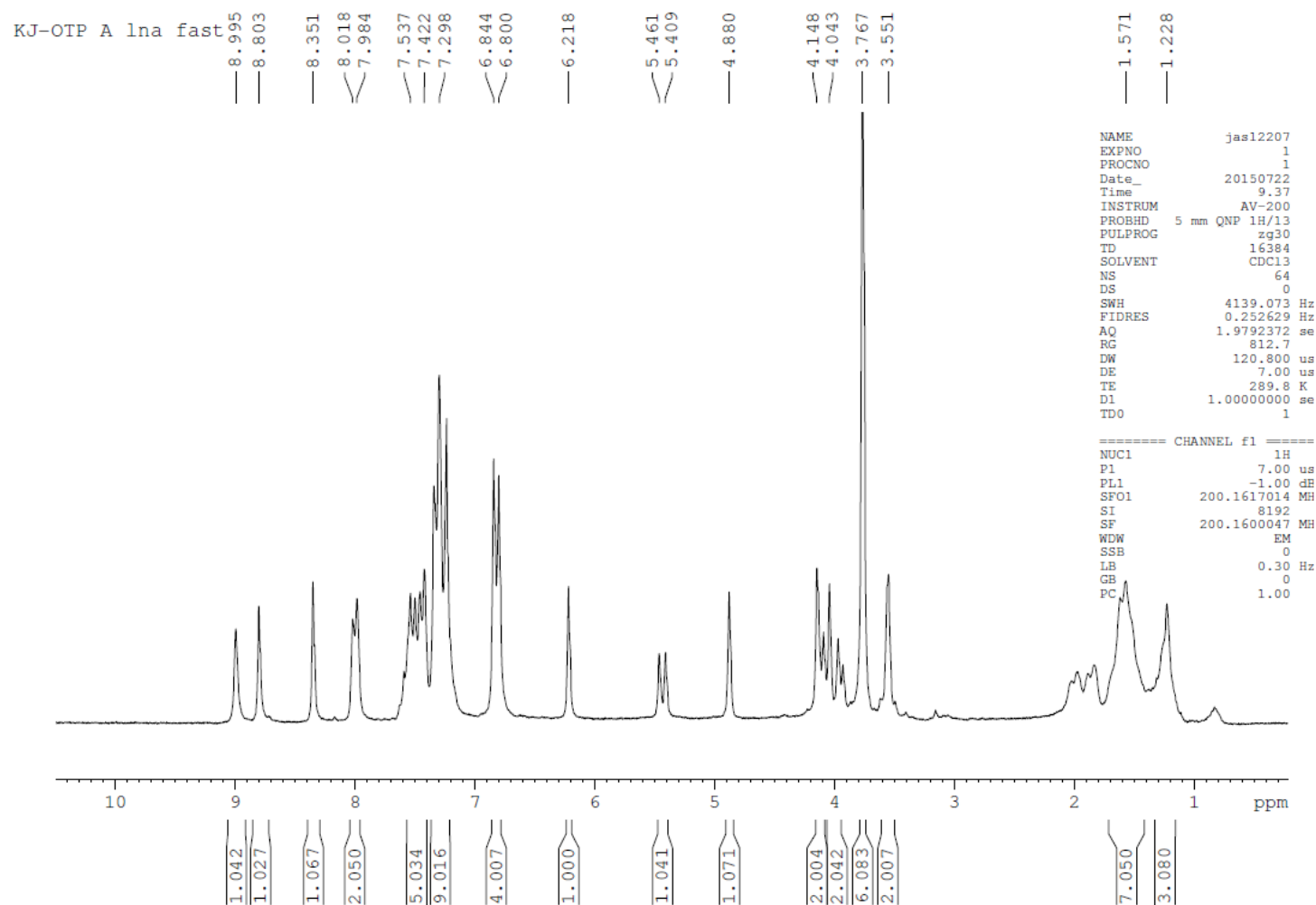


Figure S11.  $A_L$ -OTP *fast* (**2b**);  $\delta$  (ppm,  $\text{CDCl}_3$ ) 9.00 (1H, NHCO), 8.80 (1H, C8-H), 8.36 (1H, C2-H), 7.54-6.80 (18H, DMT, Bz), 6.22 (1H, C1'-H), 5.46-5.41 (1H, C3'-H), 4.88 (1H, C2'-H), 4.15-4.04 (2H, P-O- $\text{CH}_2$ C-S; 2H, O2'- $\text{CH}_2$ -C4'), 3.77 (6H, 2xOCH<sub>3</sub>), 3.55 (2H, 5' $\text{CH}_2$ ), 1.57-1.23 (10H, - $(\text{CH}_2)_5$ - „*spiro*”)

KJ-OTP A lna slow

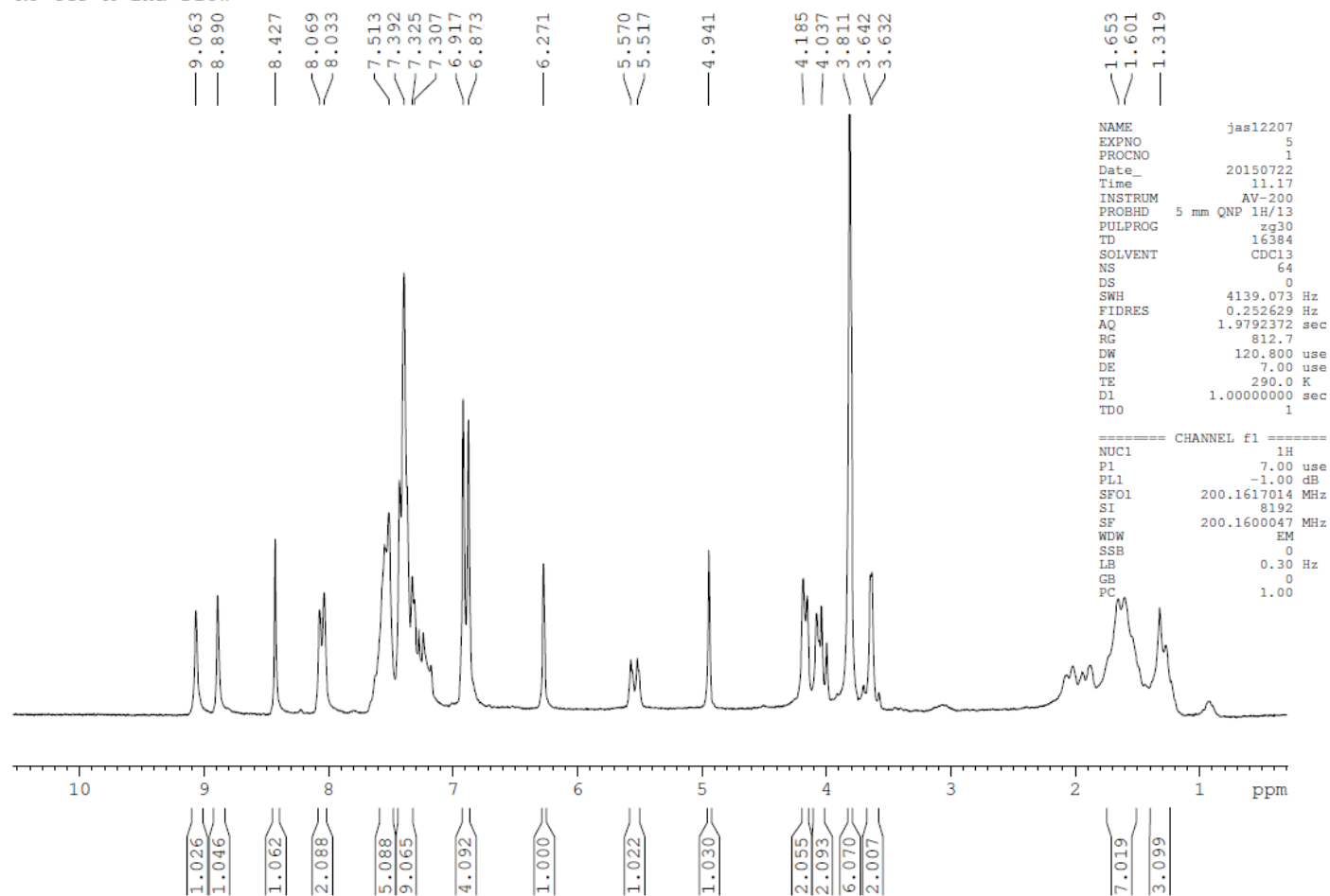


Figure S12.  $A_L$ -OTP *slow* (**2b**);  $\delta$  (ppm,  $CDCl_3$ ) 9.06 (1H, NHCO), 8.89 (1H, C8-H), 8.43 (1H, C2-H), 7.51-6.87 (18H, DMT, Bz), 6.27 (1H, C1'-H), 5.57-5.52 (1H, C3'-H), 4.94 (1H, C2'-H), 4.19-4.00 (2H, P-O-CH<sub>2</sub>C-S; 2H, O2'-CH<sub>2</sub>-C4'), 3.81 (6H, 2xOCH<sub>3</sub>), 3.64 (2H, 5'CH<sub>2</sub>), 1.65-1.32 (10H, -(CH<sub>2</sub>)<sub>5</sub>- „*spiro*”)

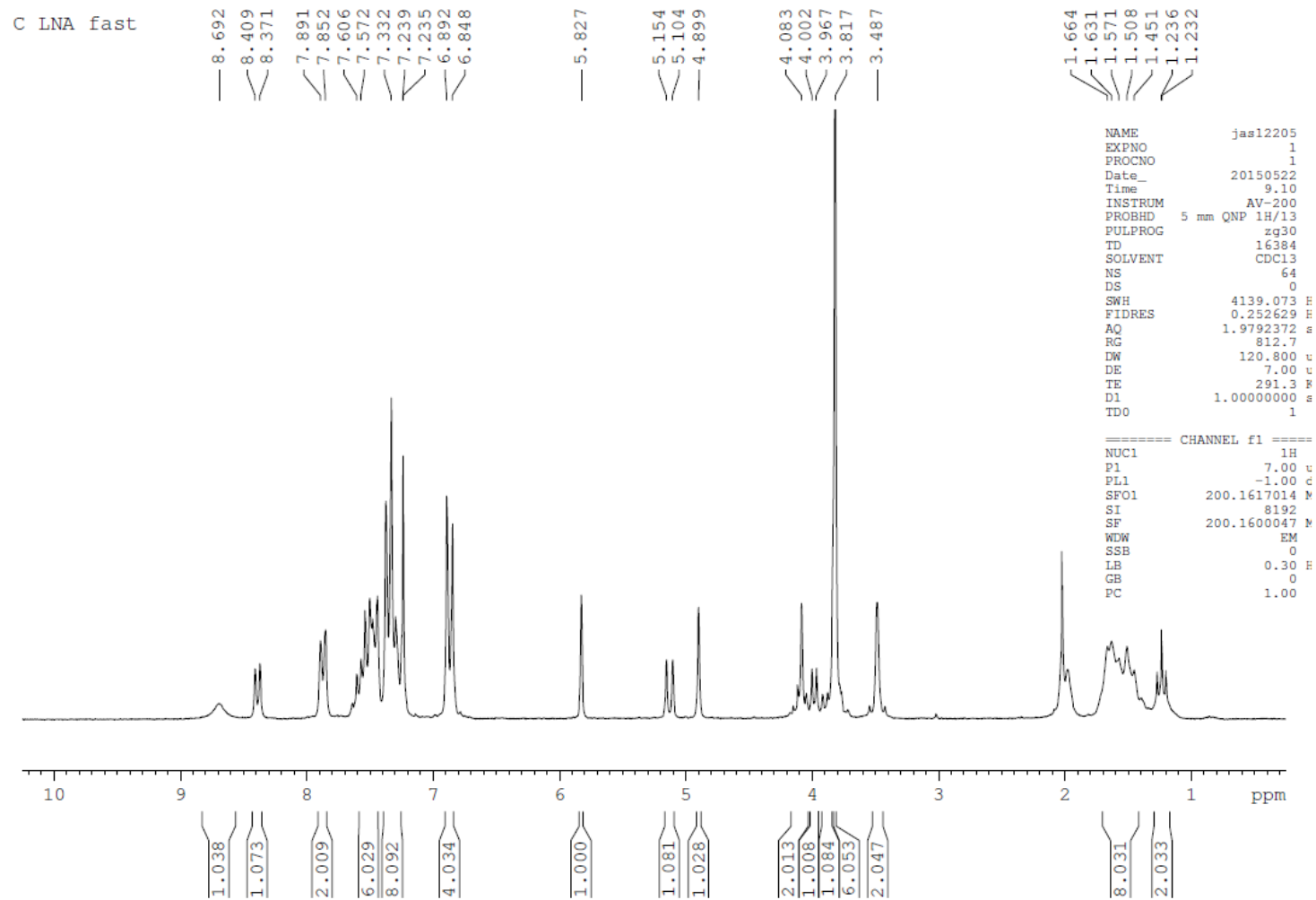


Figure S13.  $C_L$ -OTP *fast* (**2c**);  $\delta$  (ppm,  $CDCl_3$ ) 8.69 (1H, NHCO), 7.89-7.85 (2H, C6-H, C5-H), 7.60-6.85 (18H, DMT, Bz), 5.83 (1H, C1'-H), 5.15-5.10 (1H, C3'-H), 4.90 (1H, C2'-H), 4.08-3.97 (2H, P-O-CH<sub>2</sub>C-S; 2H, O<sub>2</sub>'-CH<sub>2</sub>-C4'), 3.82 (6H, 2xOCH<sub>3</sub>), 3.49 (2H, 5'CH<sub>2</sub>), 1.66-1.23 (10H, -(CH<sub>2</sub>)<sub>5</sub>- „*spiro*”)

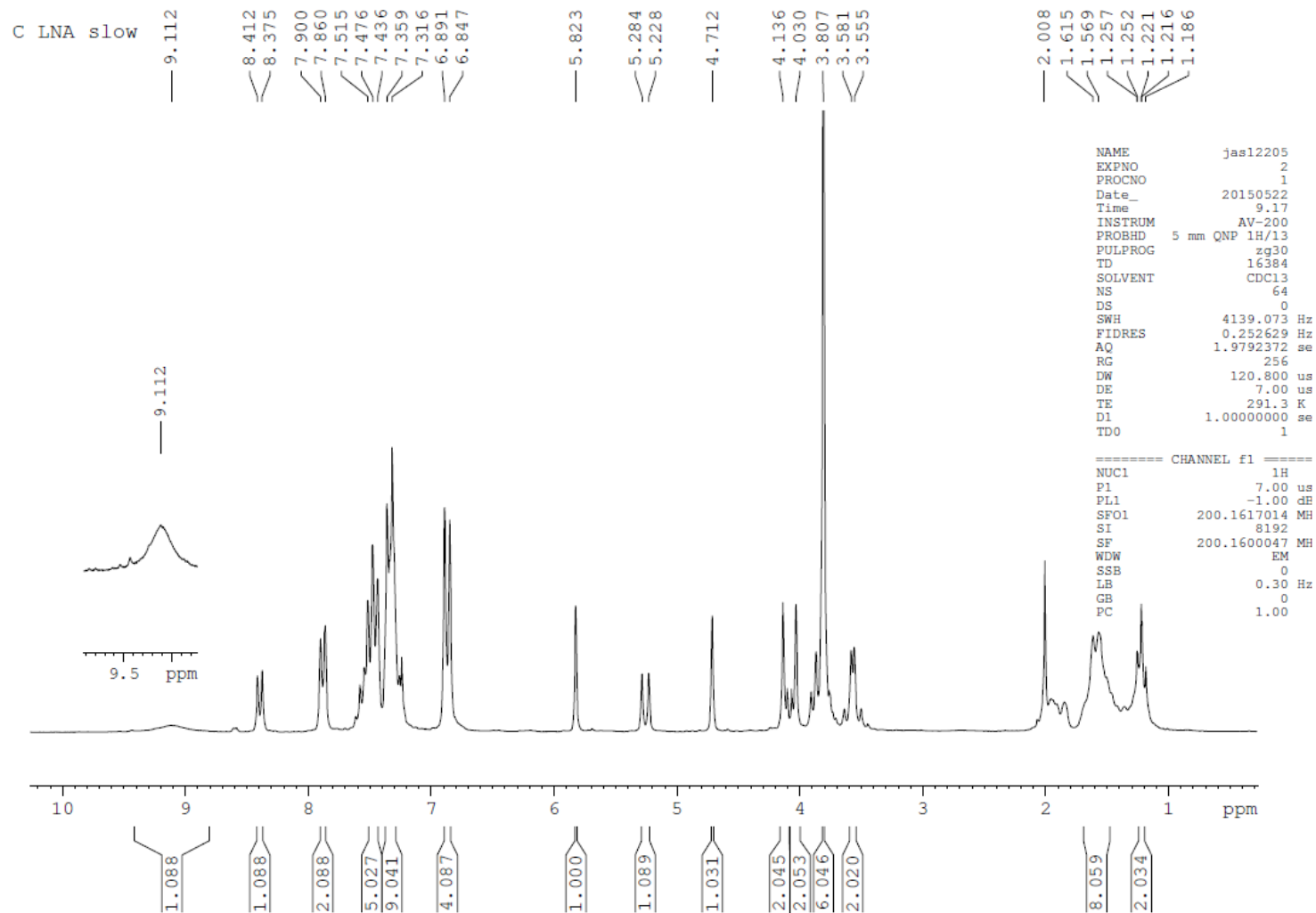


Figure S14.  $C_L$ -OTP *slow* (**2c**);  $\delta$  (ppm,  $CDCl_3$ ) 9.11 (1H, NHCO), 7.90-7.86 (2H, C6-H, C5-H), 7.52-6.85 (18H, DMT, Bz), 5.82 (1H, C1'-H), 5.28-5.23 (1H, C3'-H), 4.71 (1H, C2'-H), 4.14-3.90 (2H, P-O-CH<sub>2</sub>C-S; 2H, O2'-CH<sub>2</sub>-C4'), 3.81 (6H, 2xOCH<sub>3</sub>), 3.58 (2H, 5'CH<sub>2</sub>), 1.62-1.19 (10H, -(CH<sub>2</sub>)<sub>5</sub>-„spiro”)

OTP G lna fast

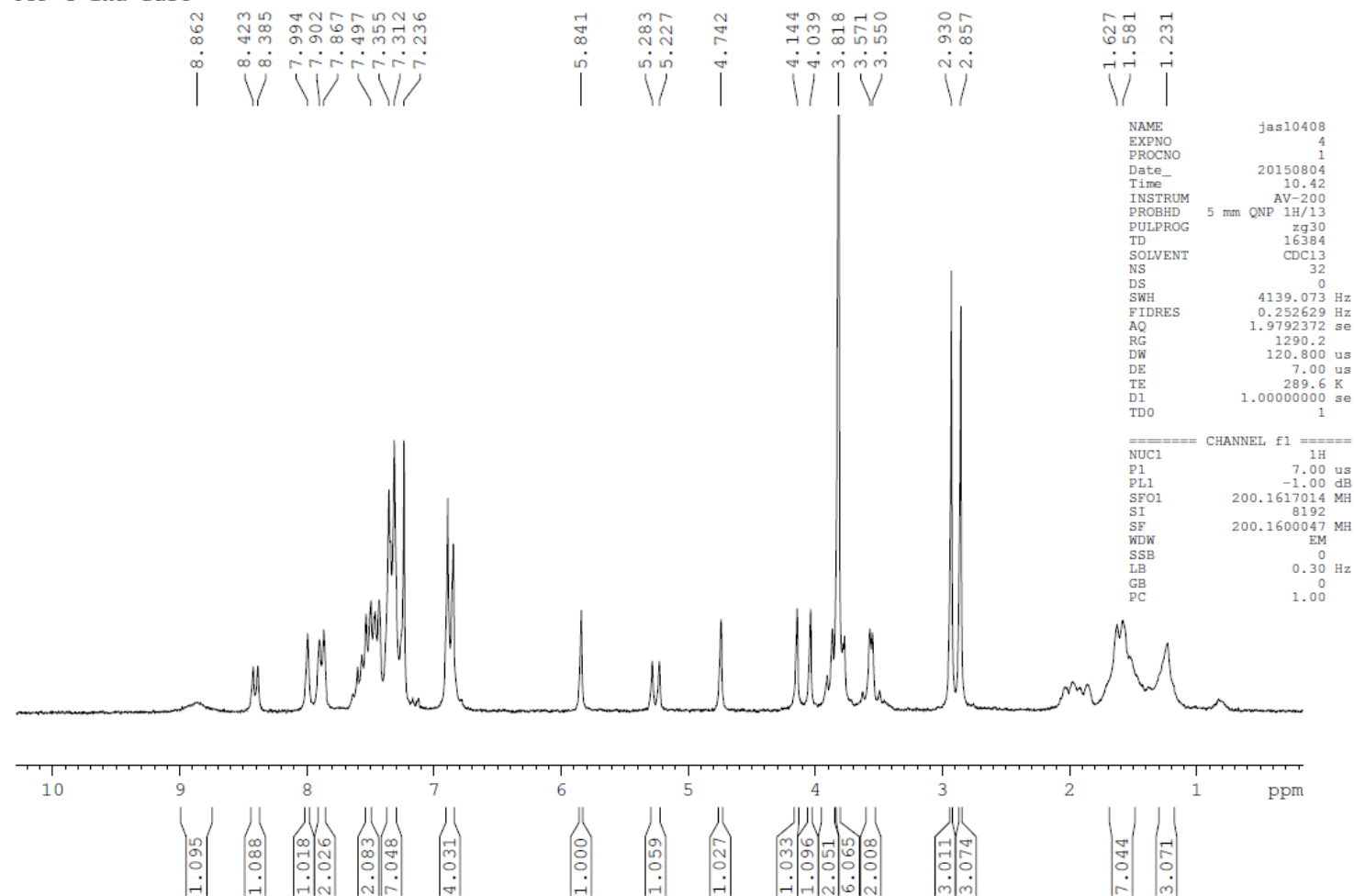


Figure S15.  $G_L$ -OTP *fast* (**2d**);  $\delta$  (ppm,  $CDCl_3$ ) 8.86 (1H, N1-H), 8.40 (1H, N=CH, dmf), 7.90 (1H, C8-H), 7.50-7.24 (13H, DMT), 5.84 (1H, C1'-H), 5.28-5.23 (1H, C3'-H), 4.74 (1H, C2'-H), 4.14-3.80 (2H, P-O-CH<sub>2</sub>C-S; 2H, O2'-CH<sub>2</sub>-C4'), 3.82 (6H, 2xOCH<sub>3</sub>), 3.57-3.55 (2H, C5'CH<sub>2</sub>), 2.93-2.86 (6H, 2xNCH<sub>3</sub>, dmf), 1.63-1.23 (10H, -(CH<sub>2</sub>)<sub>5</sub>- „*spiro*”)

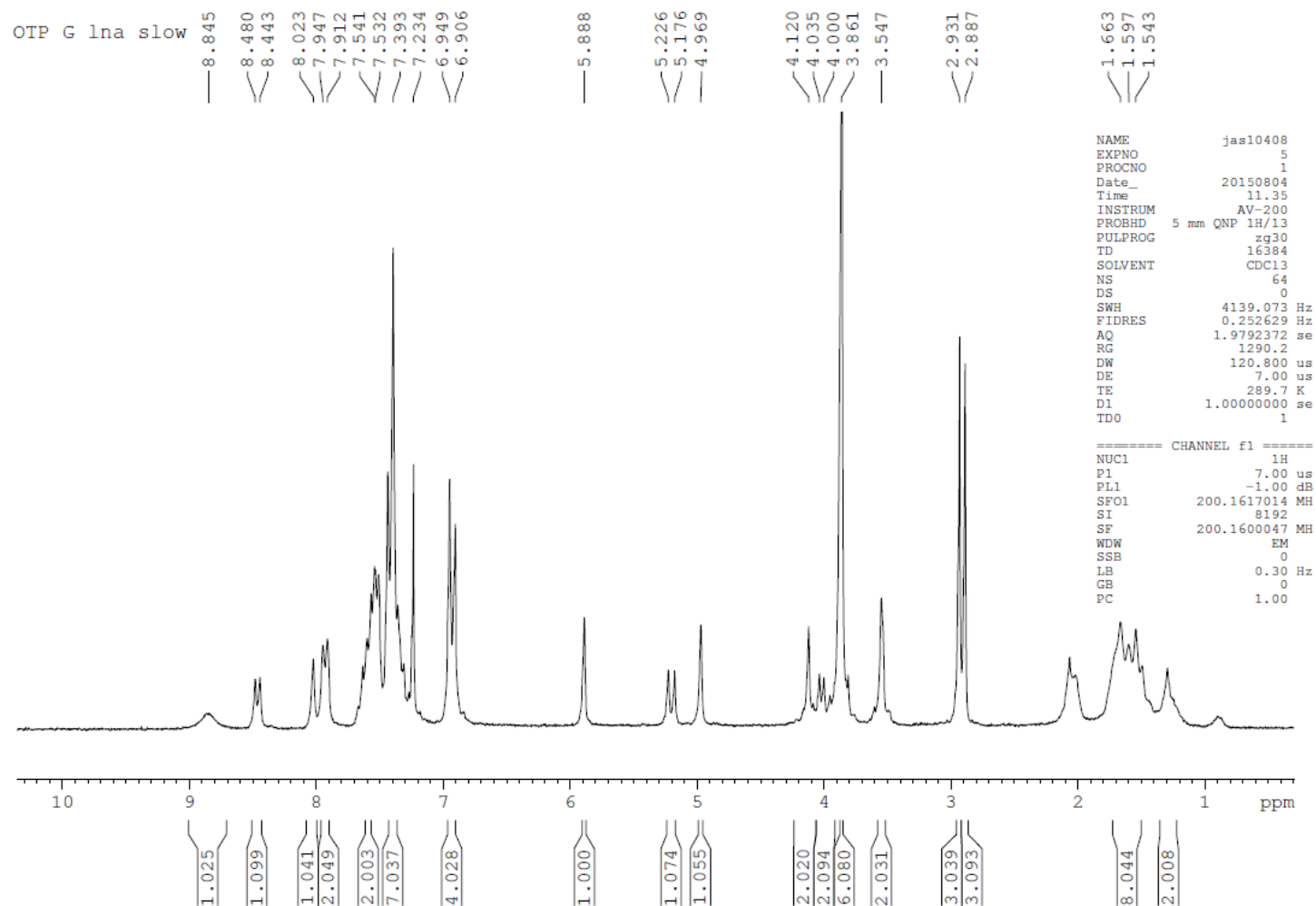


Figure S16.  $G_L$ -OTP *slow* (**2d**);  $\delta$  (ppm,  $CDCl_3$ ) 8.85 (1H, N1-H), 8.45 (1H, N=CH, dmf), 8.02 (1H, C8-H), 7.54-6.91 (13H, DMT), 5.89 (1H, C1'-H), 5.23-5.18 (1H, C3'-H), 4.97 (1H, C2'-H), 4.12-4.00 (2H, P-O-CH<sub>2</sub>C-S; 2H, O2'-CH<sub>2</sub>-C4'), 3.86 (6H, 2xOCH<sub>3</sub>), 3.55 (2H, 5'CH<sub>2</sub>), 2.93-2.89 (6H, 2xNCH<sub>3</sub>, dmf), 1.66-1.54 (10H, -(CH<sub>2</sub>)<sub>5</sub>- „*spiro*”)

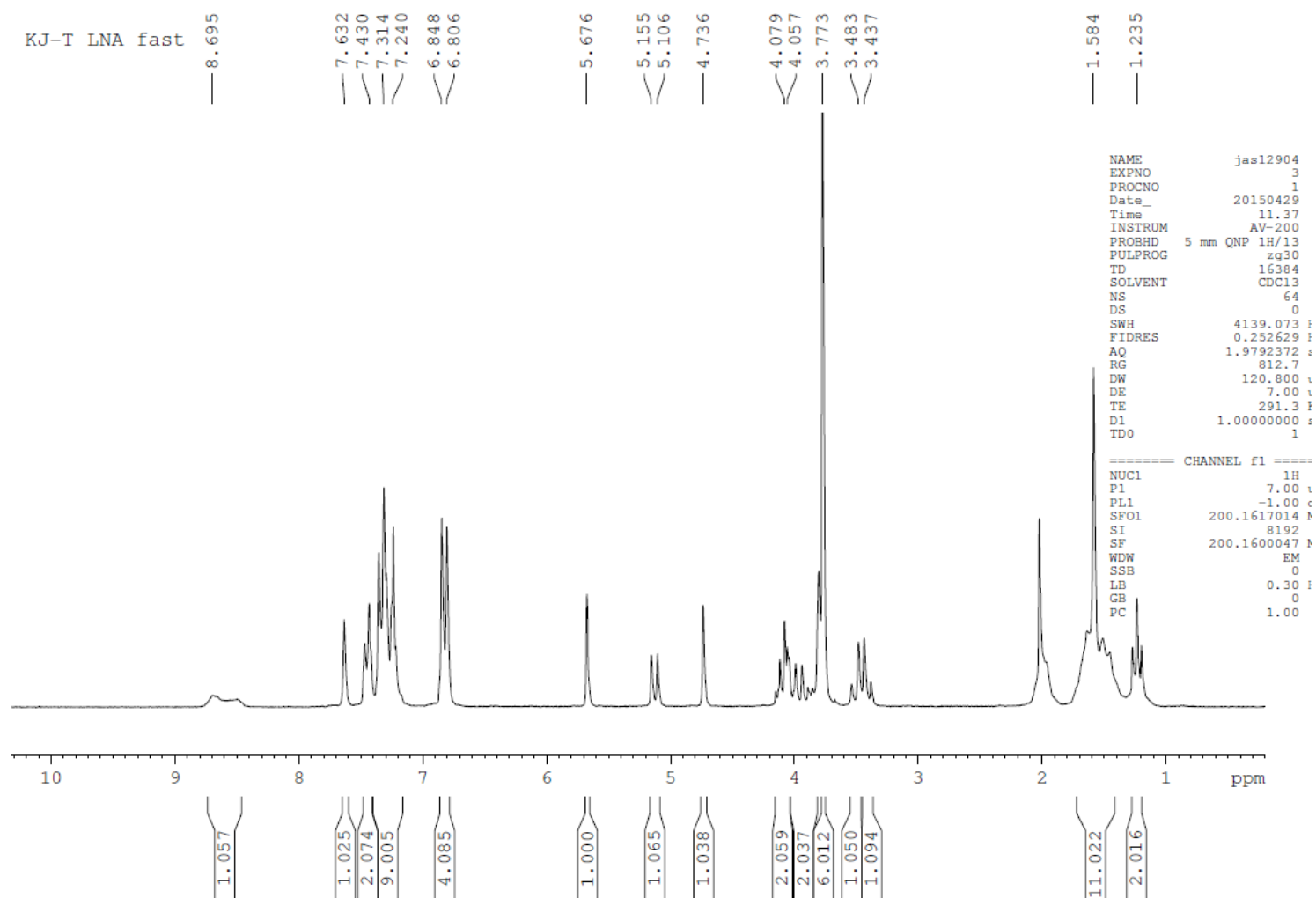


Figure S17.  $T_L$ -OTP *fast* (**2a**);  $\delta$  (ppm,  $CDCl_3$ ) 8.70 (1H, N3-H), 7.63 (1H, C6-H), 7.31-6.81 (13H, DMT), 5.68 (1H, C1'-H), 5.15-5.11 (1H, C3'-H), 4.74 (1H, C2'-H), 4.11-3.90 (2H, P-O-CH<sub>2</sub>C-S; 2H, O2'-CH<sub>2</sub>-C4'), 3.77 (6H, 2xOCH<sub>3</sub>), 3.48-3.44 (2H, 5'CH<sub>2</sub>), 1.58-1.23 (3H, C5-CH<sub>3</sub>; 10H, -(CH<sub>2</sub>)<sub>5</sub>- „*spiro*”)



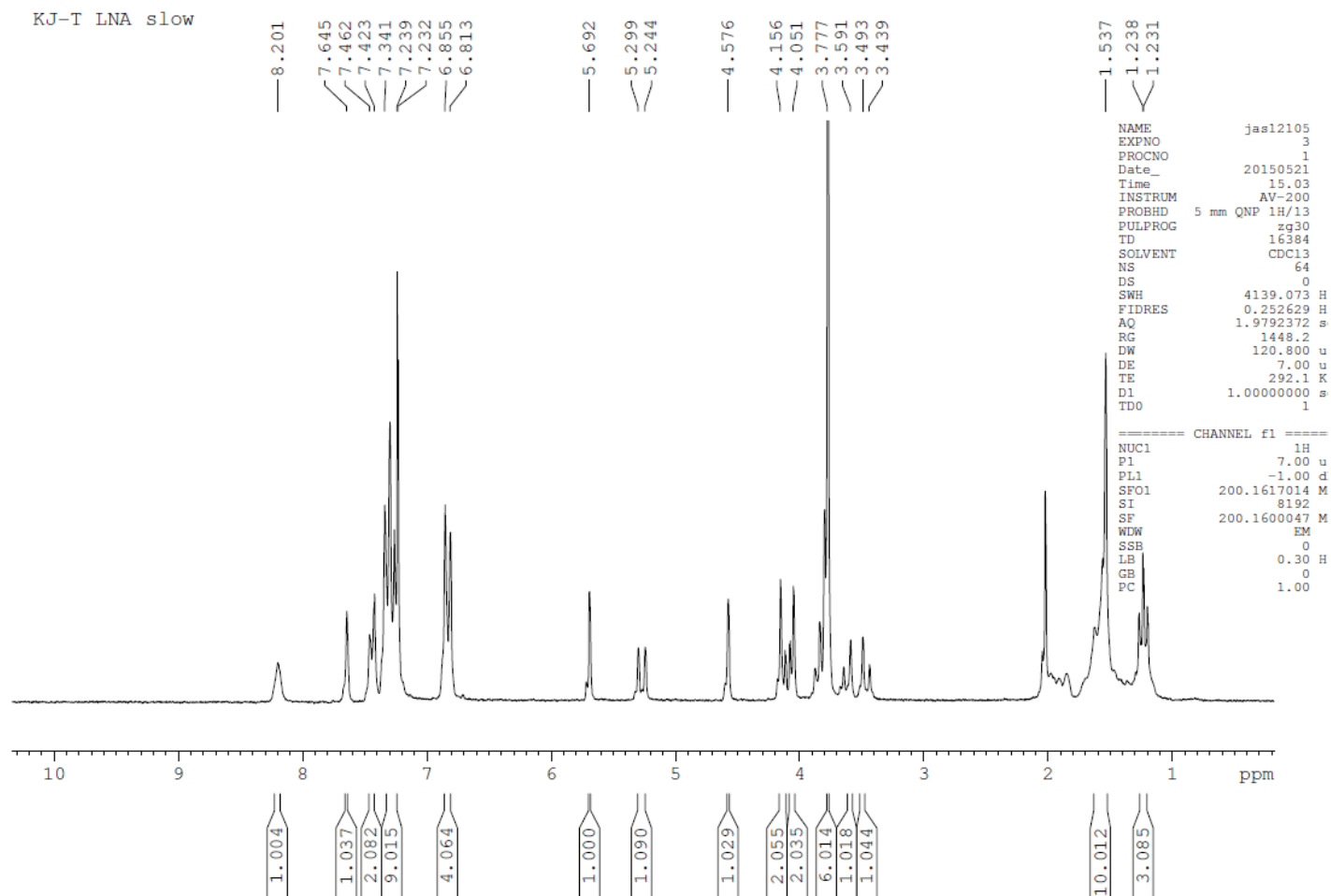


Figure S18.  $T_L$ -OTP *slow* (**2a**);  $\delta$  (ppm,  $CDCl_3$ ) 8.20 (1H, N3-H), 7.65 (1H, C6-H), 7.42-6.81 (13H, DMT), 5.69 (1H, C1'-H), 5.30-5.24 (1H, C3'-H), 4.58 (1H, C2'-H), 4.16-4.05 (2H, P-O-CH<sub>2</sub>C-S; 2H, O2'-CH<sub>2</sub>-C4'), 3.78 (6H, 2xOCH<sub>3</sub>), 3.60-3.44 (2H, 5'CH<sub>2</sub>), 1.54-1.23 (3H, C5-CH<sub>3</sub>; 10H, -(CH<sub>2</sub>)<sub>5</sub>-,,*spiro*")

VII.  $^{31}\text{P}$  NMR spectra for separated OTP-LNA monomers, recorded with a Bruker AV-200 spectrometer (200 MHz for  $^1\text{H}$ )

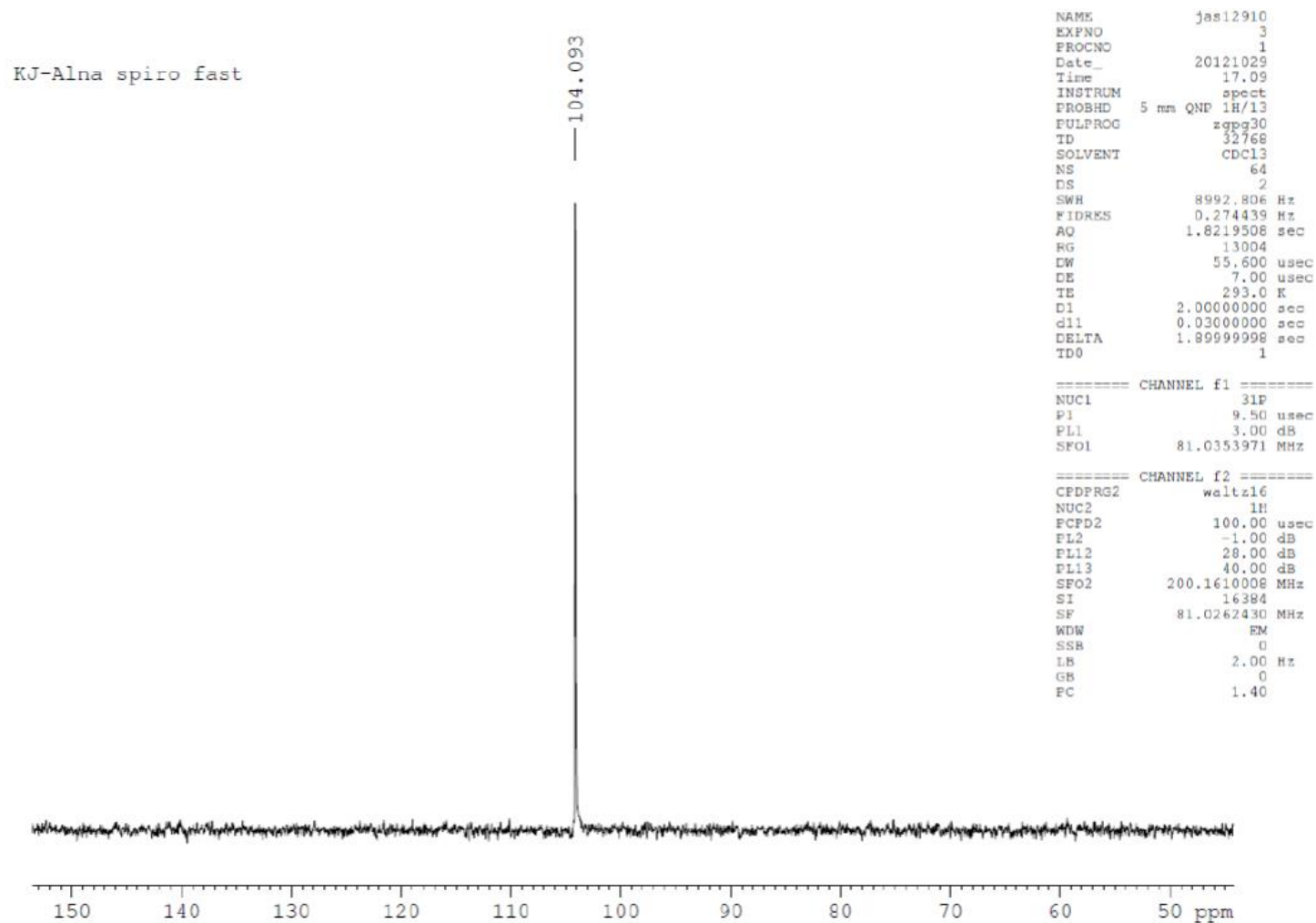


Figure S19.  $A_L$ -OTP *fast* (**2b**);  $\delta$  (ppm,  $\text{CDCl}_3$ )

KJ-Alna spiro slow

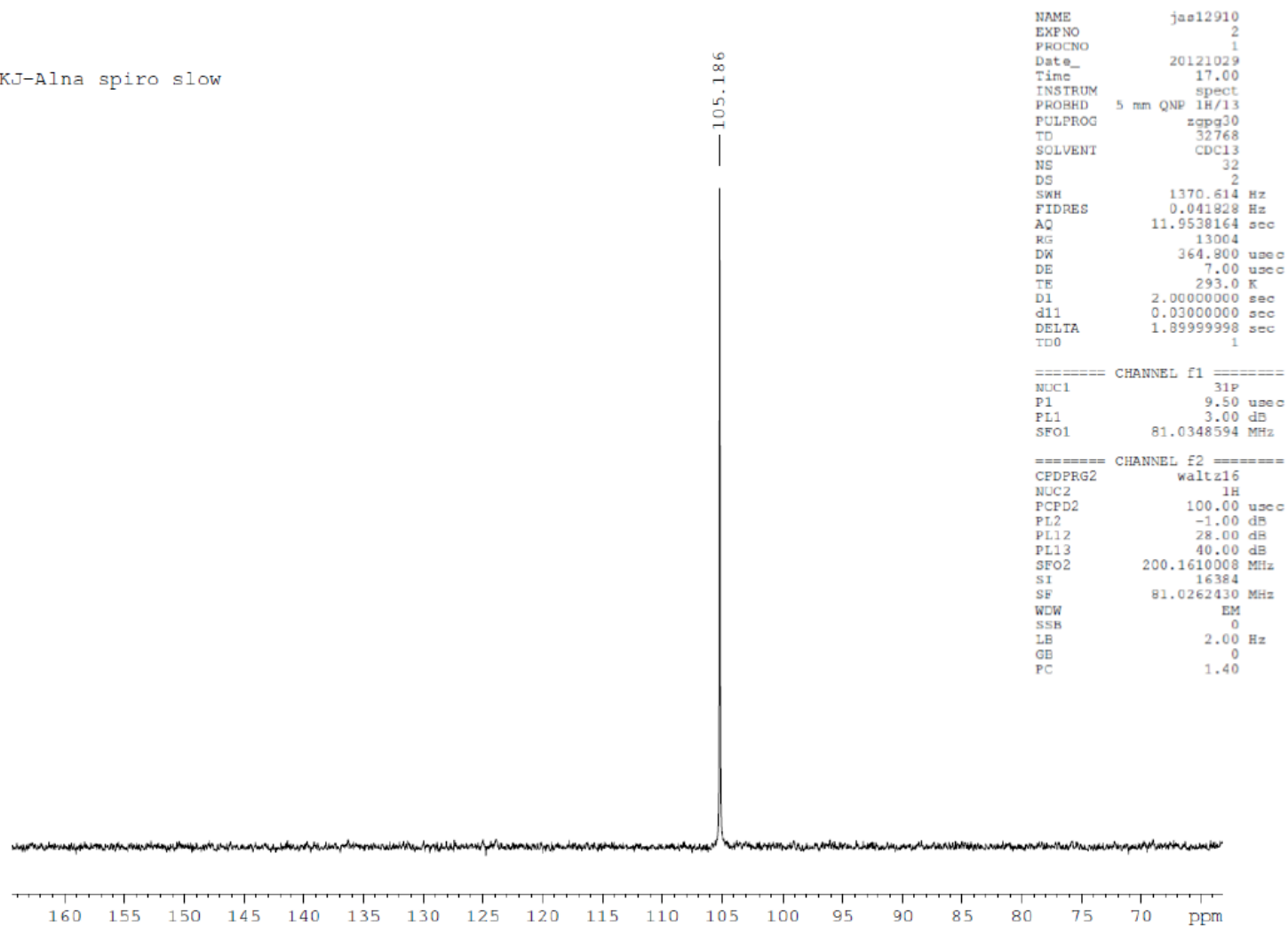


Figure S20. A<sub>L</sub>-OTP *slow* (**2b**);  $\delta$  (ppm, CDCl<sub>3</sub>)

KJ-Clna fast

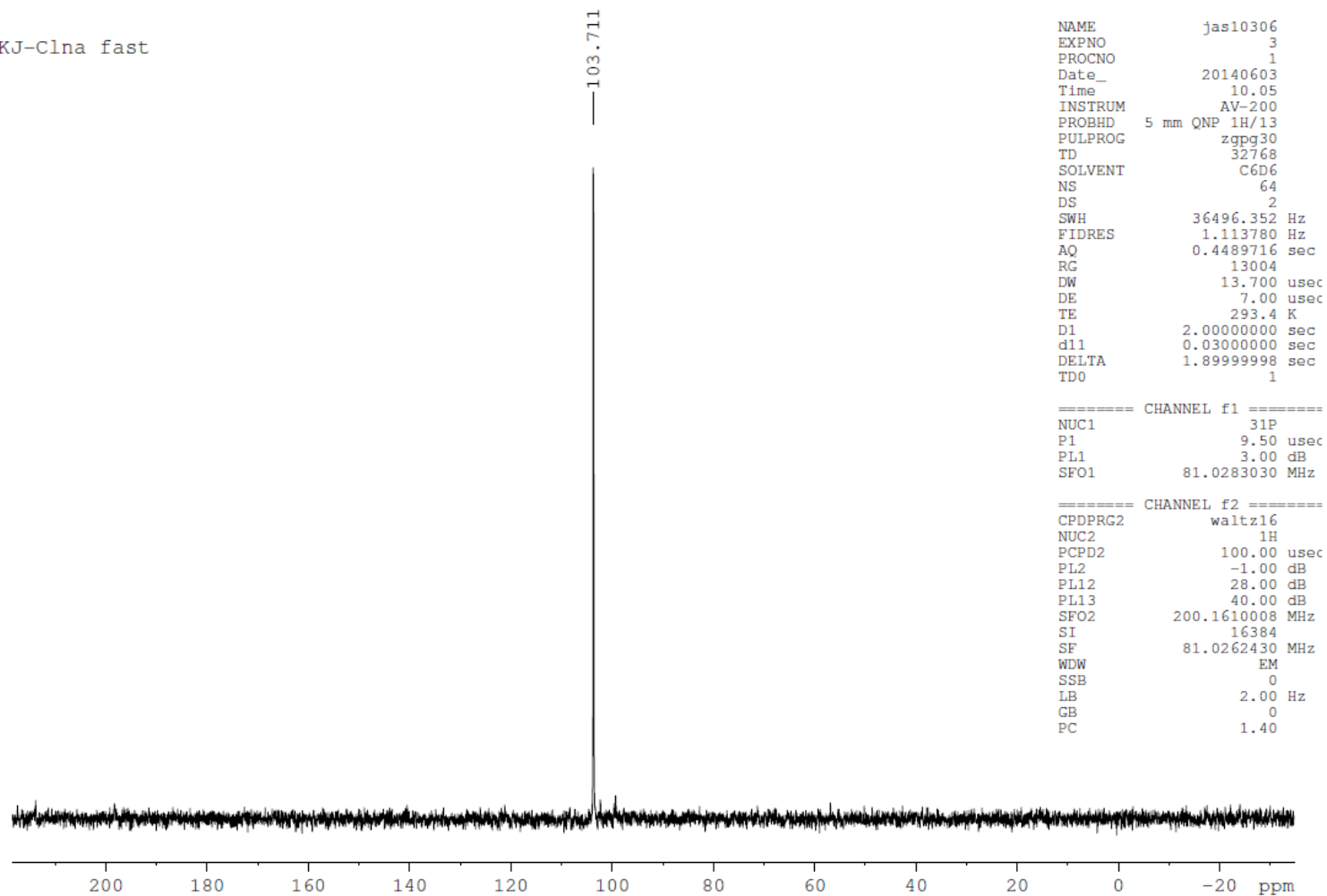


Figure S21.  $C_L$ -OTP *fast* (**2c**);  $\delta$  (ppm,  $C_6D_6$ )

KJ-Clna slow

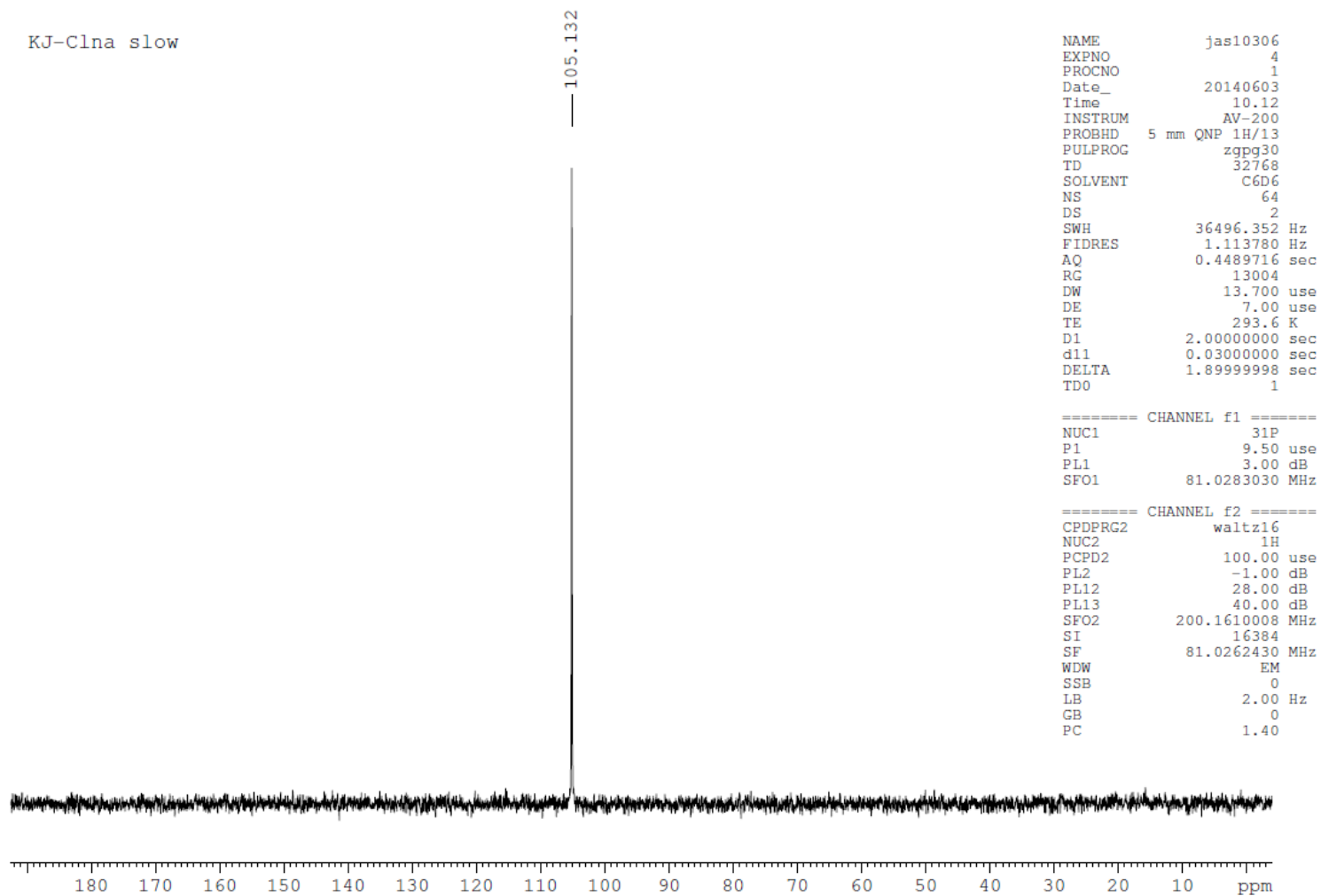


Figure S22.  $C_L$ -OTP *slow* (**2c**);  $\delta$  (ppm,  $C_6D_6$ )

kj-GL fast

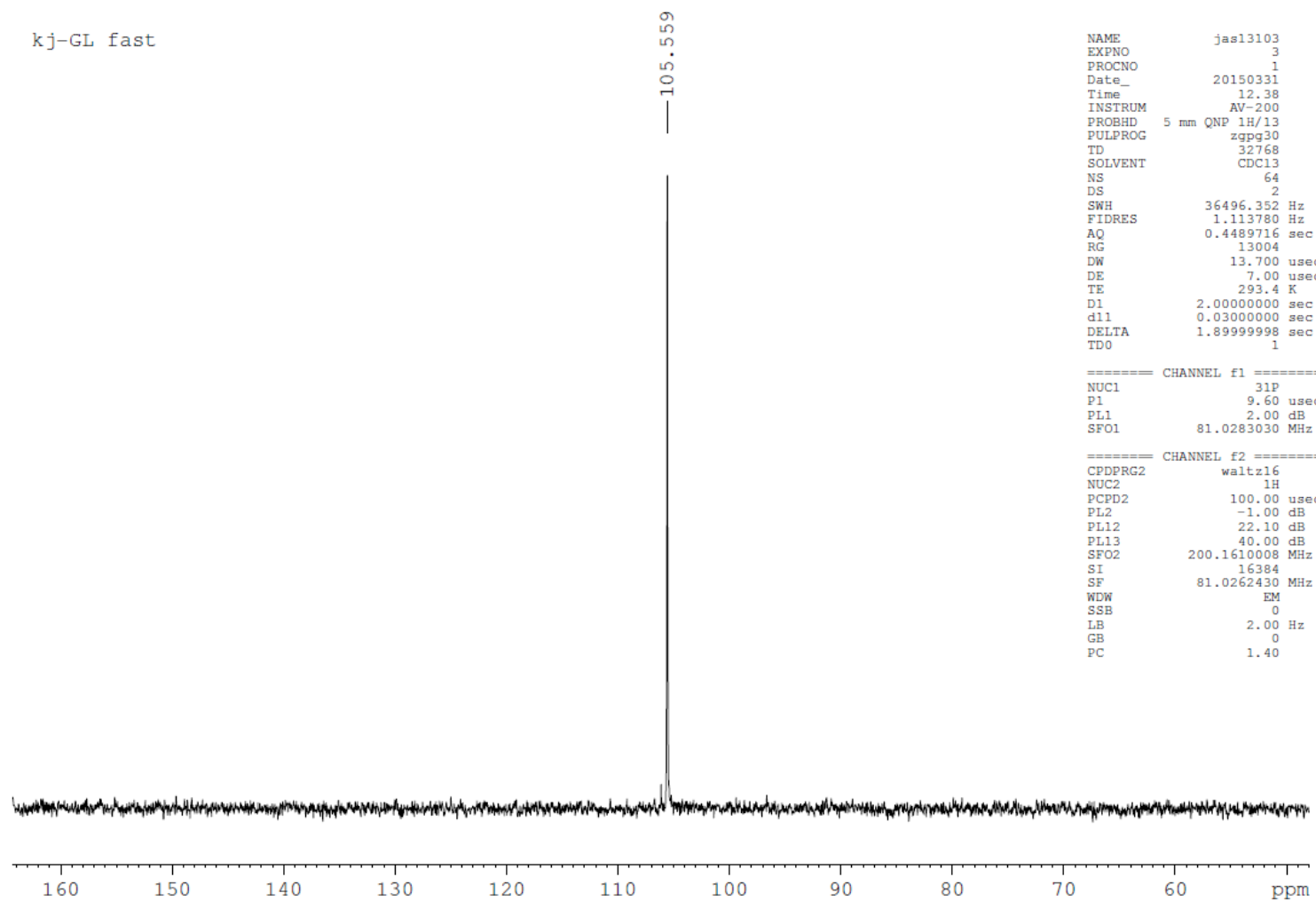


Figure S23.  $G_L$ -OTP *fast* (**2d**);  $\delta$  (ppm,  $CDCl_3$ )

kj-GL slow

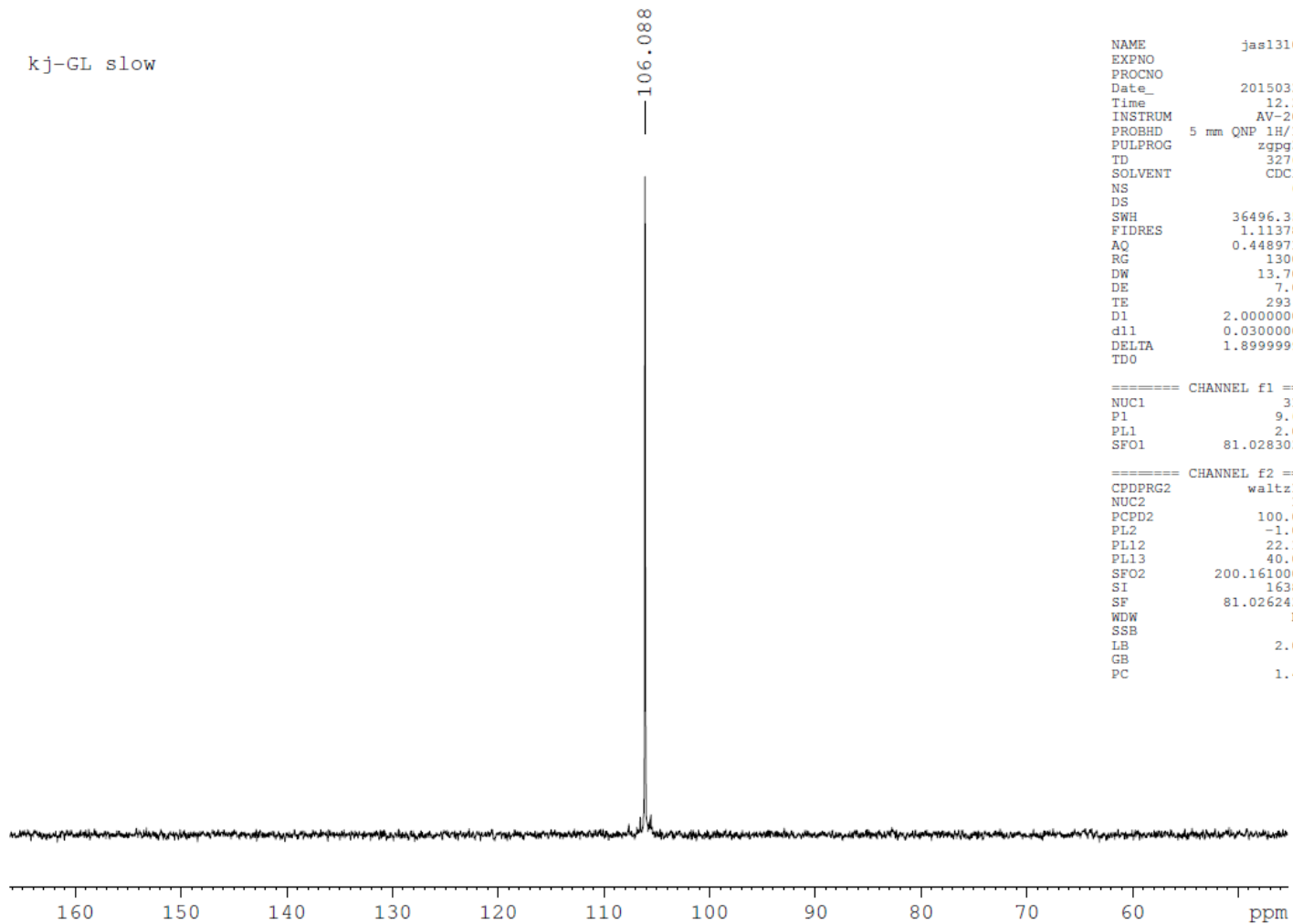


Figure S24. G<sub>L</sub>-OTP *slow* (**2d**);  $\delta$  (ppm, CDCl<sub>3</sub>)

KJ-Tl<sub>L</sub>a fast

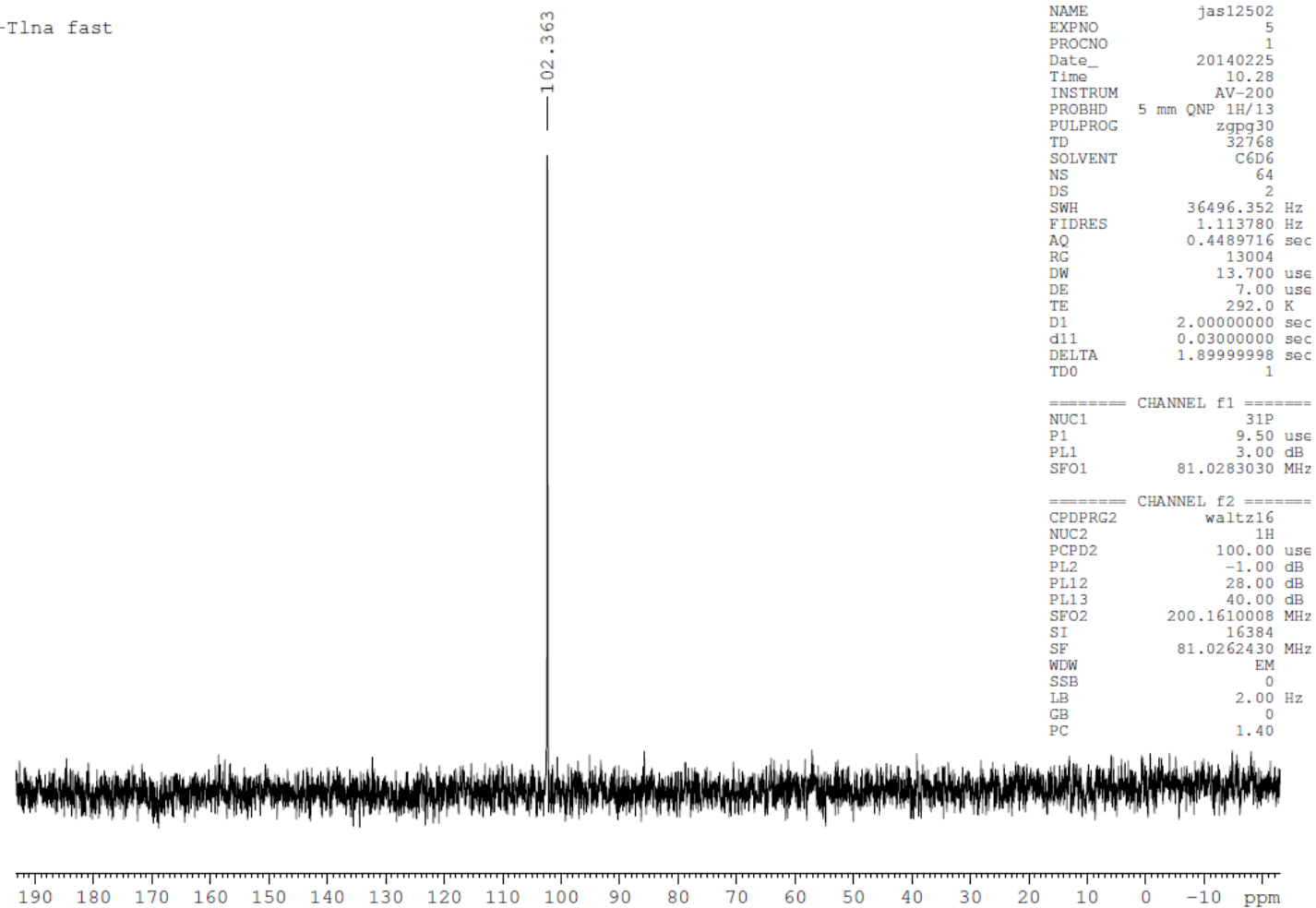


Figure S25. T<sub>L</sub>-OTP *fast* (**2a**);  $\delta$  (ppm, C<sub>6</sub>D<sub>6</sub>)



KJ-Tl1a slow

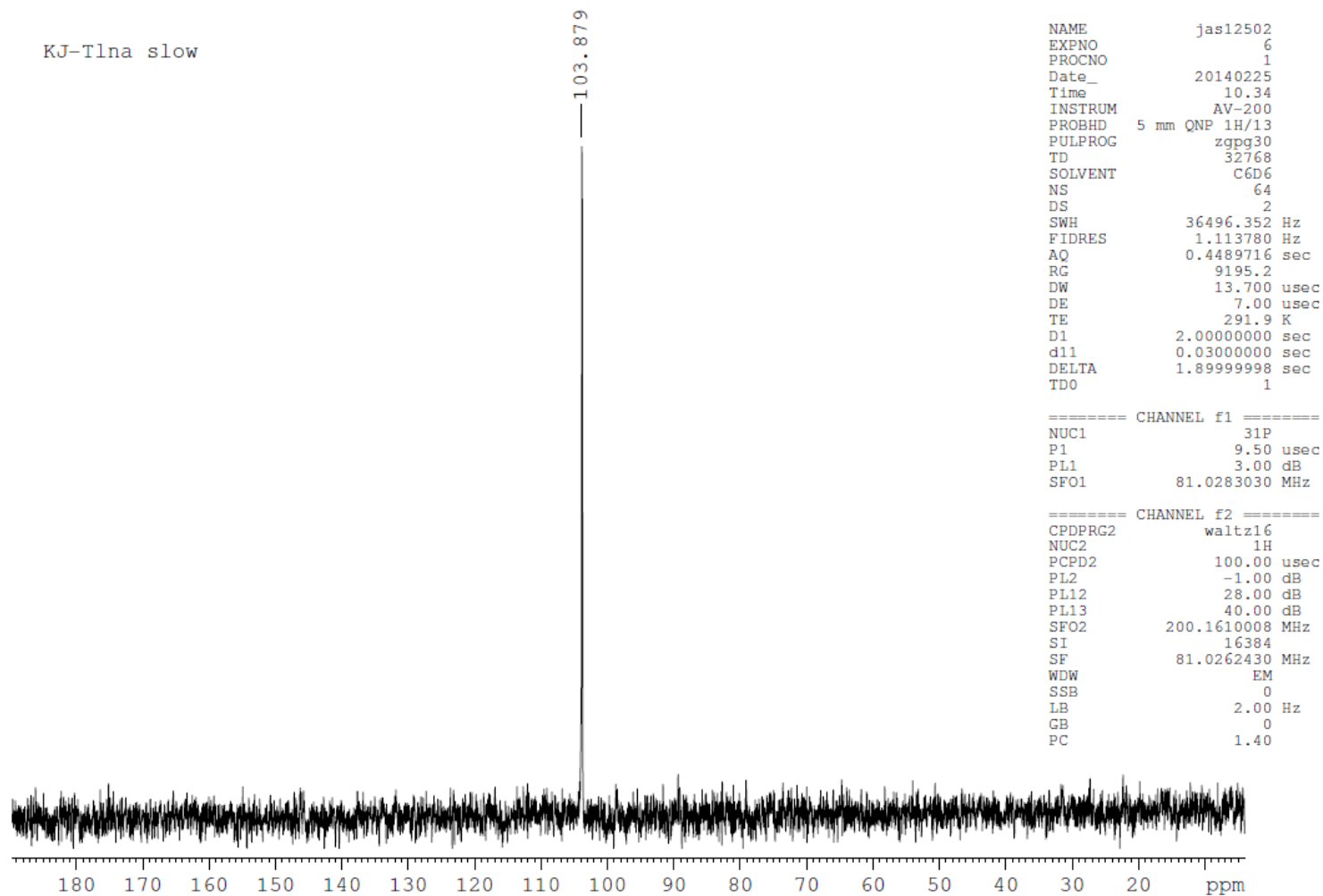


Figure S26. T<sub>L</sub>-OTP *slow* (**2a**);  $\delta$  (ppm, C<sub>6</sub>D<sub>6</sub>)

VII.  $^{13}\text{C}$  NMR spectra for separated OTP-LNA monomers, recorded with a Bruker AV-200 spectrometer (200 MHz for  $^1\text{H}$ )

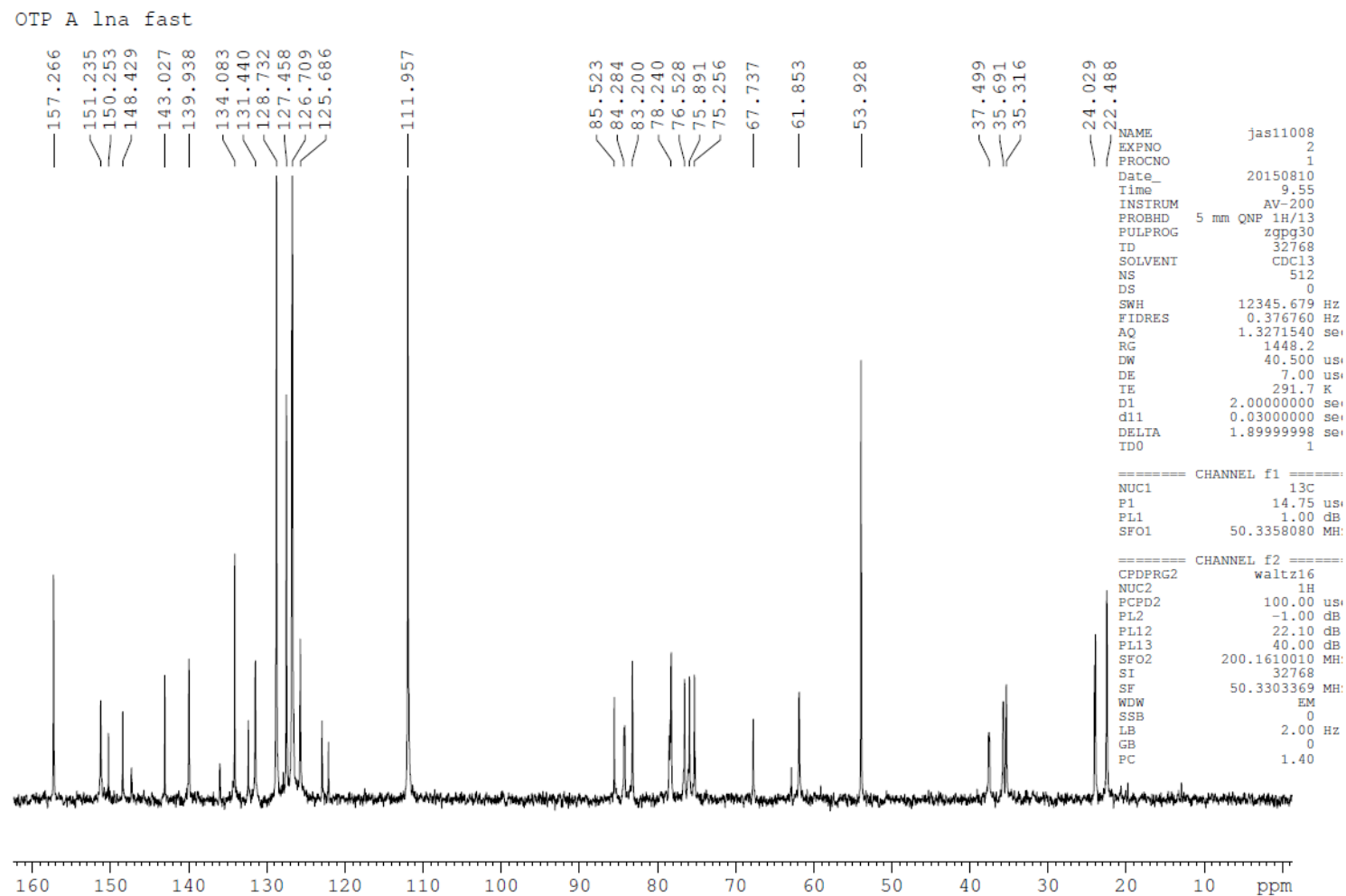


Figure S27.  $A_L$ -OTP *fast* (**2b**);  $\delta$  (ppm,  $\text{CDCl}_3$ ) 157.3, 151.2, 150.2, 148.4, 143.0, 139.9, 134.1, 131.4, 128.7, 127.5, 126.7, 125.7, 112.0, 85.5, 84.3, 83.2, 78.2, 76.5, 75.9, 75.3, 67.7, 61.9, 53.9, 37.5, 35.7, 35.3, 24.0, 22.5

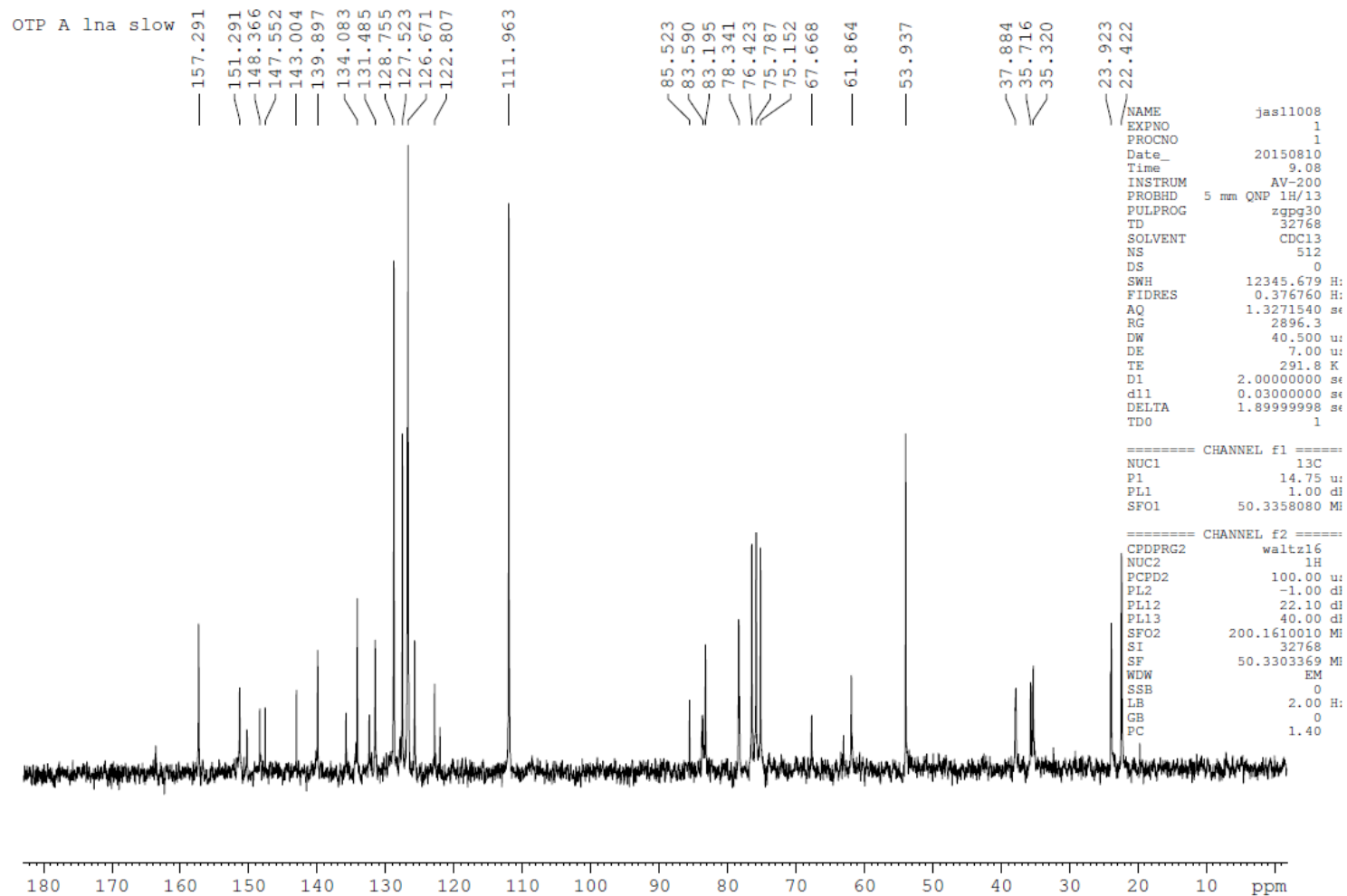


Figure S28.  $A_L$ -OTP *slow* (**2b**);  $\delta$  (ppm,  $CDCl_3$ ) 157.3, 151.3, 148.4, 147.6, 143.0, 139.9, 134.1, 131.5, 128.8, 127.5, 126.7, 122.8, 112.0, 85.5, 83.6, 83.2, 78.3, 76.4, 75.8, 75.2, 67.7, 61.9, 53.9, 37.9, 35.7, 35.3, 23.9, 22.4

KJ-Clna fast

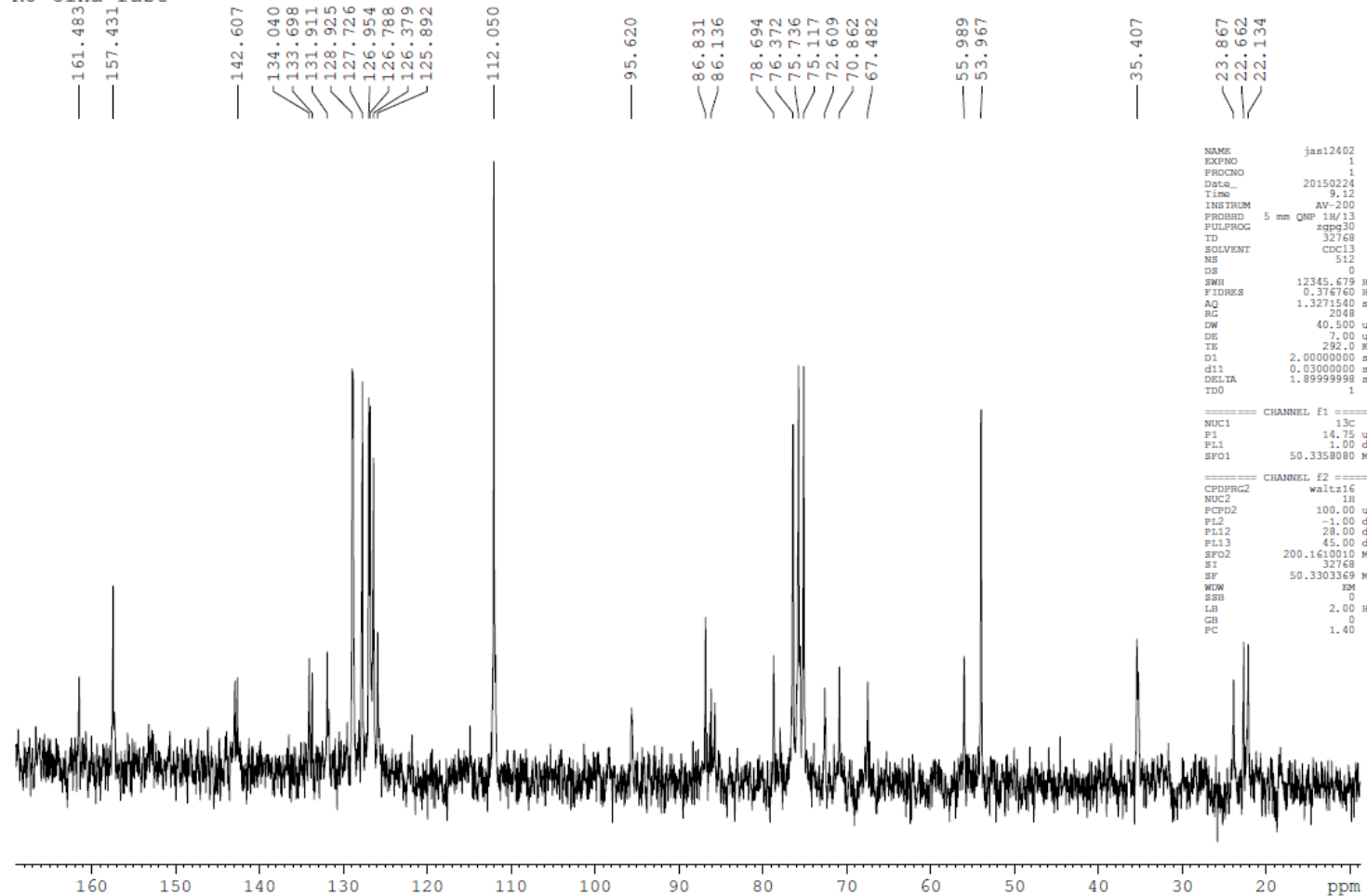


Figure S29.  $C_L$ -OTP *fast* (**2c**);  $\delta$  (ppm,  $CDCl_3$ ) 161.5, 157.4, 142.6, 134.0, 133.7, 131.9, 128.9, 127.7, 127.0, 126.8, 126.4, 125.9, 112.1, 95.6, 86.8, 86.1, 78.7, 76.4, 75.7, 75.1, 72.6, 70.9, 67.5, 56.0, 54.0, 35.4, 23.9, 22.7, 22.1

KJ-Clna slow

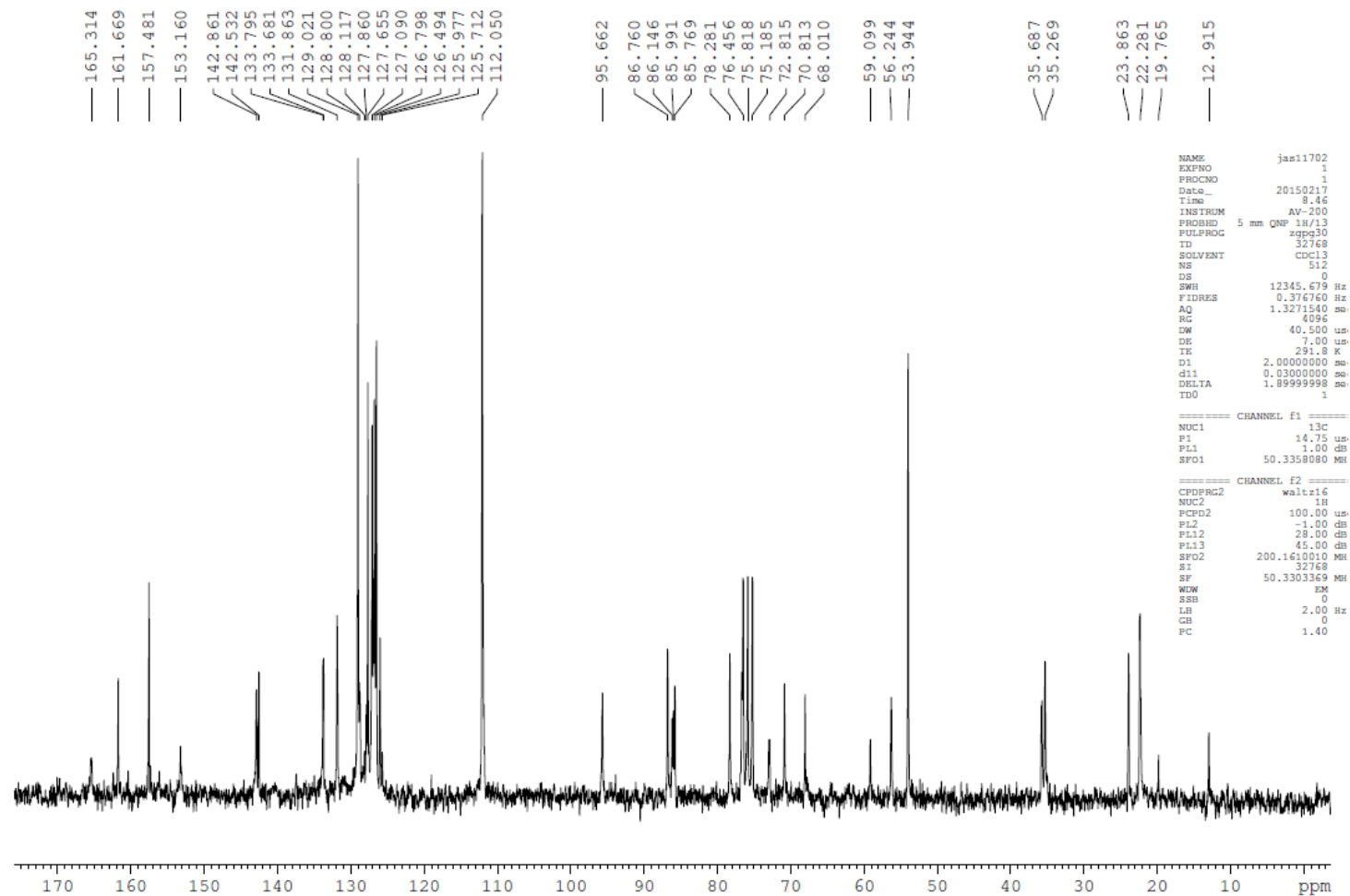


Figure S30.  $C_L$ -OTP *slow* (**2c**);  $\delta$  (ppm,  $CDCl_3$ ) 161.7, 157.5, 142.9, 133.8, 133.7, 131.9, 129.0, 128.8, 127.9, 127.1, 126.8, 126.5, 112.1, 95.7, 86.8, 86.1, 86.0, 85.8, 78.3, 76.5, 75.2, 72.8, 68.0, 56.2, 53.9, 35.7, 35.3, 23.9, 22.3

k. jastrzebska =glna-fast= 13C{1H}

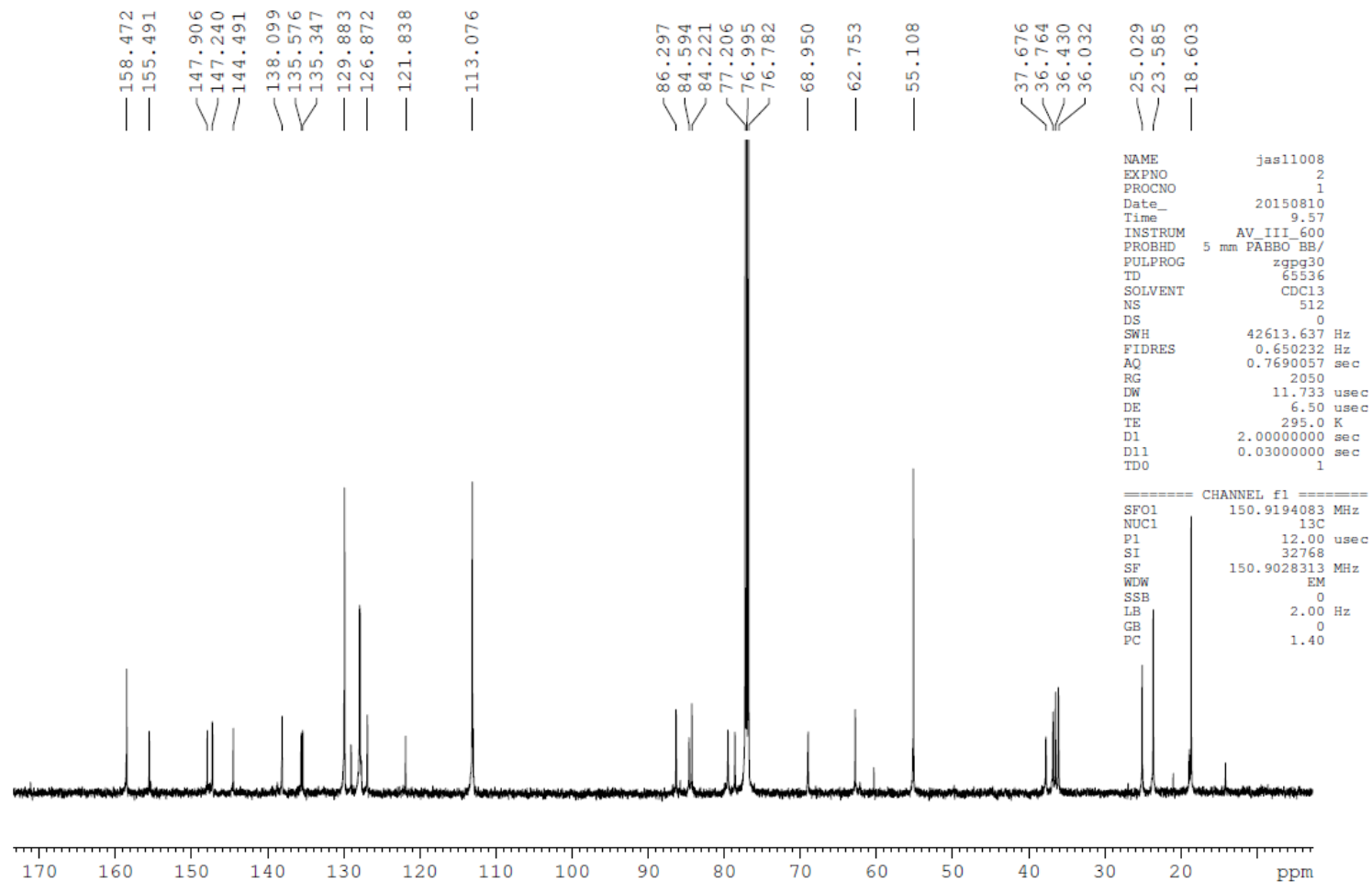


Figure S31.  $G_L$ -OTP *fast* (**2d**); SF=600 MHz for  $^1\text{H}$ ;  $\delta$  (ppm,  $\text{CDCl}_3$ ) 158.5, 155.5, 147.9, 147.2, 144.5, 138.1, 135.6, 135.3, 129.9, 126.9, 121.8, 113.1, 86.3, 84.6, 84.2, 77.2, 77.0, 76.8, 69.0, 62.8, 55.1, 37.7, 36.8, 36.4, 36.0, 25.0, 23.6, 18.6

k. jastrzebska =glna-slow= 13C{1H}

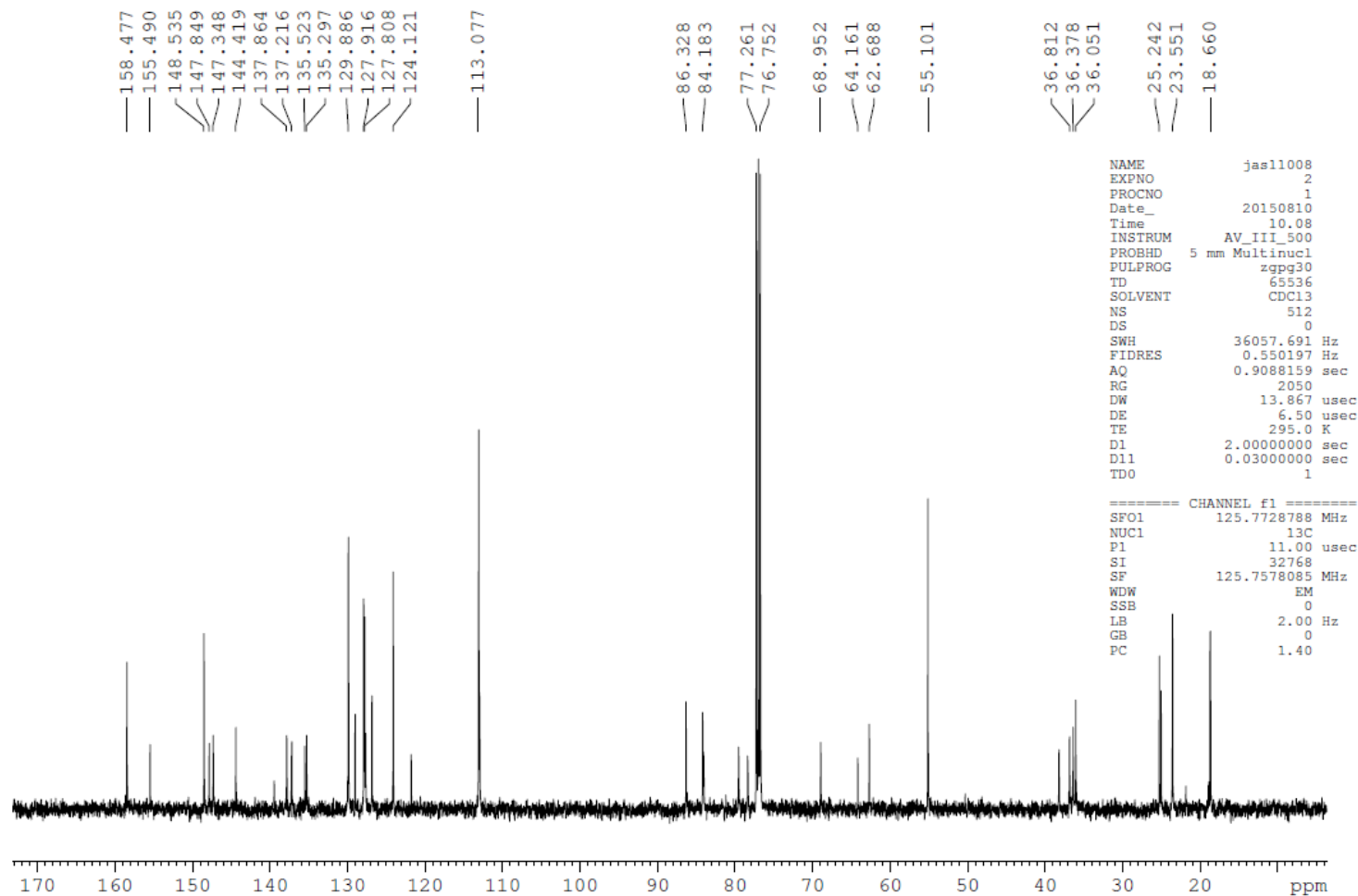


Figure S32.  $G_L$ -OTP *slow* (**2d**); SF=500 MHz for  $^1\text{H}$ ;  $\delta$  (ppm,  $\text{CDCl}_3$ ) 158.5, 155.5, 148.5, 147.8, 147.3, 144.4, 137.9, 137.2, 135.5, 135.3, 129.9, 127.8, 124.1, 113.1, 86.3, 84.2, 77.3, 76.8, 69.0, 64.2, 62.7, 55.1, 36.8, 36.4, 36.1, 25.2, 23.6, 18.7

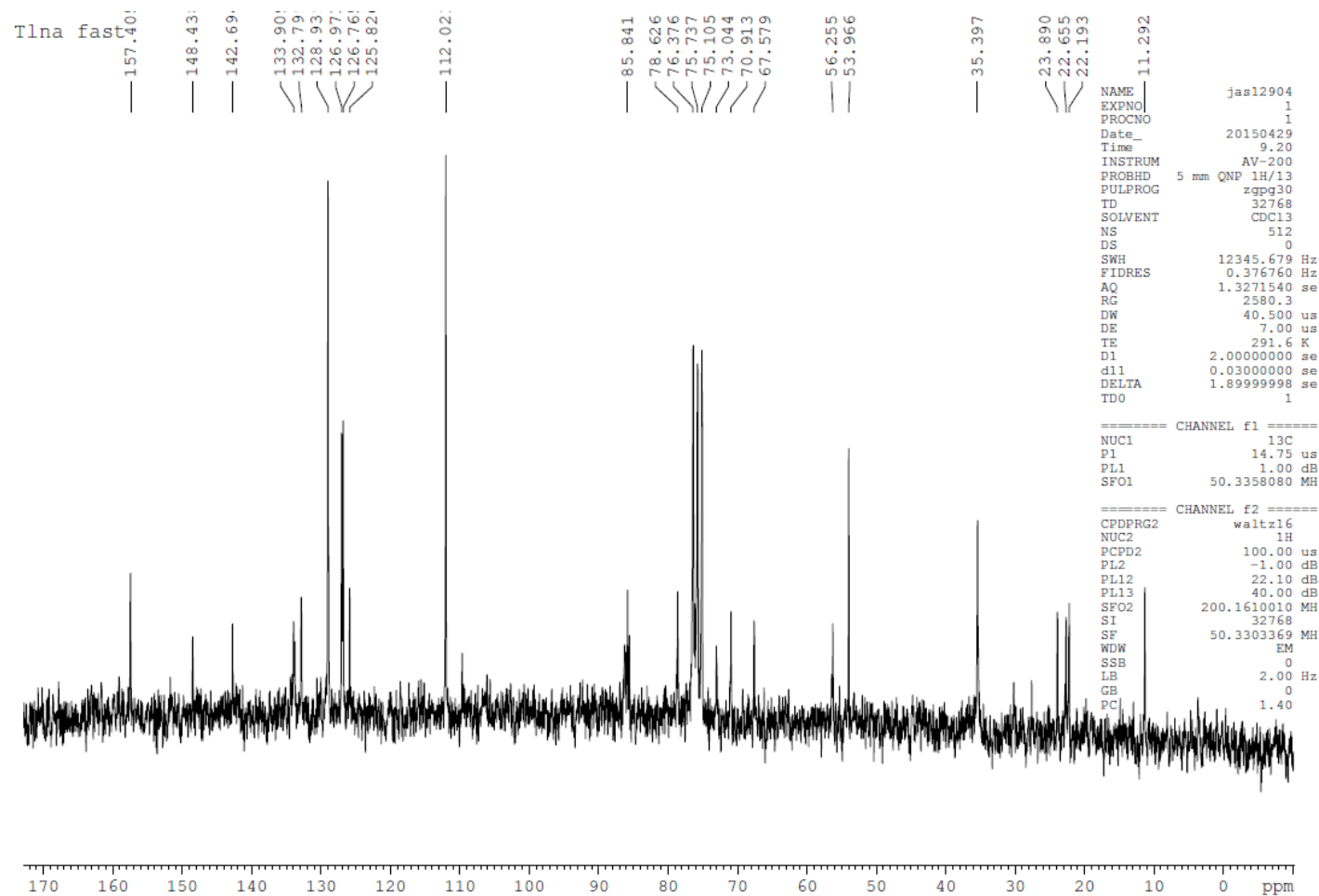


Figure S33. T<sub>L</sub>-OTP *fast* (**2a**);  $\delta$  (ppm, CDCl<sub>3</sub>) 157.4, 148.4, 142.7, 133.9, 132.8, 128.9, 127.0, 126.8, 125.8, 112.0, 85.8, 78.6, 76.4, 75.7, 75.1, 73.0, 70.9, 67.6, 56.3, 54.0, 35.4, 23.9, 22.7, 22.2, 11.3



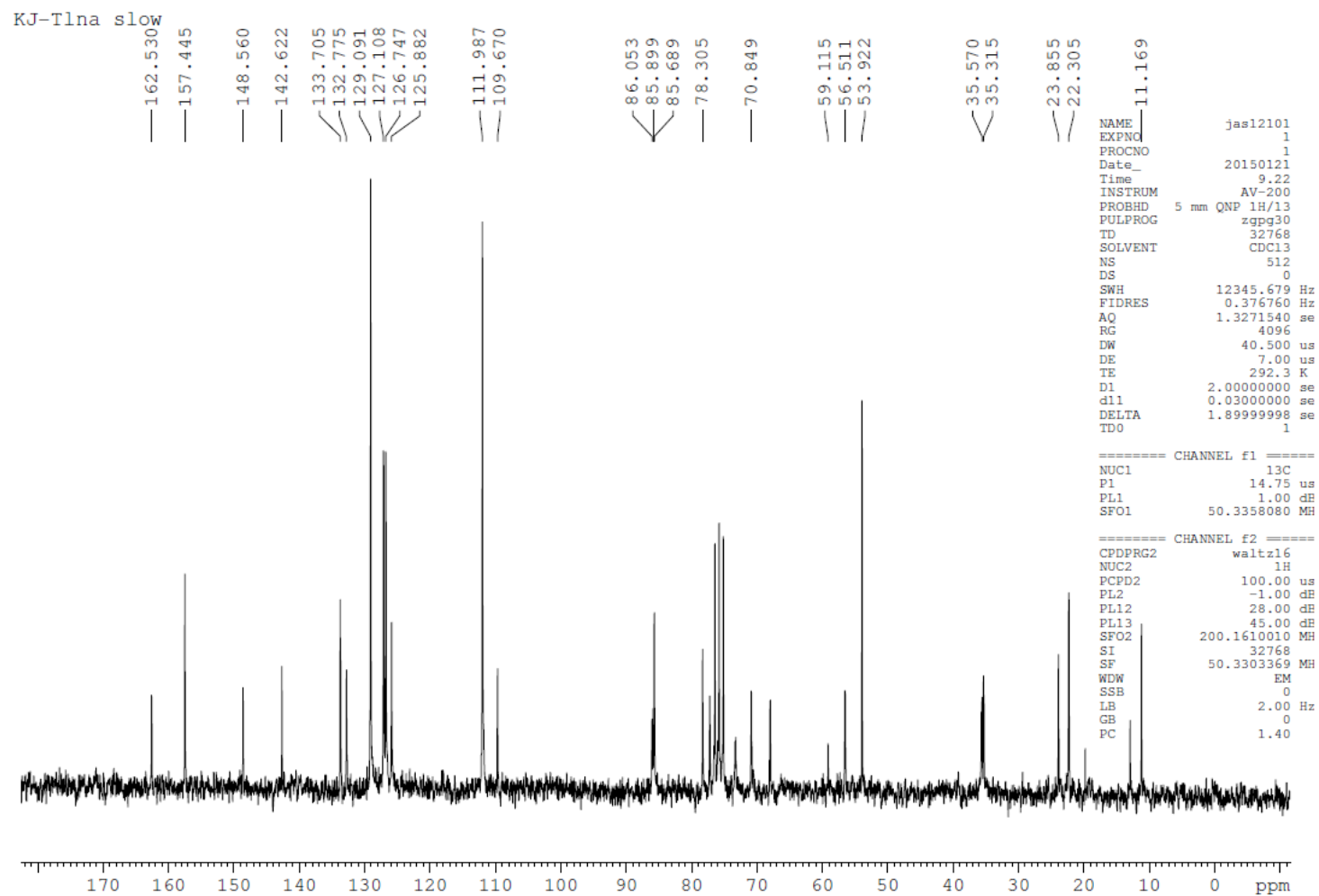


Figure S34.  $T_L$ -OTP *slow* (**2a**);  $\delta$  (ppm,  $CDCl_3$ ) 162.5, 157.4, 148.6, 142.6, 133.7, 132.8, 129.1, 127.1, 126.7, 125.9, 112.0, 109.7, 86.1, 85.9, 85.7, 78.3, 70.8, 56.5, 53.9, 35.6, 35.3, 23.9, 22.3, 11.2

VIII. Profiles from an RP-HPLC analysis of **PS-(DNA/LNA)** oligomers carrying the 5'-*O*-DMT tag.

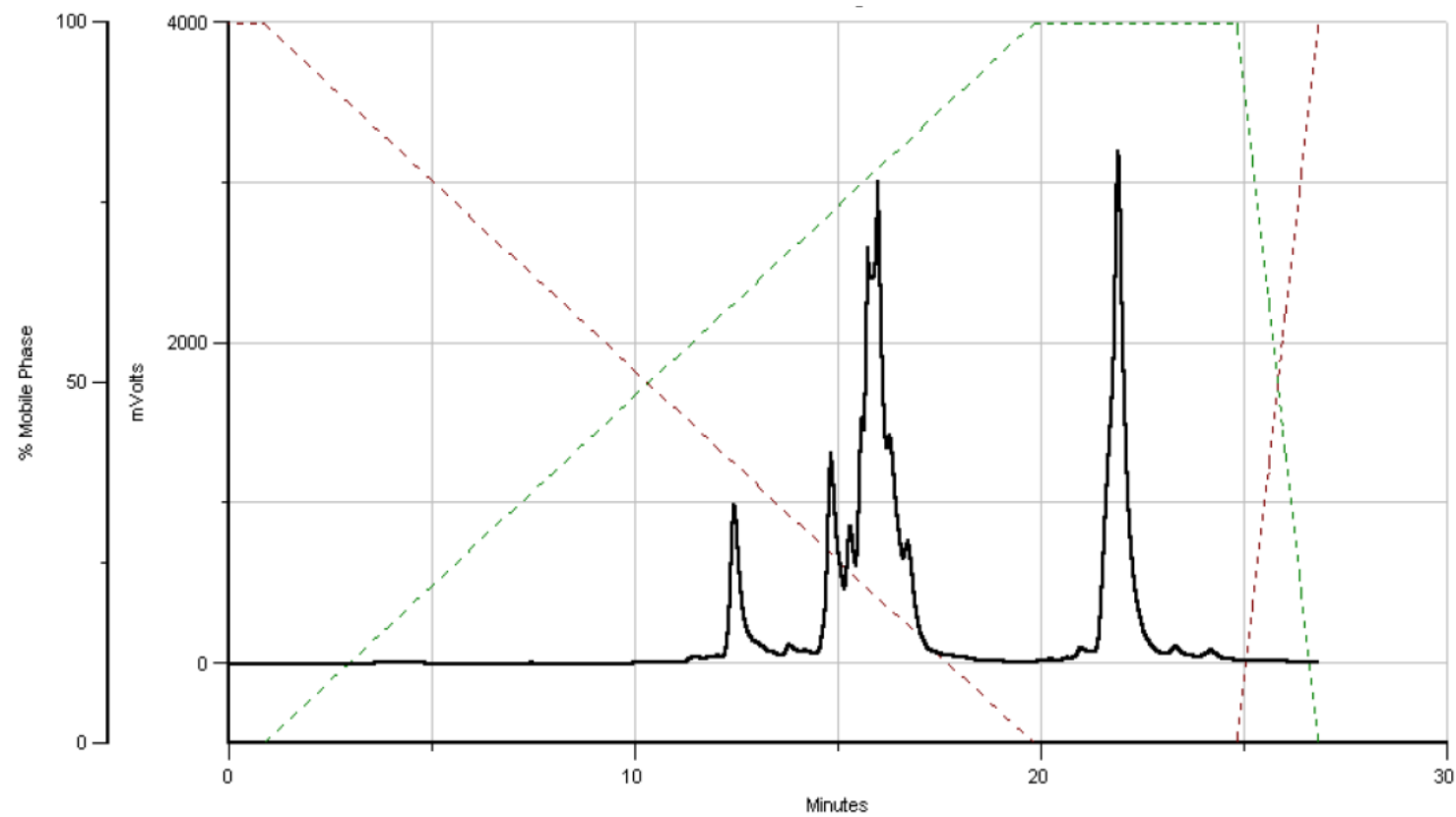


Figure S35. **A2R** [ $R_P$ -PS]-d(GACA<sub>L</sub>TCA<sub>L</sub>CTAG)

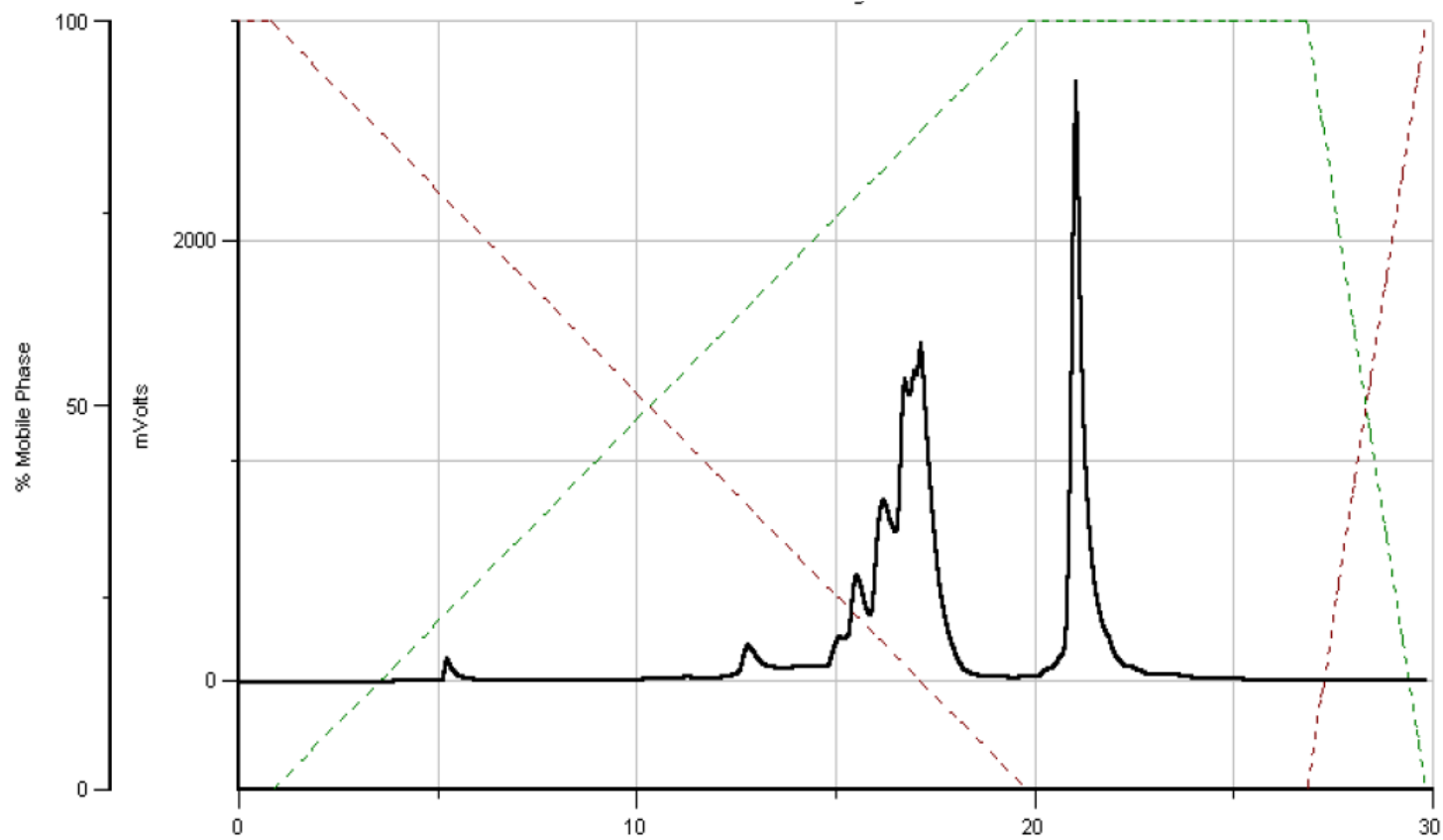


Figure S36. **A2S** [ $S_p$ -PS]-d(GACA<sub>L</sub>TCA<sub>L</sub>CTAG)

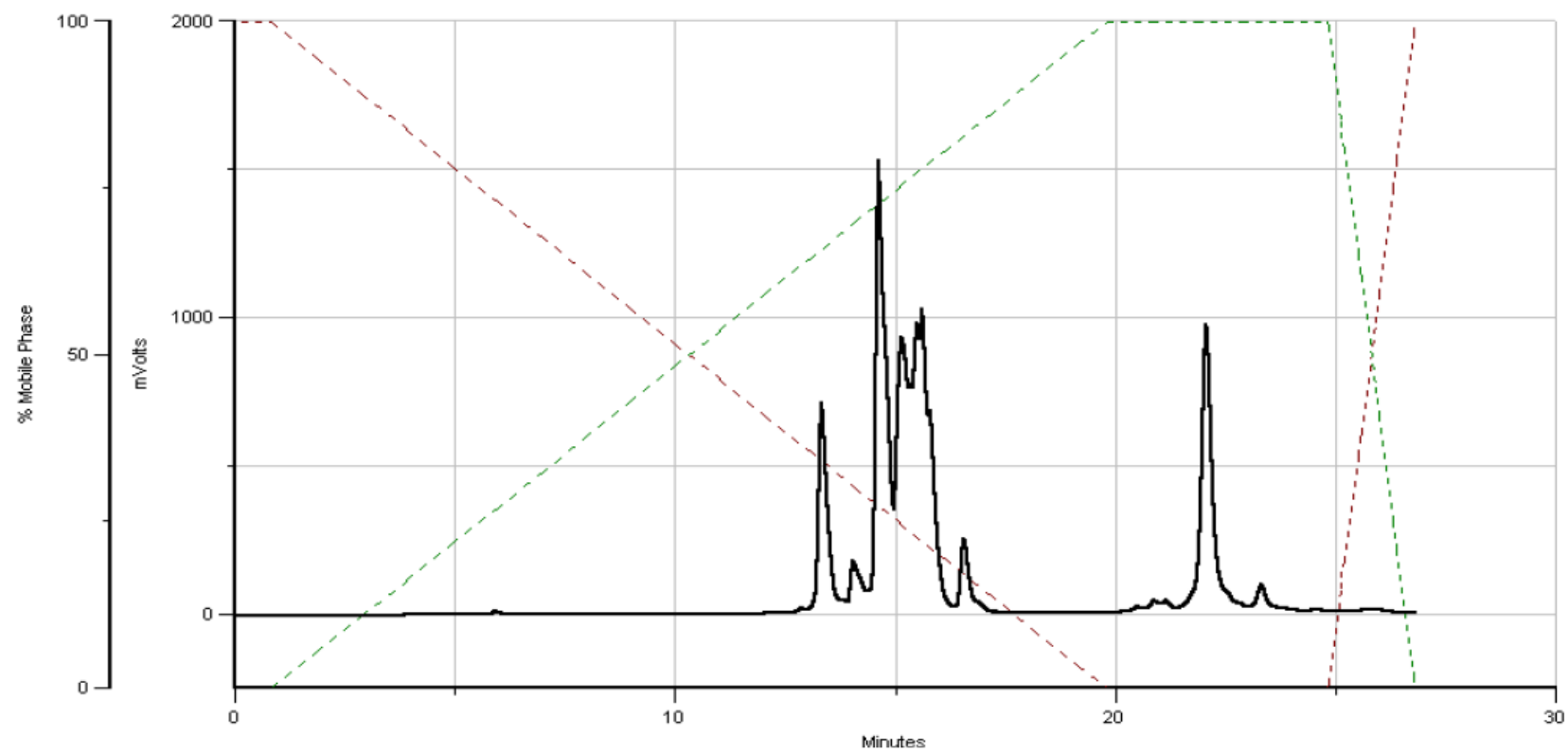


Figure S37. **C2R** [ $R_p$ -PS]-d(GAC<sub>L</sub>ATC<sub>L</sub>ACTAG)

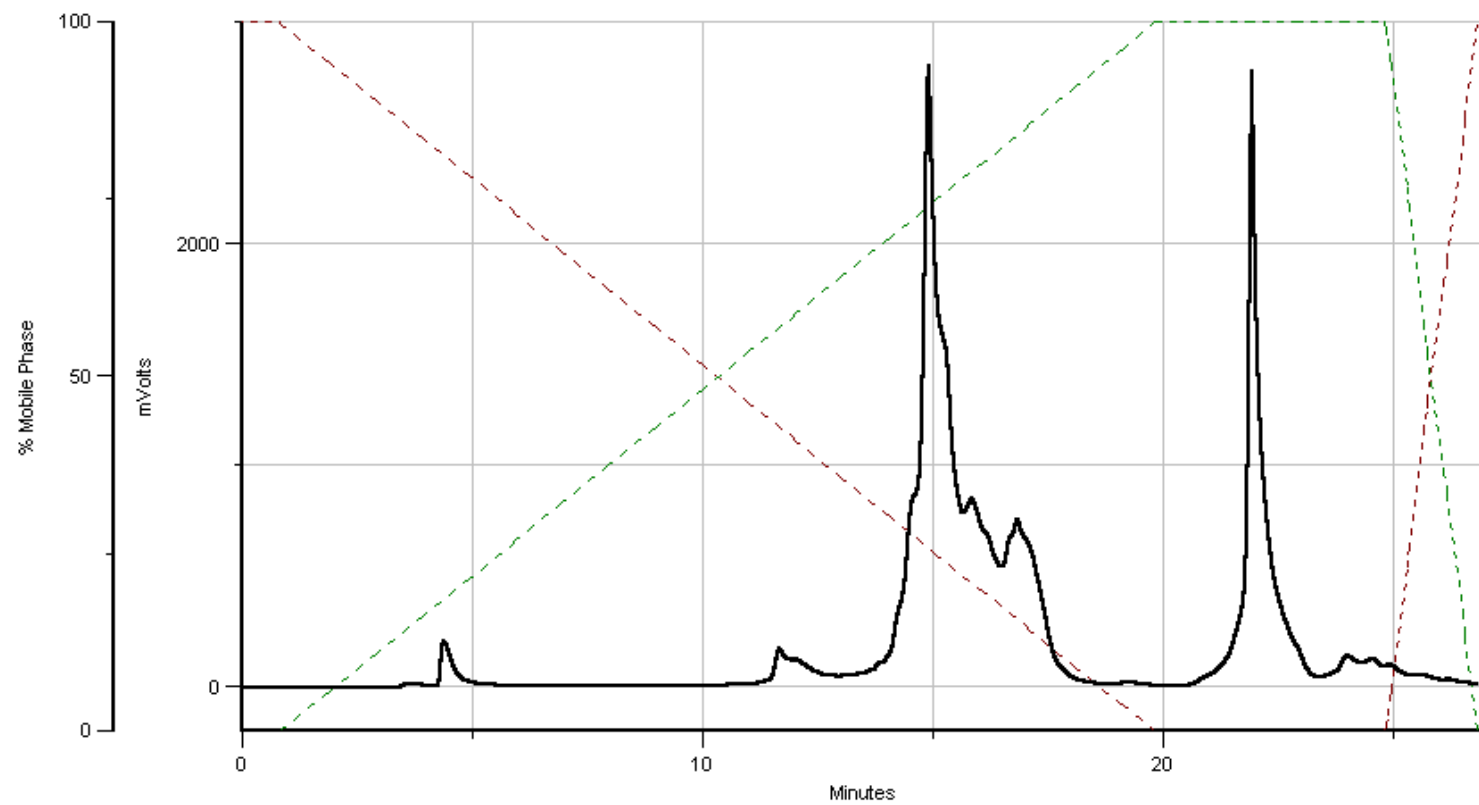


Figure S38. C2S [Sp-PS]-d(GACLATCLACTAG)

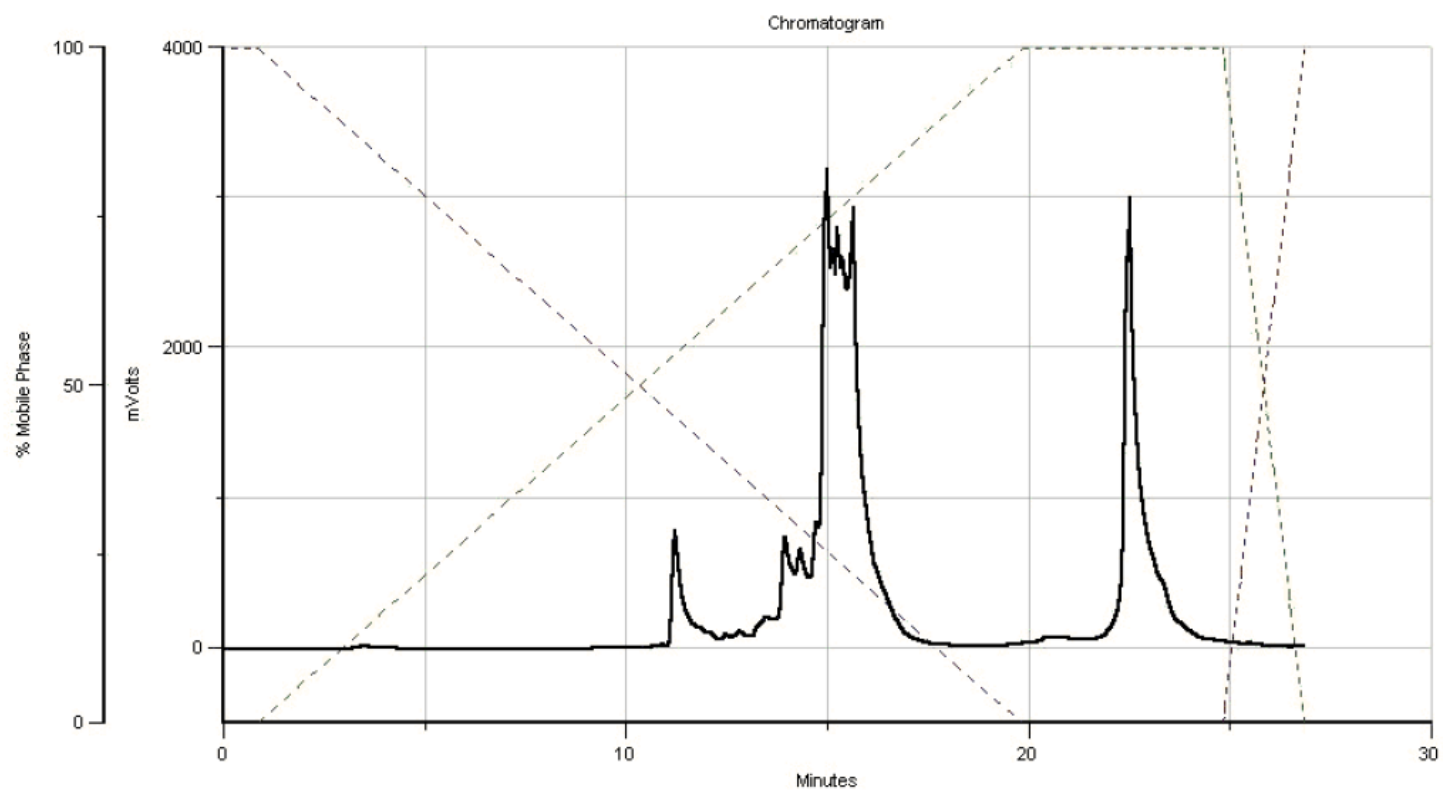


Figure S39. **C3R** [ $R_p$ -PS]-d(GAC<sub>L</sub>ATC<sub>L</sub>AC<sub>L</sub>TAG)

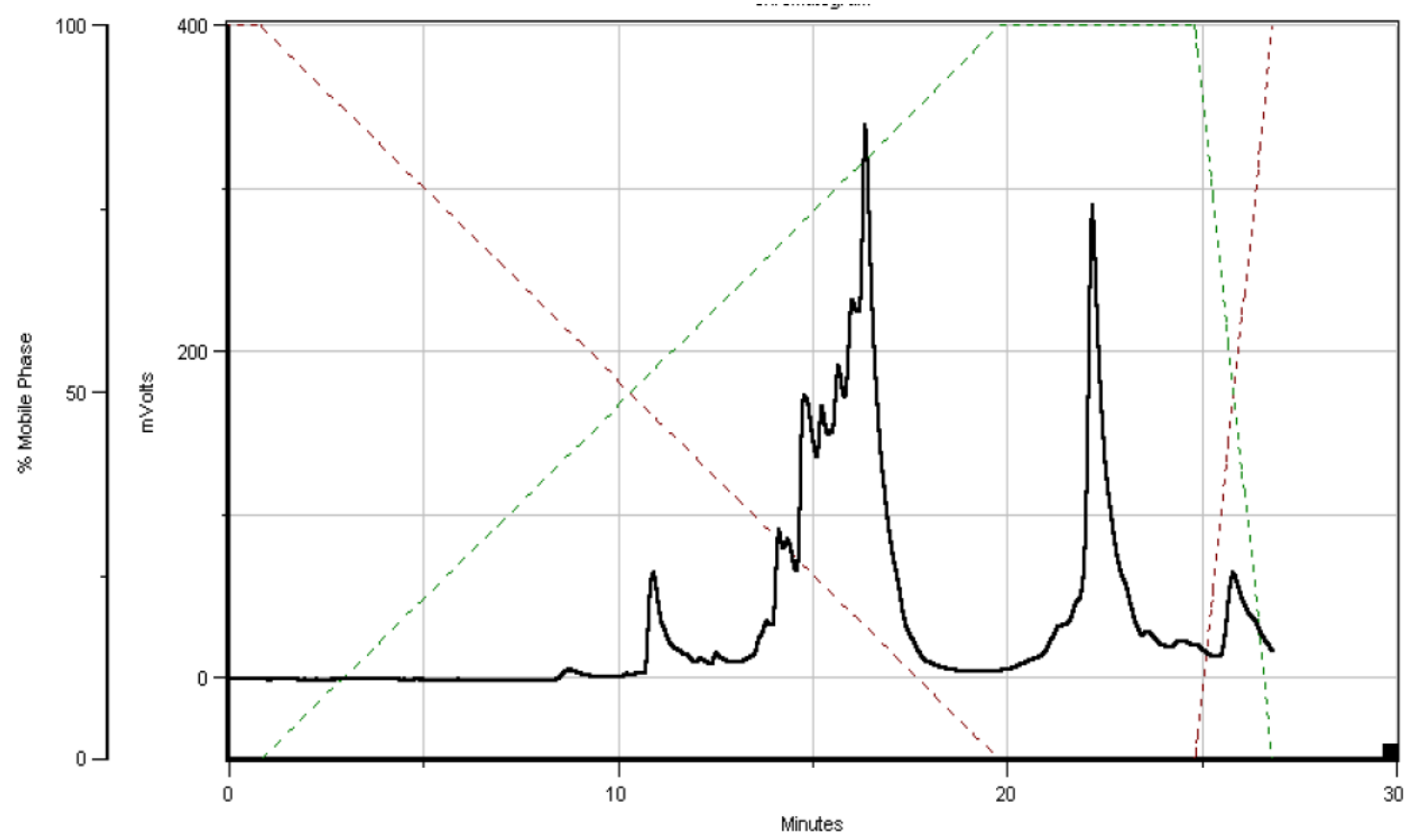


Figure S40. C3S [S<sub>P</sub>-PS]-d(GAC<sub>L</sub>ATC<sub>L</sub>AC<sub>L</sub>TAG)

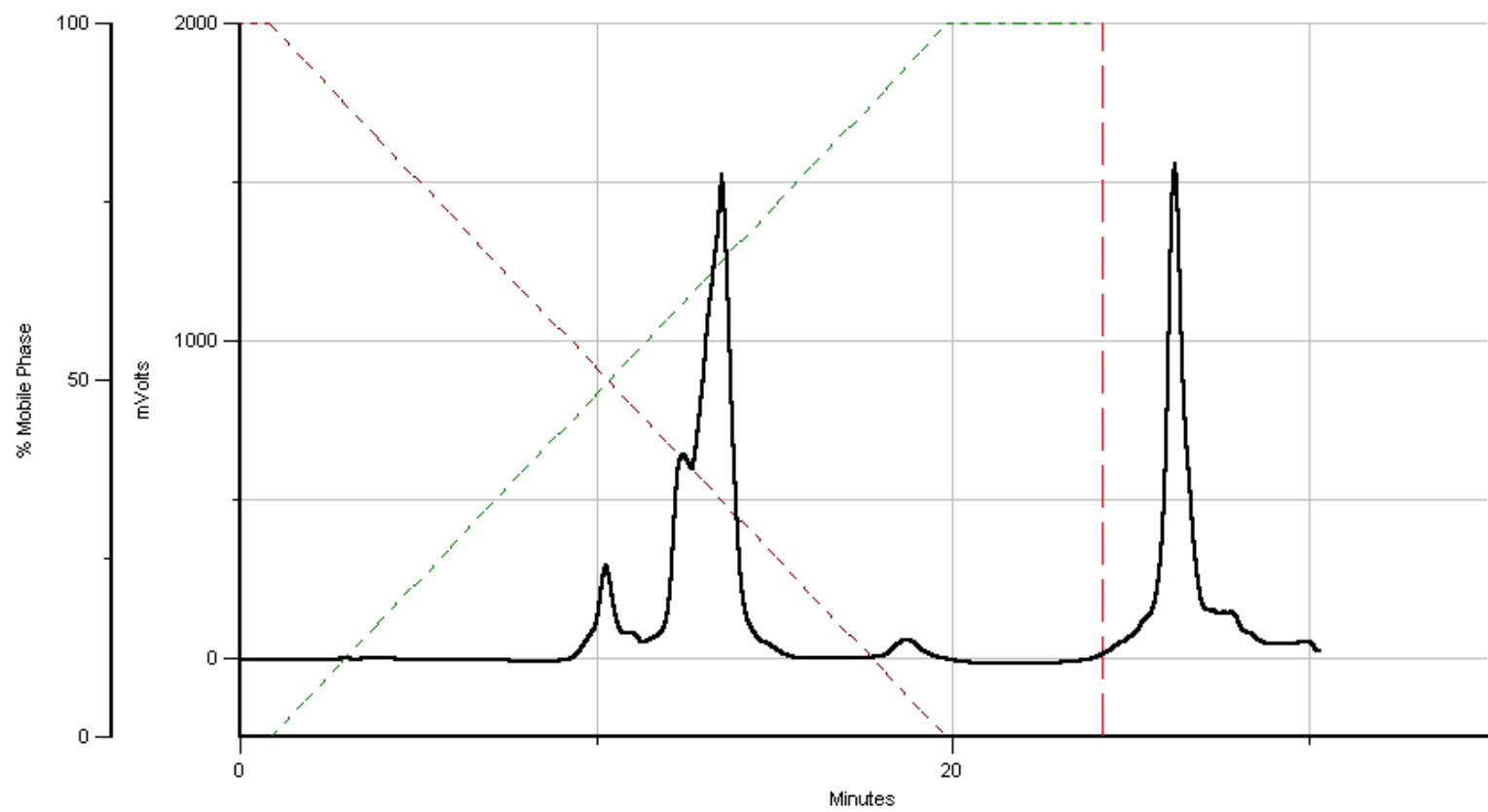


Figure S41. **G2R** [*R<sub>p</sub>*-PS]-d(GAG<sub>L</sub>ACTAG)



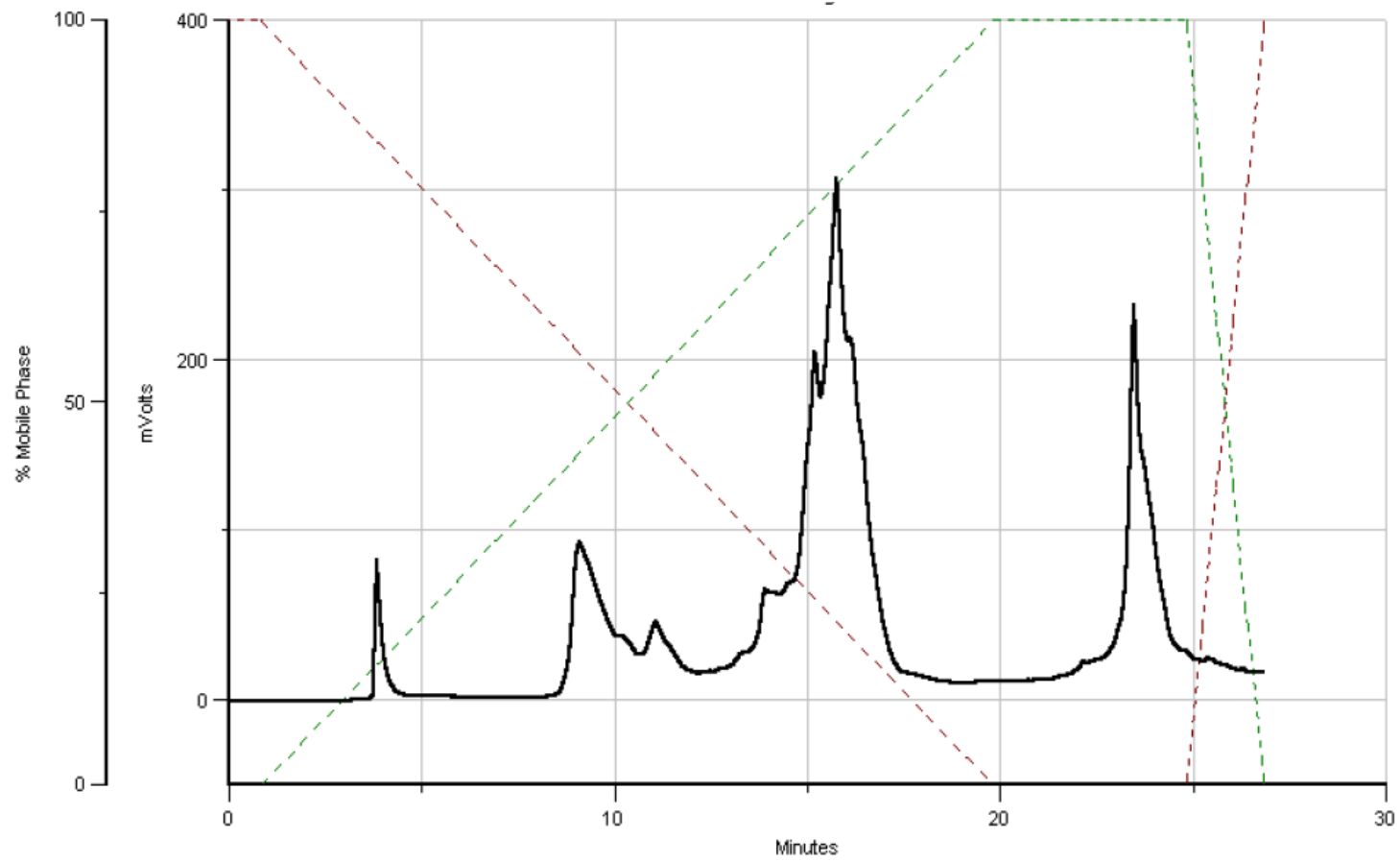


Figure S42. **G2S** [ $S_P$ -PS]-d(GAG<sub>L</sub>ATG<sub>L</sub>ACTAG)

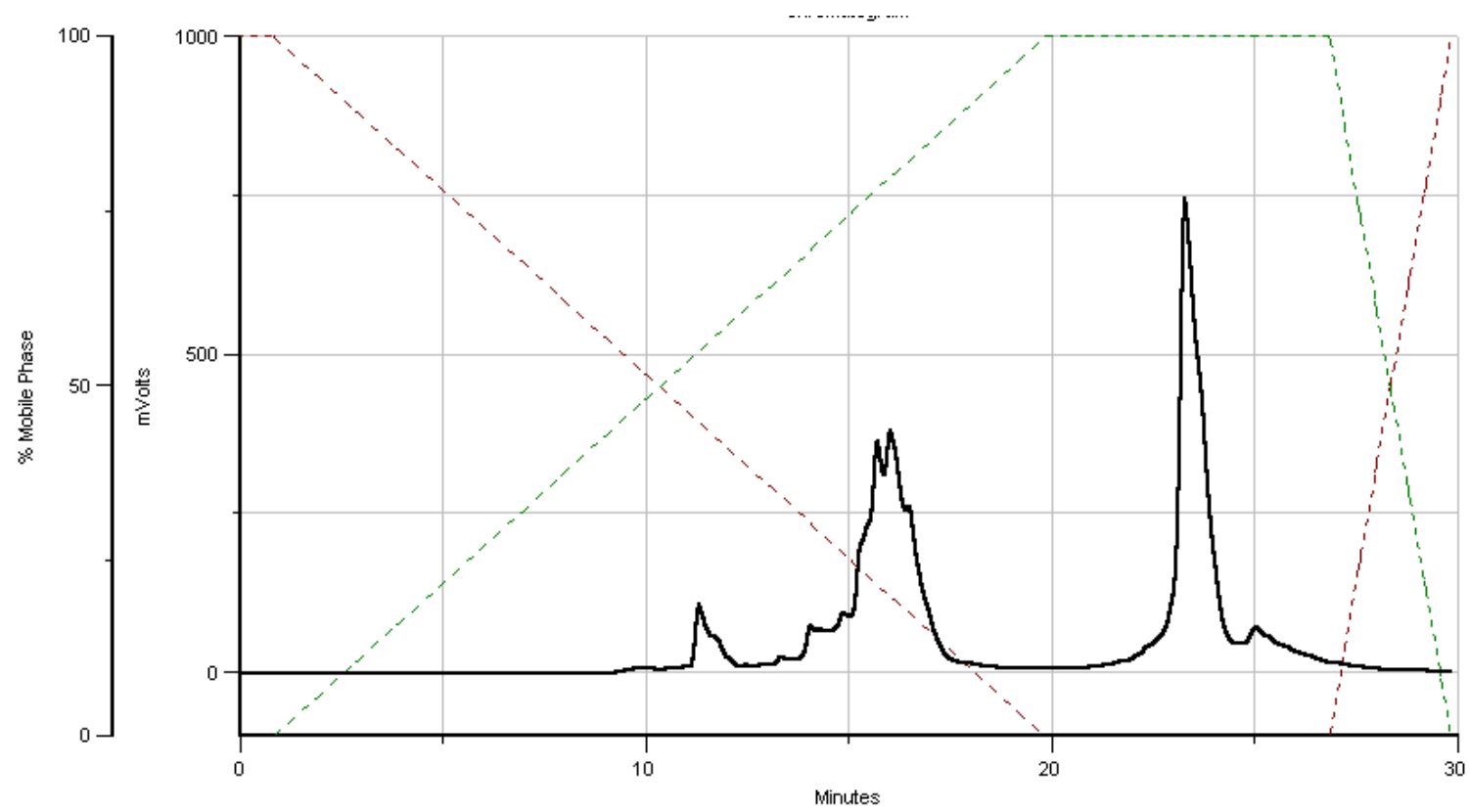


Figure S43. **T2R** [*R<sub>p</sub>*-PS]-d(GACAT<sub>L</sub>CACT<sub>L</sub>AG)

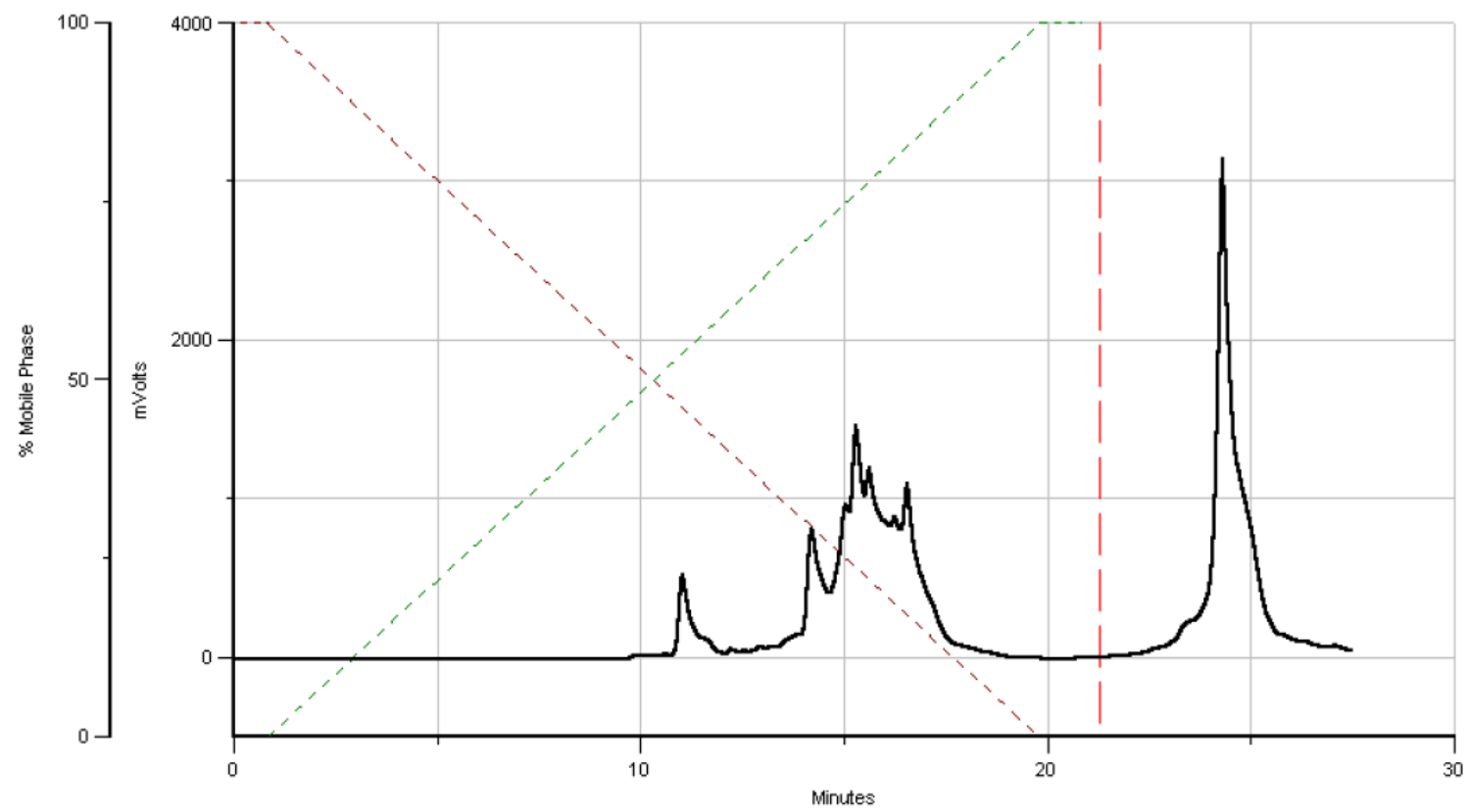


Figure S44. T2S [ $S_p$ -PS]-d(GACAT<sub>L</sub>CACT<sub>L</sub>AG)

IX. Profiles from an RP-HPLC analysis of **PS-(DNA/LNA)** oligomers after removal of the 5'-O-DMT tag.

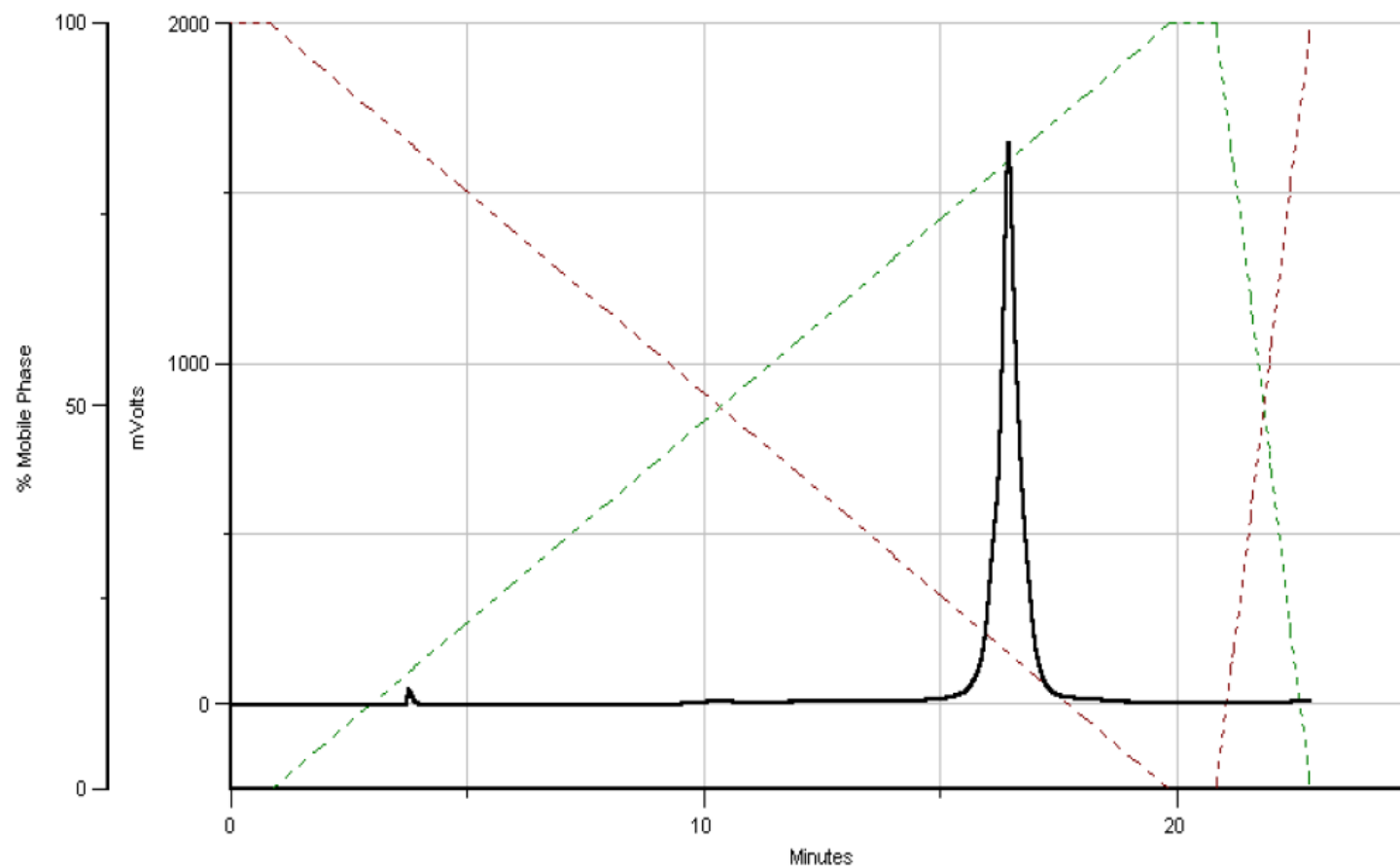


Figure S45. **A2R** [ $R_P$ -PS]-d(GACA<sub>L</sub>TCA<sub>L</sub>CTAG)

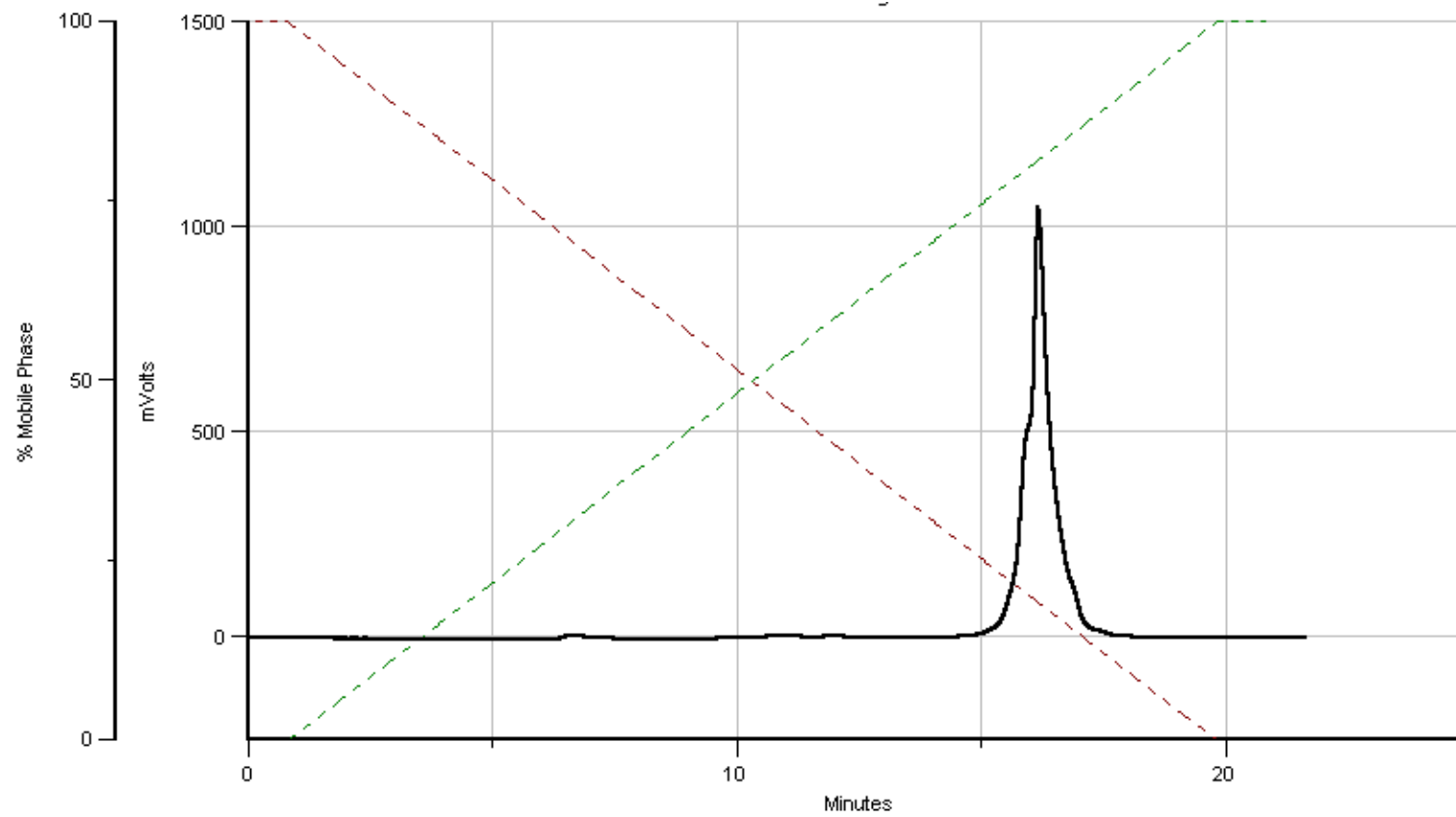


Figure S46. **A2S** [S<sub>P</sub>-PS]-d(GACA<sub>L</sub>TCA<sub>L</sub>CTAG)

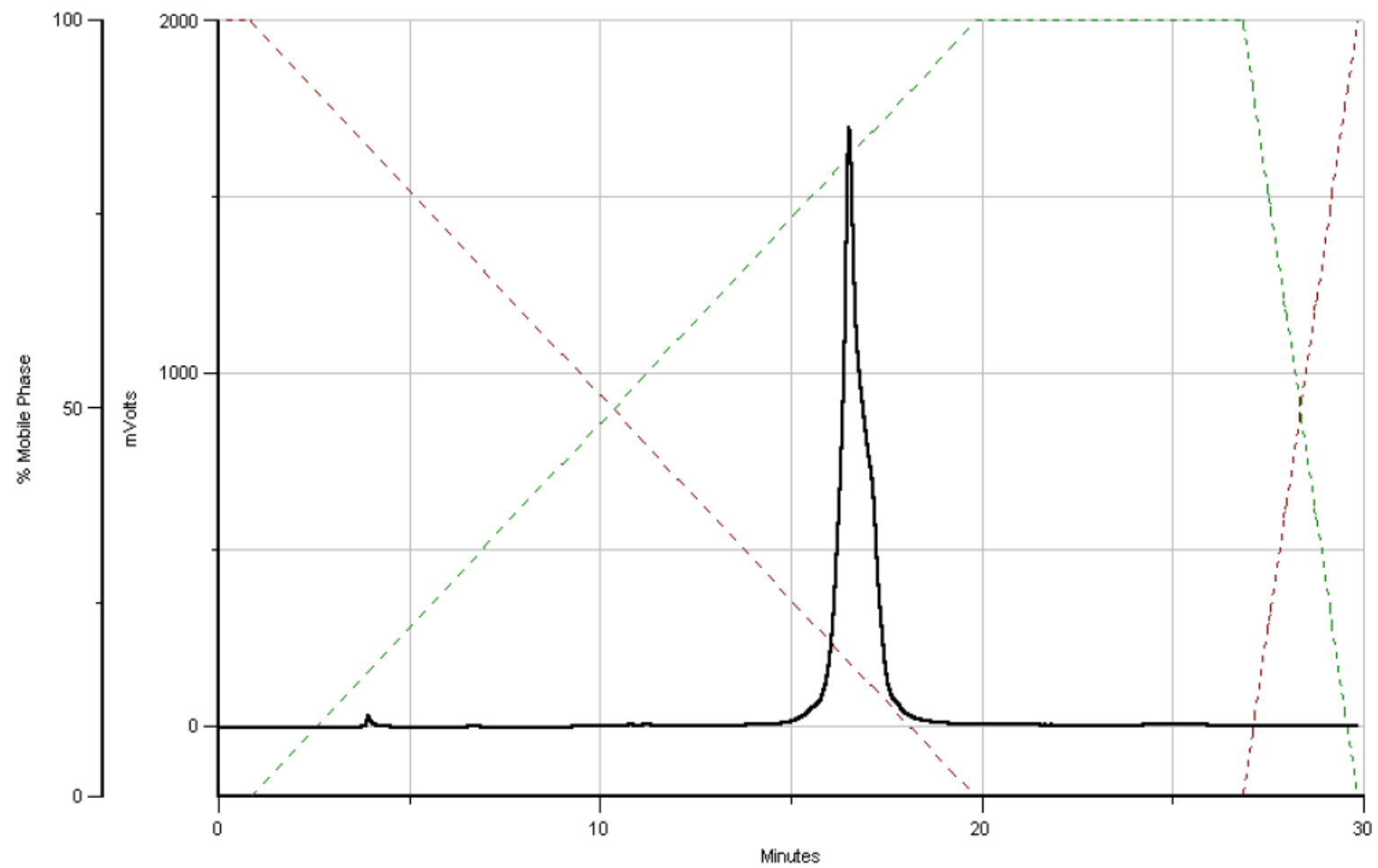


Figure S47. **C2R** [*R<sub>p</sub>*-PS]-d(GAC<sub>1</sub>ATC<sub>1</sub>ACTAG)

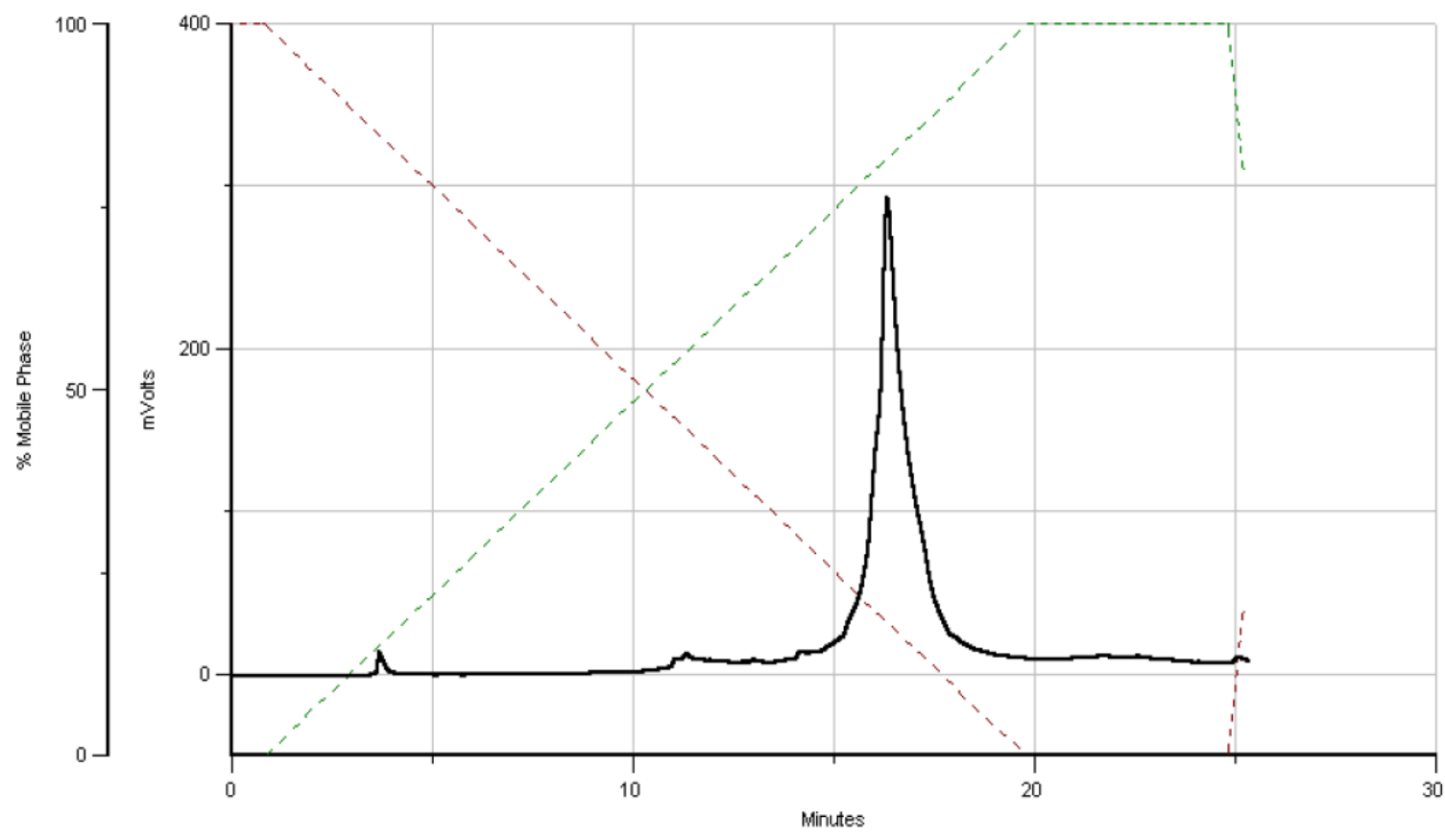


Figure S48. **C2S** [ $S_P$ -PS]-d(GAC<sub>L</sub>ATC<sub>L</sub>ACTAG)

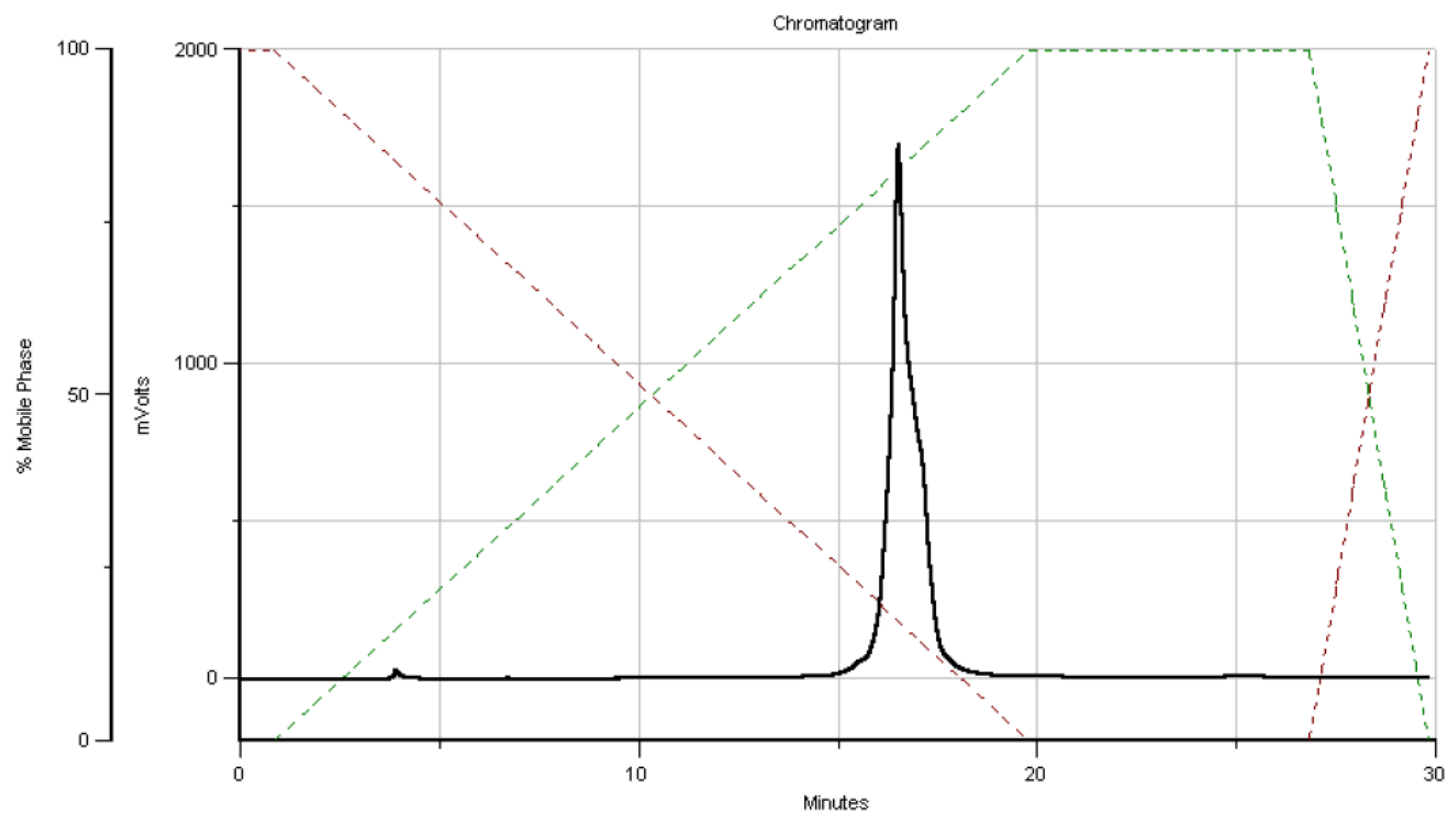


Figure S49. **C3R** [ $R_p$ -PS]-d(GAC<sub>L</sub>ATC<sub>L</sub>AC<sub>L</sub>TAG)



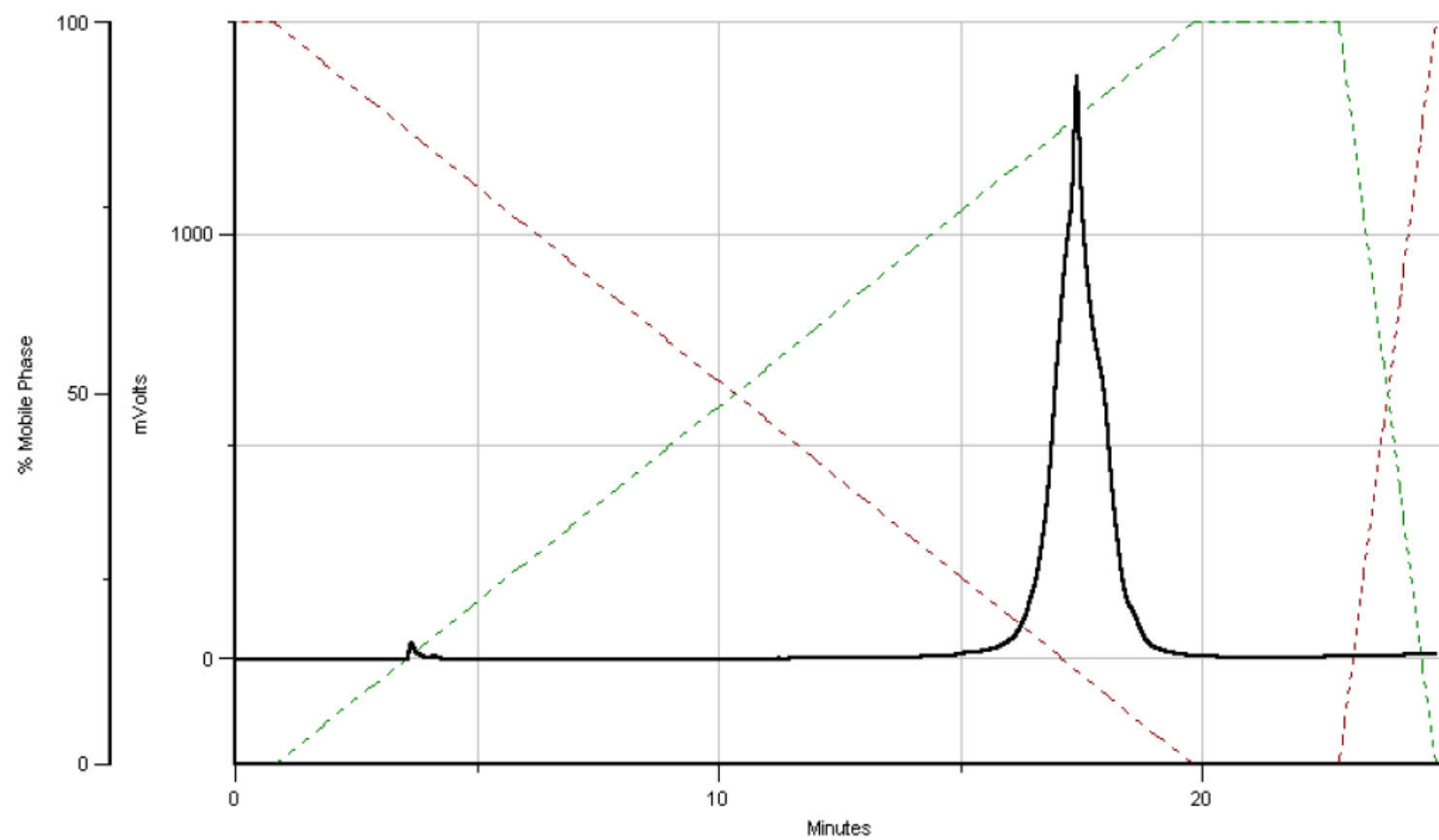


Figure S50. **C3S** [ $S_P$ -PS]-d(GAC<sub>L</sub>ATC<sub>L</sub>AC<sub>L</sub>TAG)

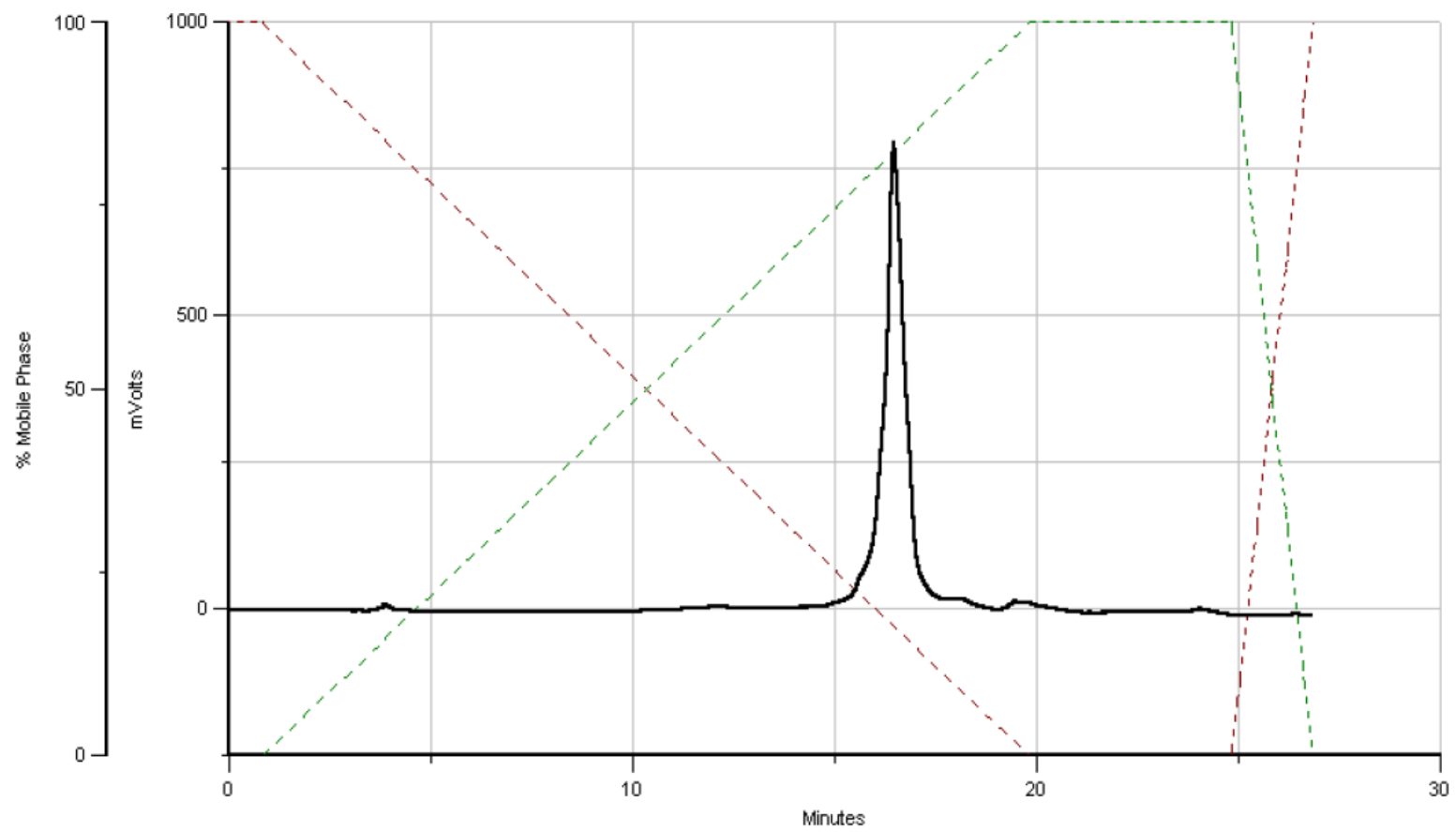


Figure S51. **G2R** [ $R_p$ -PS]-d(GAG<sub>L</sub>ATG<sub>L</sub>ACTAG)

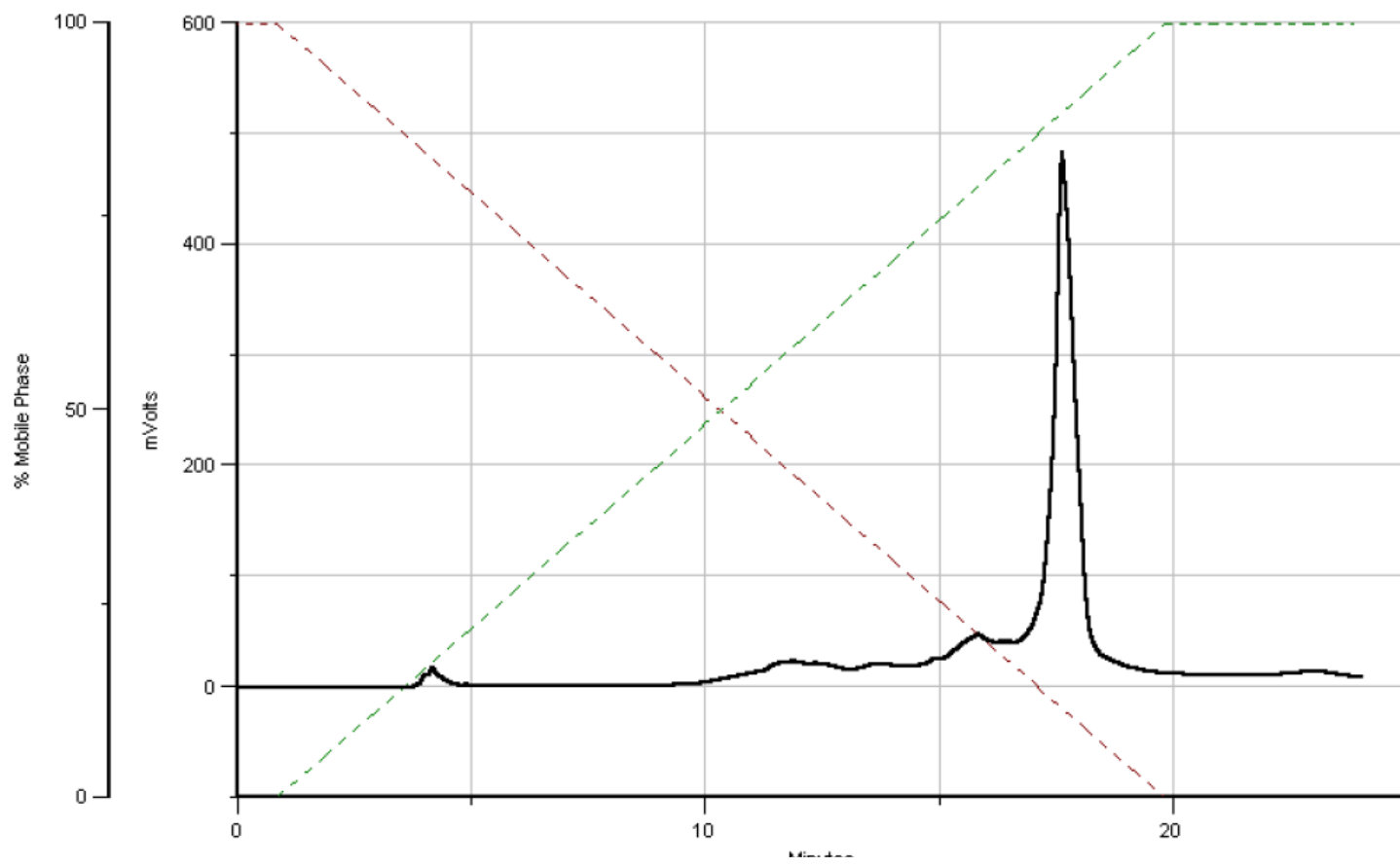


Figure S52. **G2S** [ $S_P$ -PS]-d(GAG<sub>L</sub>ATG<sub>L</sub>ACTAG)

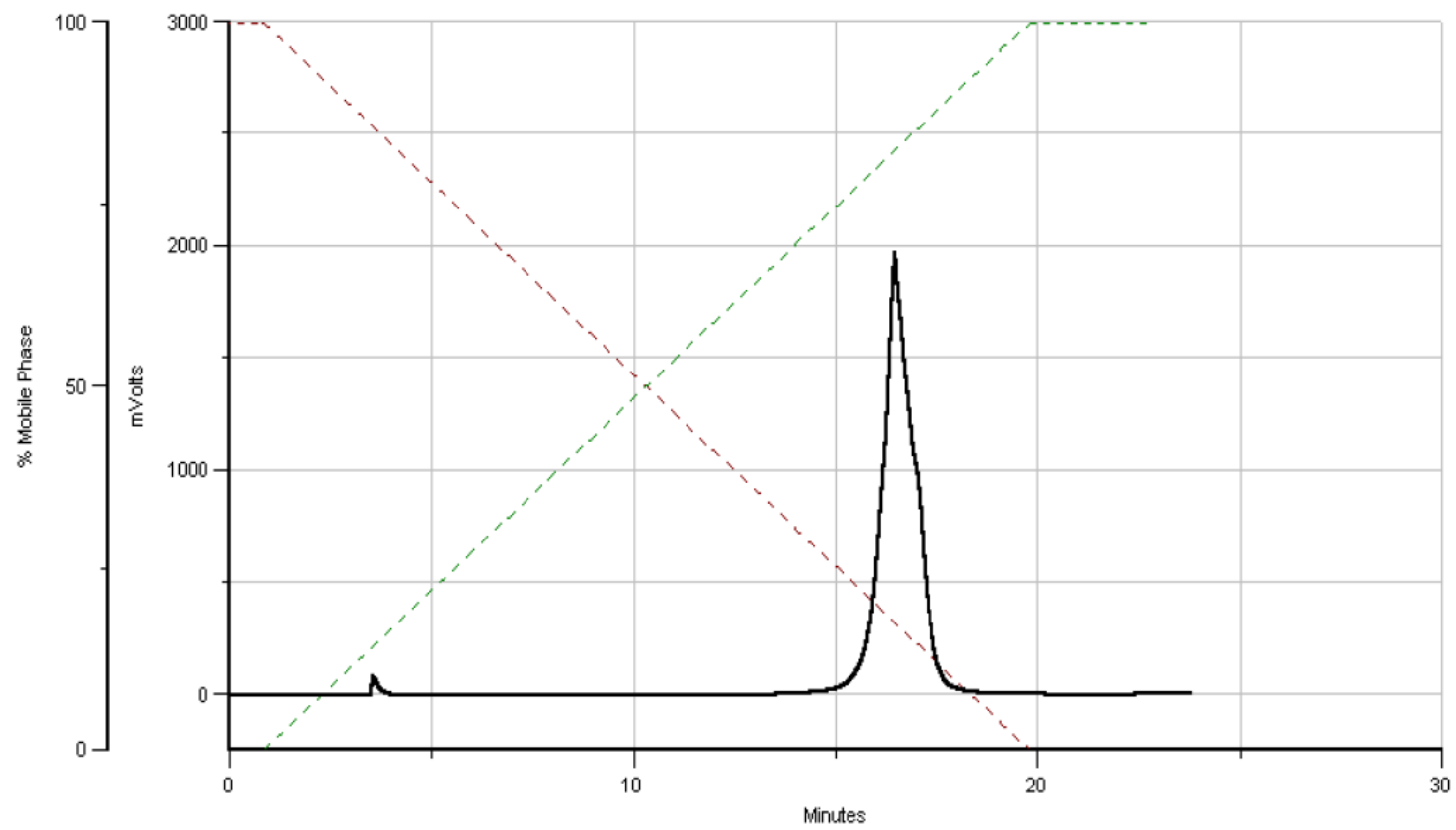


Figure S53. **T2R** [ $R_p$ -PS]-d(GACAT<sub>L</sub>CACT<sub>L</sub>AG)

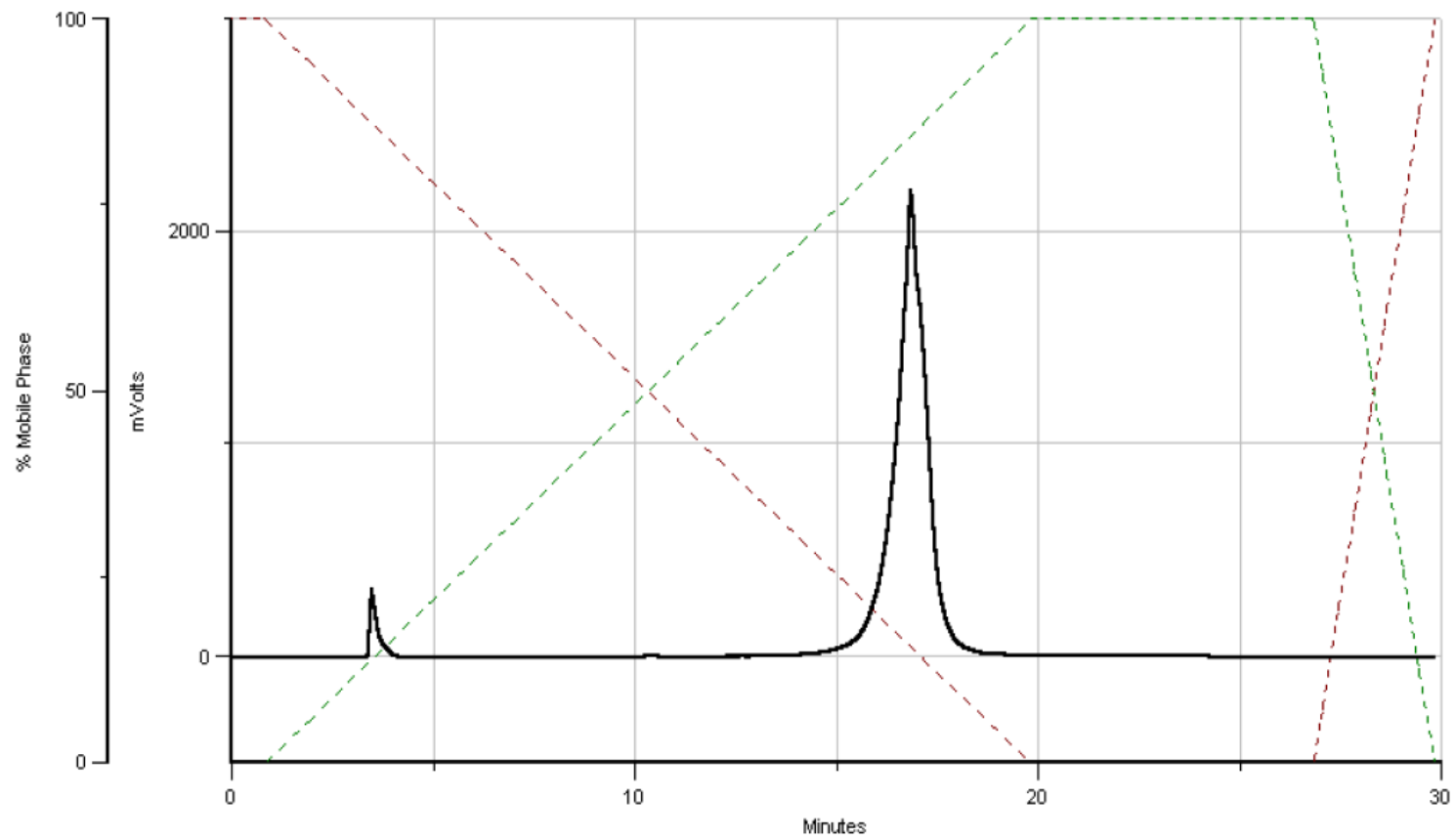


Figure S54. **T2S** [ $S_P$ -PS]-d(GACAT<sub>L</sub>CACT<sub>L</sub>AG)

## X. Enzymatic hydrolysis of $(A_L)_{PS}T$ obtained from **2b** *fast* and **2b** *slow*.

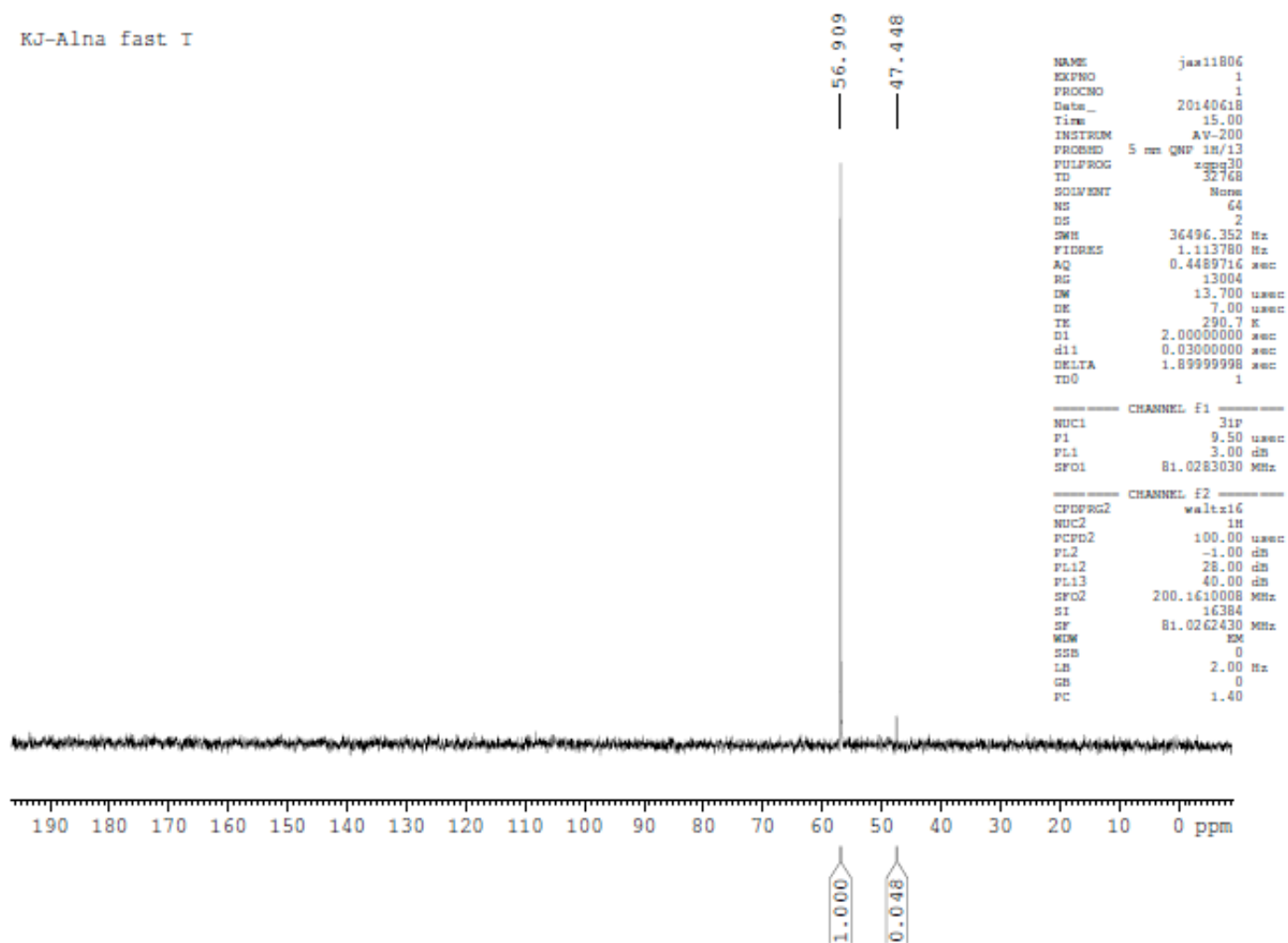


Figure S55. A  $^{31}P$  NMR spectrum for  $(A_L)_{PS}T$  obtained from **2b** *fast*. A signal at 47.4 ppm corresponds to the product of hydrolysis and not to the second P-diastereoisomer.

KJ-Alna fast T

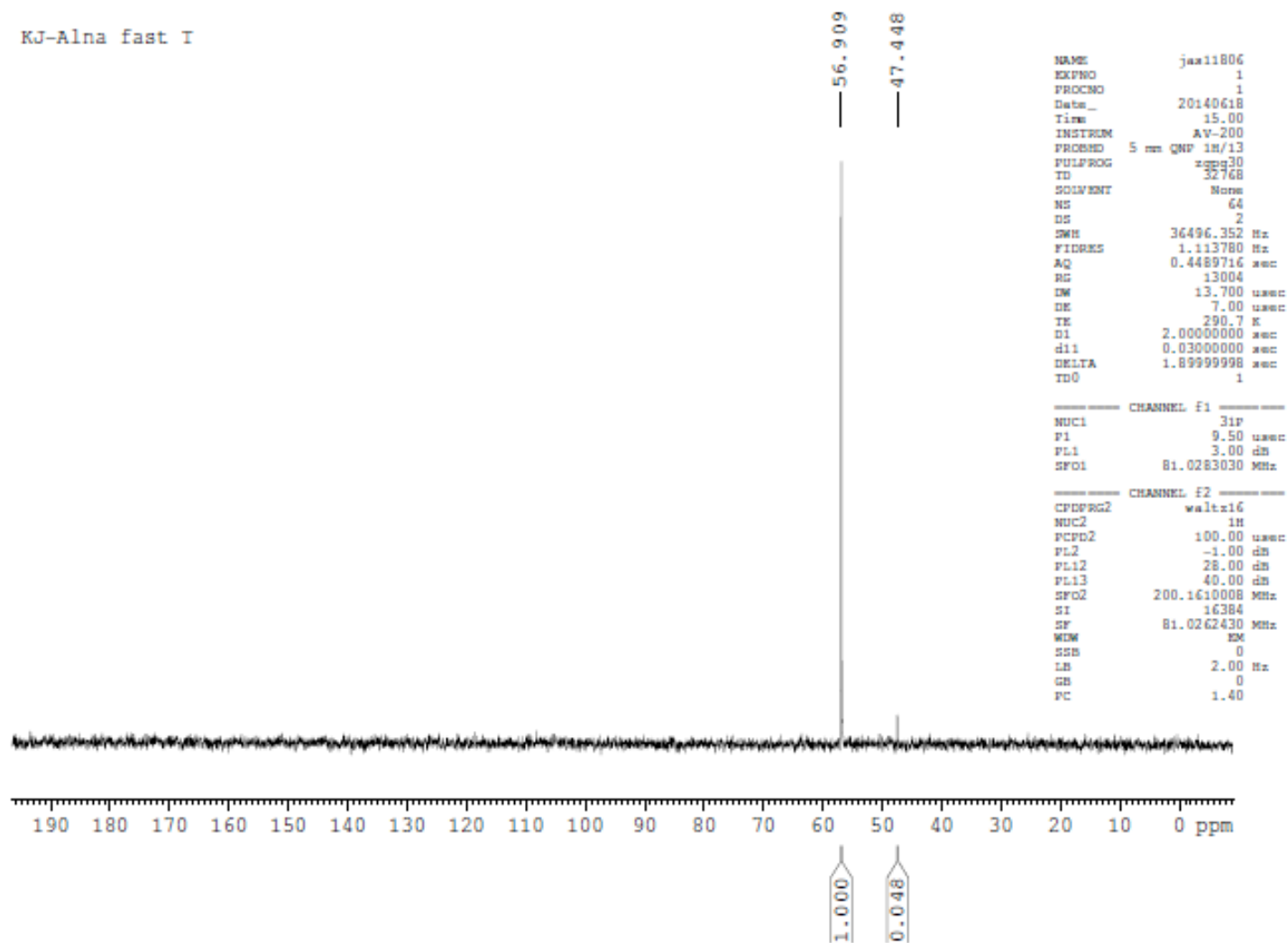


Figure S56. A  $^{31}\text{P}$  NMR spectrum for  $(A_L)_{\text{PS}}\text{T}$  obtained from **2b** *slow*. A signal at 47.4 ppm corresponds to the product of hydrolysis and not to the second P-diastereoisomer.

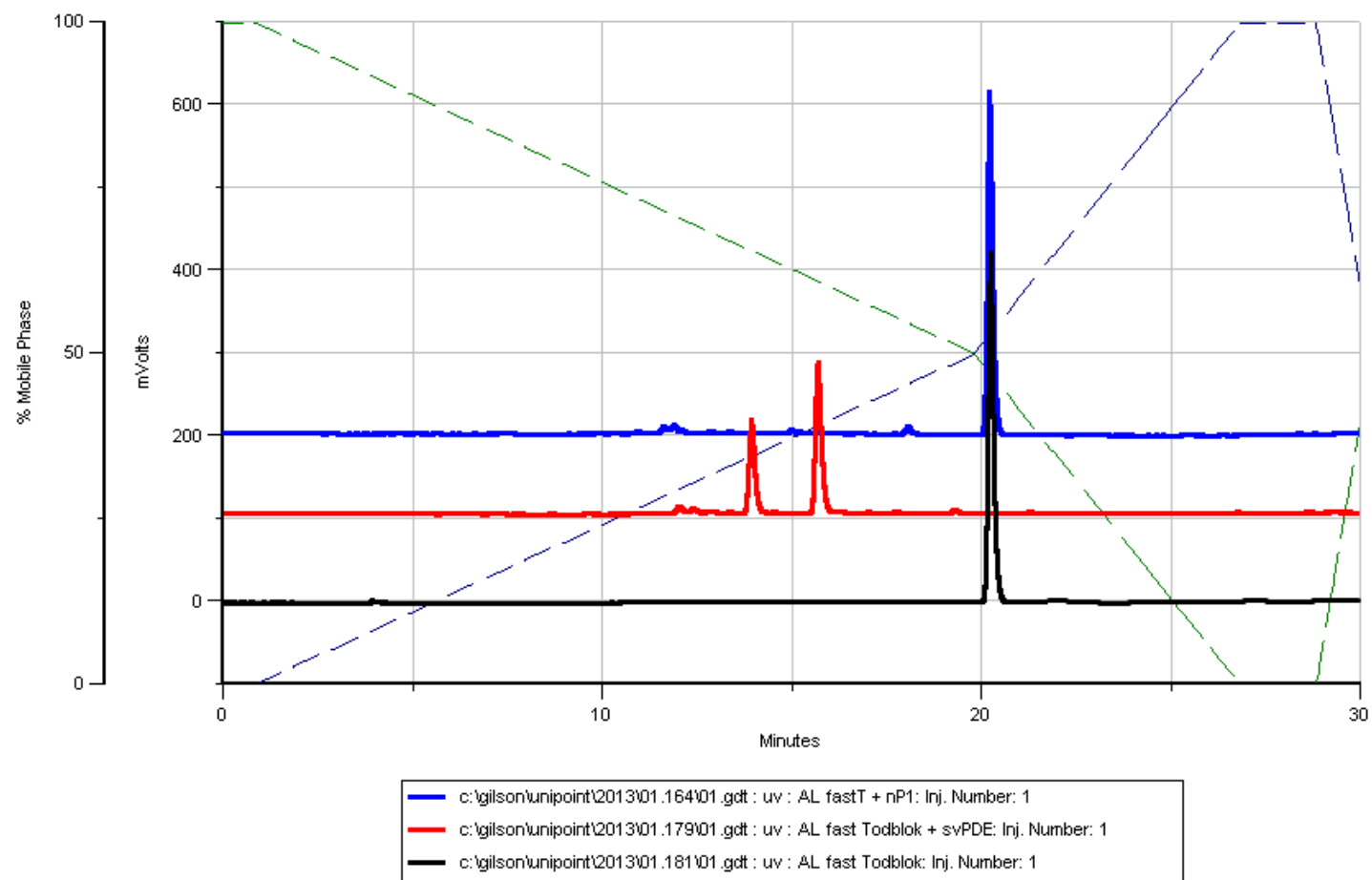


Figure S57. RP HPLC profiles for:  $(A_L)_{PS}T$  from **2b** *fast* (black line),  $(A_L)_{PS}T$  from **2b** *fast* + *svPDE* (red line),  $(A_L)_{PS}T$  from **2b** *fast* + *nPI* (blue line). ACE 5 C 18-AR Column, 250×4.6 mm; flow rate 1mL/min, A buffer: 0.1 M TEAB, B buffer: 40% CH<sub>3</sub>CN in 0.1 TEAB, Gradient: 0-50% of B buffer in 20 min, 50-100% of B buffer in 7 min.



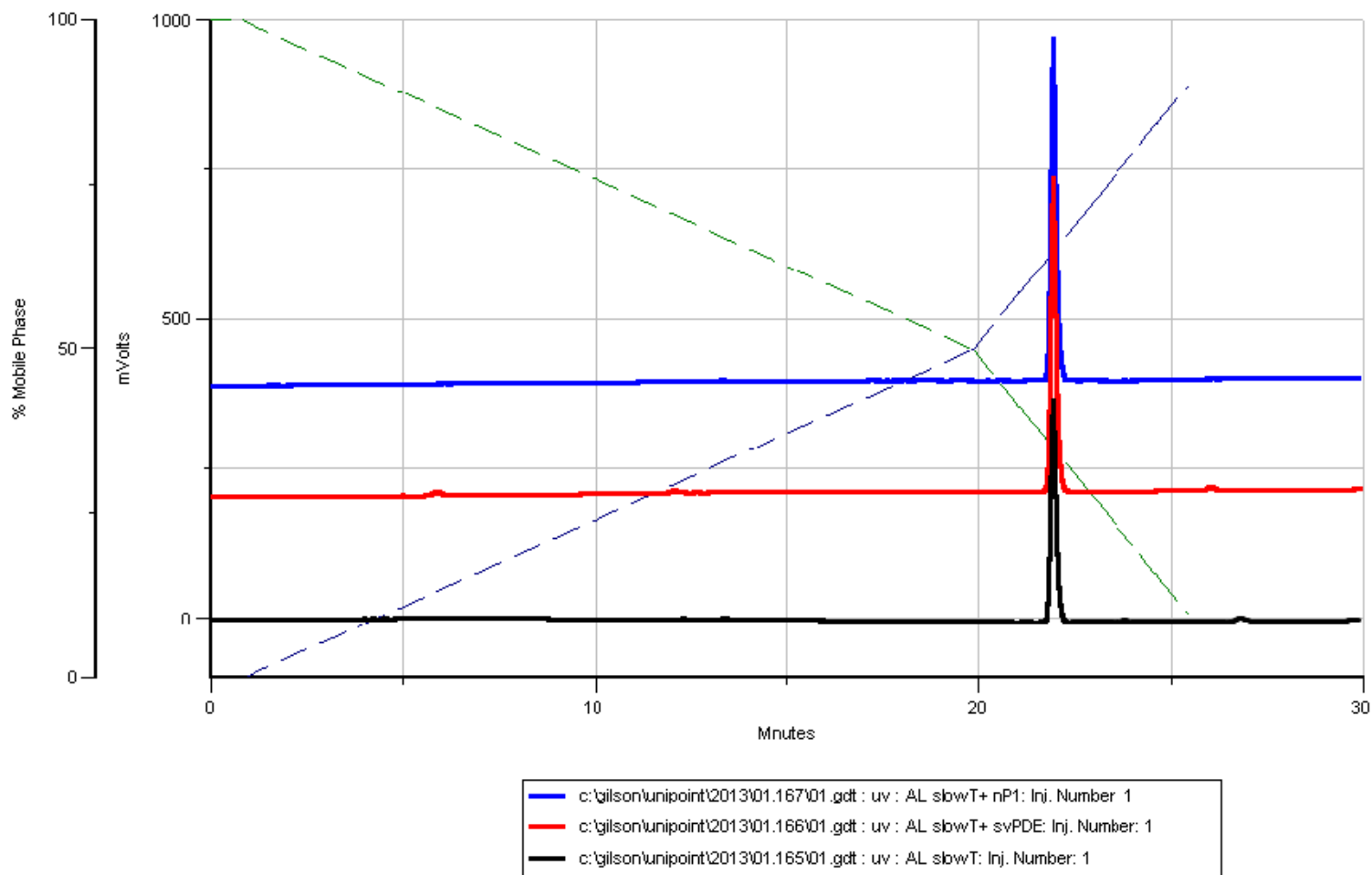


Figure S58. RP HPLC profiles for: (A<sub>L</sub>)<sub>PS</sub>T from **2b** *slow* (black line), (A<sub>L</sub>)<sub>PS</sub>T from **2b** *slow* + svPDE (red line), (A<sub>L</sub>)<sub>PS</sub>T from **2b** *slow* + nP1 (blue line). ACE 5 C 18-AR Column, 250×4.6 mm; flow rate 1mL/min, A buffer: 0.1 M TEAB, B buffer: 40% CH<sub>3</sub>CN in 0.1 TEAB, Gradient: 0-50% of B buffer in 20 min, 50-100% of B buffer in 7 min.